BIG DATA ANALYTICS FOR ASSESSING SURFACE TRANSPORTATION SYSTEMS

by

Jairaj Desai

A Dissertation

Submitted to the Faculty of Purdue University

In Partial Fulfillment of the Requirements for the degree of

Doctor of Philosophy

Lyles School of Civil Engineering

West Lafayette, Indiana

May 2022

THE PURDUE UNIVERSITY GRADUATE SCHOOL
STATEMENT OF COMMITTEE APPROVAL

Dr. Darcy Bullock, Chair
Lyles School of Civil Engineering

Dr. Ayman Habib
Lyles School of Civil Engineering

Dr. James Krogmeier
School of Electrical and Computer Engineering

Dr. Andrew P. Tarko
Lyles School of Civil Engineering

Approved by:
Dr.Dulcy Abraham

To my parents, Tejal and Chetas, for your constant love, support, patience and for believing in me when I myself never did. I owe it all to you.

To my friends, Vishesh and Aman, for your unwavering belief, words of encouragement and cherished friendship, I am ever grateful. I'd truly be lost without you.

To my aunt and uncle, Dharmi and Firoz, your love and hospitality knows no bounds. I would not be here without your support.

ACKNOWLEDGMENTS

First and foremost, I would like to thank my advisor Dr. Darcy Bullock for his mentorship, support, words of encouragement and belief in me throughout my time here at Purdue University. I am extremely grateful to him for giving me this opportunity and for helping me grow both personally and professionally over my time here working with the Joint Transportation Research Program. I would also like to thank Dr. Ayman Habib, Dr. James Krogmeier and Dr. Andrew Tarko for sharing their feedback and guidance that helped my research and subsequently this dissertation. My sincere thanks to all my colleagues without whose help and support none of this would have been possible – Dr. Jijo Mathew, Meg Hunter, Justin Mahlberg, Daniel Saldivar, Rahul Sakhare, Howell Li, Woosung Kim, Mingmin Liu and Ben Scholer. A special thank you to Debbie Horton, Bridget Brunton and Kym Pelfree for their invaluable support.

TABLE OF CONTENTS

LIST OF TABLES

LIST OF FIGURES

ABSTRACT

Most new vehicles manufactured in the last two years are connected vehicles (CV) that transmit back to the original equipment manufacturer at near real-time fidelity. These CVs generate billions of data points on an hourly basis, which can provide valuable data to agencies to improve the overall mobility experience for users. However, with this growing scale of CV big data, stakeholders need efficient and scalable methodologies that allow agencies to draw actionable insights from this large-scale data for daily operational use. This dissertation presents a suite of applications, illustrated through case studies, that use CV data for assessing and managing mobility and safety on surface transportation systems.

A systematic review of construction zone CV data and crashes on Indiana's interstates for the calendar year 2019, found a strong correlation between crashes and hard-braking event data reported by CVs. Trajectory-level CV data analyzed for a construction zone on interstate 70 provided valuable insights into travel time and traffic signal performance impacts on the surrounding road network. An 11-state analysis of electric and hybrid vehicle usage in proximity to public charging stations highlighted regions under and overserved by charging infrastructure, providing quantitative support for infrastructure investment allocations informed by real-world usage trends. CV data were further leveraged to document route choice behavior during active freeway incidents providing stakeholders with a historical record of observed routing patterns to inform future alternate route planning strategies. CV trajectory data analysis facilitated the identification of trip chaining activities resulting in improved outlier curation and realistic estimation of travel time metrics.

The overall contribution of this thesis is developing analytical big data procedures to process billions of CV data records to inform engineering and public policy investments in infrastructure capacity, highway safety improvements, and new EV infrastructure. These scalable and efficient analysis techniques proposed in this dissertation will help agencies at the federal, state and local levels in addition to private sector stakeholders in assessing transportation system performance at-scale and enable informed data-driven decision making.

1. INTRODUCTION

Transportation agencies around the world have for the past few decades relied primarily on deploying fixed intelligent transportation system (ITS) sensor-based infrastructure on road networks to monitor traffic, roadway and vehicle conditions. These sensors collect a wide range of data from simple vehicle volumes to estimated vehicle speeds and roadway conditions. While ITS sensors have been widely deployed and promise a high degree of accuracy in detecting vehicles, their deployment carries with it an inherently high installation, maintenance and repair cost and additionally spatially limits the area of detection. Additionally, both in-roadway (loop detectors for example) and over-roadway (cameras and speed radar for example) sensors require significant disruption to traffic for installation and repair, structural cuts to pavements for embedding the sensors, and are highly cost and labor intensive [1]. Traditional ITS sensors for monitoring travel times and roadside detection can even incur costs of up to $10,000 per mile and $100,000 per year respectively [2]. However, Connected Vehicle (CV) data presents an opportunity for widespread monitoring of transportation systems at much lower costs than ITS sensors.

CV data presents significant benefits for practitioners and researchers when compared to ITS sensors in assessing and subsequently addressing safety, mobility and environmental issues in the transportation domain. The US Department of Transportation (USDOT) identified four Vehicle-to-Infrastructure (V2I) research programs, namely V2I Safety, Dynamic Mobility Applications (DMA), Applications for the Environment: Real-time Information Synthesis (AERIS) and Road-Weather Management (RWM) [3] that could significantly benefit from the incorporation of CV data-driven methodologies. A 2021 survey of 50 smart cities in 26 states across the country found only 8 percent of respondents currently using CV data [4], a number that is expected to grow sharply as CVs make up more and more of the new car market with every passing year, with some estimates predicting the CV data market to be worth $334 billion by the year 2030 [5]. It is estimated that by that same year, CVs will make up approximately 95 percent of the global new car market, a sharp increase up from about 50 percent in recent years [6]. Federal and state agencies would be primely placed to take advantage of this market shift by themselves transitioning to CV data monitoring now, away from ITS-sensor based monitoring.

At the federal level, the USDOT has signaled a significant importance on data-driven decision making through its Work Zone Data Exchange (WZDx) initiative aimed at providing drivers and Original Equipment Manufacturers (OEMs) with the most up to date information on active work zones throughout the nation in a bid to improve safety [7]. The Federal Highway Administration (FHWA) has observed that many agencies have been and continue to use floating car and floating phone studies to mimic real-time trajectory data, however they run the risk of presenting non-representative data samples and lack real-time information [8].

The Joint Office of Energy and Transportation is also taking a data-driven approach towards building a nationwide Electric Vehicle (EV) charging network over the coming years by providing states and communities with access to a host of foundational datasets as they vie for federal and state funding to improve infrastructure readiness for the impending widespread adoption of EVs [9]. The USDOT continues to inculcate multiple data sources (many of them real-time) into improving the safety and efficiency of multimodal transportation systems, and has in recent times opened up its data sharing policies to stimulate collaboration among governmental, industrial and academic partners [10]. On the private sector front, multiple automotive OEMs have already begun or are in the process of aggregating, analyzing and in some cases, monetizing their CV data including GM [11], Ford [12], Honda [13] and Volkswagen [14] among others.

The United States Congress recently passed the Bipartisan Infrastructure Deal (also known as the Infrastructure Investment and Jobs Act[IIJA]) which reauthorizes surface transportation programs for five years, and provides for nearly $110 billion in funding to repair existing transportation infrastructure (including roadways and significant bridges) [15]. The new National Electric Vehicle Infrastructure (NEVI) Formula Program, a part of this act, targets having a nationwide network of 500,000 EV chargers by the year 2030 [16] and requests each state submit its infrastructure deployment plan in order access the apportioned funds. Equitably allocating and effectively utilizing this investment will require that relevant stakeholders have access to real-world insights on infrastructure usage to ensure resource allocations reflect observed trends and demands. One of the prime objectives behind the research in this dissertation is to propose scalable and efficient CV data analysis techniques that can provide these operational insights to decision-makers.

1.1 Motivation

There is an emerging shift in agencies desire to reduce ITS infrastructure investments and increase system wide performance monitoring using real-time CV data. The motivation of this research is to address the aforementioned need by leveraging large-scale CV big data towards assessing surface transportation systems using visualizations, novel methodologies and associated performance measures to facilitate informed data-driven decision making by transportation stakeholders.

Although there is strong interest by agencies in CV data, it also comes with concerns. High volumes of trajectory data may soon become unwieldy for many agencies, with estimates for 2019 putting the global volume of generated CV data at 95 petabytes [17]. This dissertation discusses the development of methodologies and visualizations that will allow researchers and practitioners to easily gain operational insights from CV big data to assess transportation system performance, and presents opportunities to implement CV data-based monitoring into their day-to-day operations. Various performance measures are proposed for assessing mobility and safety on interstates, assessing charging infrastructure usage and for real-time monitoring of route choice behavior to assist agencies with daily monitoring as well as historical reviews of traffic patterns.

1.2 Scope and Organization

The scope of this dissertation is the development of methodologies and visualizations that leverage large-scale CV big data towards assessing surface transportation systems. The contents of this dissertation are organized in chapters as follows:

- To demonstrate CV data-driven visualizations and methodologies that aid in monitoring work zone mobility performance and impact on surrounding road networks (chapter 2)

- To present a systematic review of secondary crashes on Indiana Interstates for 2019 and document their impact on freeway mobility with quantitative performance measures based on CV data (chapter 3)

- To evaluate the use of hard-braking events as a proactive surrogate safety performance metric for tracking interstate work zone safety in place of reactive metrics relying on crash reporting (chapter 4)

- To develop methodologies leveraging CV data towards assessing EV charging infrastructure usage, and identifying gaps in infrastructure availability for streamlining future investment opportunities (chapter 5)

- To develop methodologies that utilize CV data in analyzing route choice behavior among motorists navigating through or around an active freeway incident resulting in a partial or complete road closure (chapter 6)

Overall conclusions drawn from the research in this dissertation and findings from each of the above chapters are summarized briefly in chapter 7.

2. MONITORING MOBILITY IN AND AROUND INTERSTATE CONSTRUCTION WORK ZONES

The information presented in this chapter is published in "Agile Work Zone Management Based on Connected Vehicle Data" [18] and in "Methodology for Applying Connected Vehicle Data to Evaluate Impact of Interstate Construction Work Zone Diversions" [19].

This chapter discusses visualizations and methodologies for monitoring work zone mobility and impact of freeway construction on freeway as well as arterial mobility using CV and supporting data. The analysis, methodology, and results discussed in this study can be used by agencies for planning monitoring strategies for large construction projects that have significant impact on alternative routes.

2.1 Agile Work Zone Management Based on Connected Vehicle Data

2.1.1 Overview

Peak period lane closures can result in significant queueing on major interstates. Many state agencies thus have a lane closure policy in place based upon historical time of day and day of week traffic volumes. The COVID-19 pandemic resulted in a significant reduction in traffic volumes in Indiana during March-May 2020. In some periods, traffic volume reductions were over 35%. During this period, the Indiana Department of Transportation (INDOT) implemented an agile lane closure policy based upon observed volumes and monitored those exceptions using connected vehicle data. This chapter reports on the analysis of 11 lane closure exceptions on 4 interstates across Indiana. Congestion comparisons were made for each exception for the same time period in 2020 and 2019. Even with the lane closure exceptions, the study found 10 of 11 sections actually had fewer mile-hours of congestion and the total mile-hours of congestion for all 11 sections reduced from 1281 mile-hours in 2019 to 244 mile-hours in 2020. Overall, crashes decreased from 125 in 2019 to 70 in 2020. Year-over-year comparisons for these exceptions demonstrated significant opportunities for agile work zone lane closure practices when coupled with close monitoring of crash and congestion measures derived from connected vehicle data.

2.1.2 Introduction

Lane closures for construction and maintenance activities often lead to significant queueing and congestion. Many state agencies have lane closure policy provisions that limit lane closures to periods with lower traffic volumes to reduce significant queueing. However, certain exceptions to a pre-defined policy are often required. Criterion for permitting a lane closure exception differs on a state-by-state basis as does the exception granting and approval process [20]. The 2017 Indiana Interstate Highway Congestion Policy (IHCP) states as overall guidance that construction work that results in queuing outside of limits set by the congestion policy should be avoided where feasible while there are processes in place when granting exceptions [21].

In cases where lane closures are deemed essential, traffic counts and queue analysis tools are typically used to analyze exception requests. These tools are based upon volumes that can be difficult to accurately forecast and traffic models that do not always reflect local conditions. However, with the advent of commercially available connected vehicle data, it is now possible to monitor interstate congestion and queuing on a minute-by-minute interval. The motivation of this paper is to report on the use of daily connected vehicle dashboards to assess lane closure exception requests, and then follow up with assessment of those lane closure exceptions.

As a result of a statewide stay-at-home order to address COVID-19 initiated in March 2020, traffic on state highways in Indiana saw a 30% to 45% decrease in passenger vehicles in March. Figure 1 shows representative traffic volume changes in March compared to base levels. When compared to a control week beginning February 22nd, weekly average personal travel nationwide in the US as well as in Indiana was down approximately 30% for 6 weeks starting March 27th, 2020 [22]. This reduction in traffic volumes resulted in an opportunity for the Indiana Department of Transportation (INDOT) to implement agile lane closure exceptions. This paper uses crash data and connected vehicle data to assess the implementation of these lane closure exceptions and their impact on traffic.

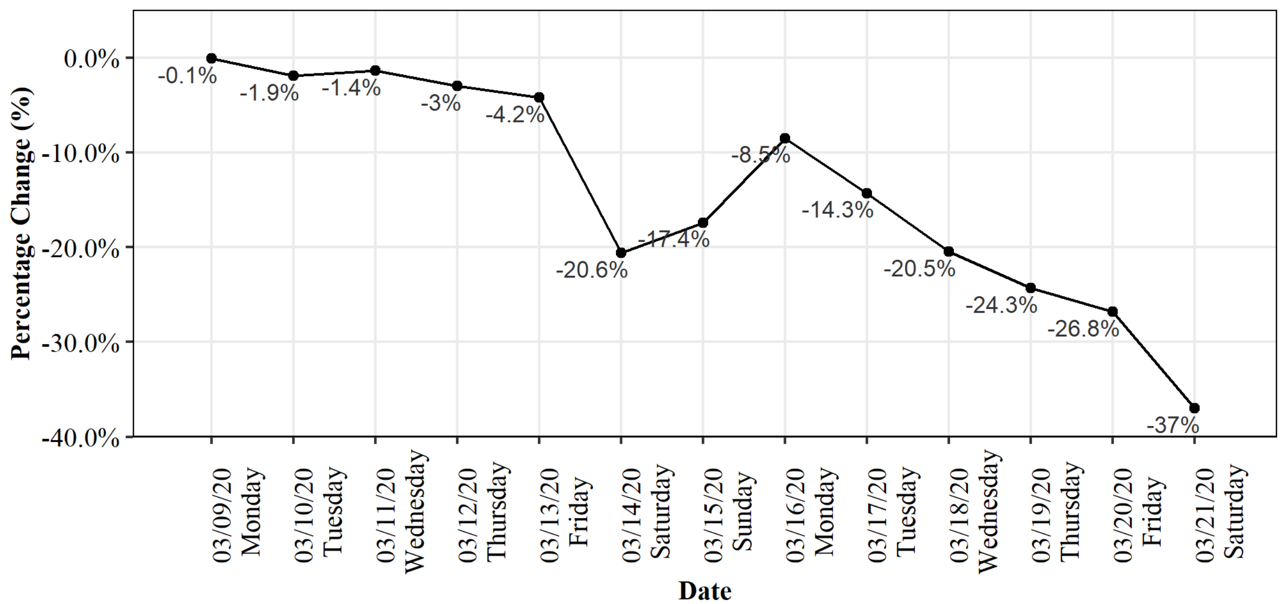

Figure 1. Percentage change in Indiana traffic volume from March 9-21, 2020 compared to same day in base week of March 2-8, 2020

2.1.3 Literature Review

While agile project management methodologies first originated in the software development industry, they have quickly found favor in the construction industry in the pre-design, design and actual construction phases as well [23], [24]. Some of the biggest advantages of using an agile approach include decreased uncertainty associated with models and improved risk management on complex projects.

States such as New Jersey have in the past developed uniform procedures for determining the impact of lane closures on traffic using hourly traffic volumes [25] which depend on adjustments made to Annual Average Daily Traffic (AADT) values. These practices are commonly used by many other states and INDOT has followed those practices that use historical traffic volumes with queueing models to determine the feasibility of approving a lane closure exception [20].

2.1.4 Objectives

Existing lane closure policies that often see no updates for extended periods of time, are based upon historical traffic counts and use generic queue calculations to evaluate exception requests.

Using real-time CV data has the potential to further improve flexibility on lane closure policies to strike an acceptable balance between time delay costs to motorists and maximizing closure times to benefit construction activity. The objectives of this study are:
(a) To evaluate the impact of agile lane closure policies on congestion.

(b) To evaluate the impact of agile lane closure policies on crash frequency.

(c) To evaluate the use of real-time connected vehicle data for fine tuning agile lane closure policies.

2.1.5 Study Location

This study evaluated 11 lane closure exceptions granted across the state of Indiana on 4 different interstate routes (Interstates 65, 69, 70 and 265). Table 1 lists these 11 lane closure exceptions, and columns 2 and 3 identify the route and the mile marker range they were active on. Details regarding congestion and crash count calculations are described in subsequent sections.

Figure 2 shows a statewide map with each of the 11 exceptions marked, showing a majority of the granted exceptions were on rural stretches of interstate roadways that do not typically carry heavy daily commuter traffic.

Table 1. Lane closure exceptions evaluation area mile marker ranges and year-over-year mile-hours of congestion and crash count comparisons

2020 Exception	Route	Evaluation Area Mile Marker Range	Mile-hours of congestion (MHC)		% change in MHC	Crash count		% change in Crashes
			2020	*2019*		*2020*	*2019*	
E1	I65	MM 205 – 230	12	179	-94%	12	18	-33%
E2	I70 W	MM 103 – 105	1	6	-85%	1	1	0%
E3	I70 E	MM 95 – 104	96	26	276%	3	8	-63%
E4	I65	MM 158 – 168	8	69	-88%	3	14	-79%
E5	I65	MM 20 – 22	1	18	-96%	3	0	-
E6	I70	MM 3 – 7	48	59	-19%	6	4	50%
E7	I65	MM 147 – 149	12	23	-48%	10	4	150%
E8	I65	MM 106 – 108	7	61	-89%	10	17	-41%
E9	I70	MM 37 – 41	21	28	-26%	2	2	0%
E10	I69	MM 263 – 271	19	578	-97%	7	29	-76%
E11	I265	MM 0 – 7	19	234	-92%	13	28	-54%
Total			244	1281	-81%	70	125	-44%

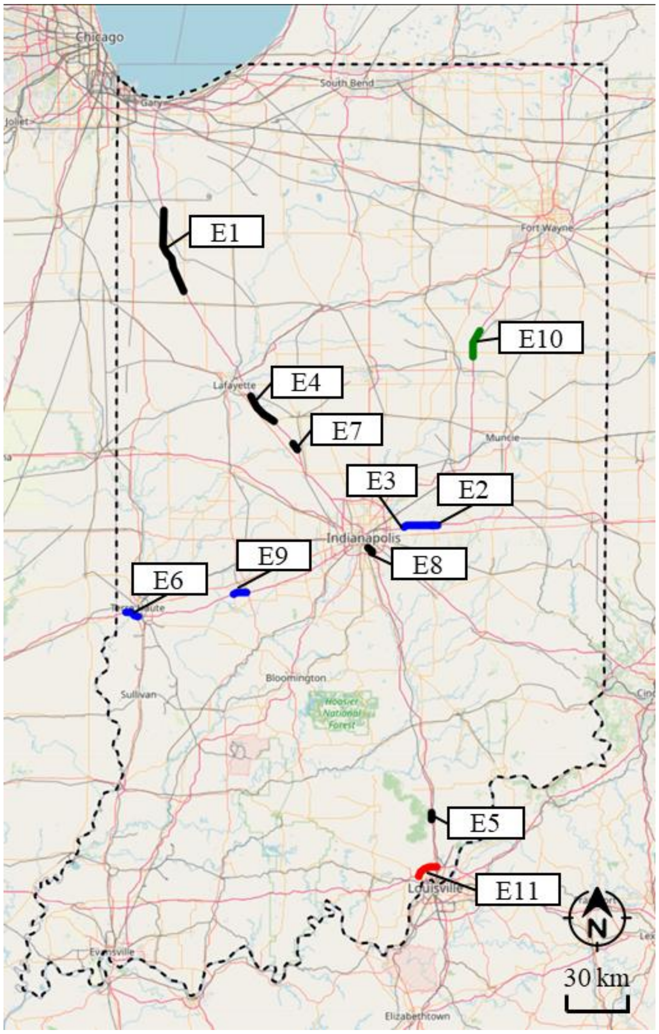

Figure 2. Statewide map of 11 Lane Closure Exceptions on Interstates

2.1.6 Methodology

Table 1 details the evaluation area mile marker range for each exception, and together the 11 exceptions cover 75 miles of Indiana Interstates. Exception E1 was granted from April 2 through May 8, 2020 while exceptions E2 through E11 were granted for an additional 5 days ending on May 13, 2020.

2.1.6.1 Assessing Congestion

Although there are a variety of definitions of congestion, for simplicity, segments of interstate are typically considered to be operating in the congested regime in Indiana when speeds are below 45

MPH [26]. Using this definition, commercially available connected vehicle data were employed to calculate mile-hours of congestion, meant to numerically represent the spatial and temporal extent of congestion on a stretch of roadway [27] as shown in (1) below.

$$MH_{<45} = \Sigma_{i=1 \text{ to } n}(L_i \times t_i) \quad (1)$$

where,

$MH_{<45}$ = total mile-hours of congestion

n = total number of segments in a stretch of interstate

L_i = length of segment i in miles

t_i = time in hours for which segment i was congested

Mile-hours of congestion values for every exception were calculated for its corresponding period of activity in 2020 as well as in 2019 and are listed in their respective columns in Table 1. All but one exception (E3) showed a decrease in mile-hours of congestion for 2020 and an overall decrease of 81% was seen in congestion across all exceptions.

2.1.6.2 Assessing Crash Data

Similarly, individual crash reports for the same 6-week period in 2019 and 2020 were obtained from the state's online repository and aggregate counts by exception have been listed in corresponding columns in Table 1. Crashes decreased by 44% overall in the evaluation areas for these exceptions in 2020. Three exceptions (E5, E6, E7) showed an increase in crash counts in 2020 that is discussed in the text that follows. The literature suggests crash rates are likely to increase on a roadway that is under construction compared to the same roadway having no construction activity [28]. Thus, compared to base level crash counts from 2019, there were substantial safety improvements as a result of the timely implementation of these lane closure exceptions.

2.1.7 Year-over-year Comparisons

2.1.7.1 Mile-hours of Congestion and Crash Count Comparisons

Figure 3 shows mile-hours of congestion comparisons for the 11 exceptions for 2019 and 2020. Callout (i) points to exception E3 depicting highest percentage increase in mile-hours of congestion in 2020 (276%), while callout (ii) points to exception E10 depicting highest percentage decrease in mile-hours of congestion in 2020 (97%).

Figure 4 shows a similar graphical comparison as in Figure 3, but for year-over-year crash counts. All exceptions except E5, E6 and E7 showed a significant reduction in crashes in 2020.

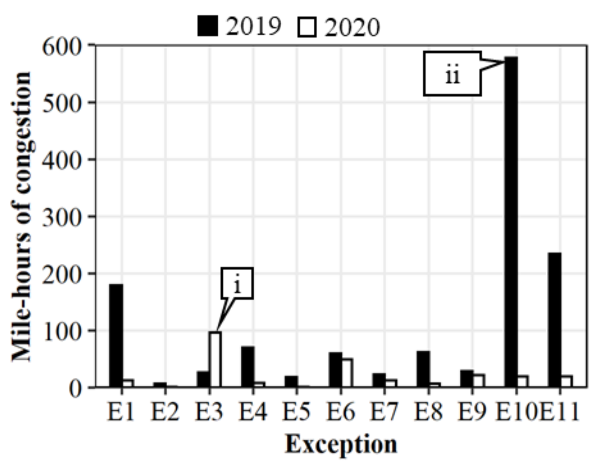

Figure 3. Year-over-year mile-hours of congestion comparisons for 11 exceptions

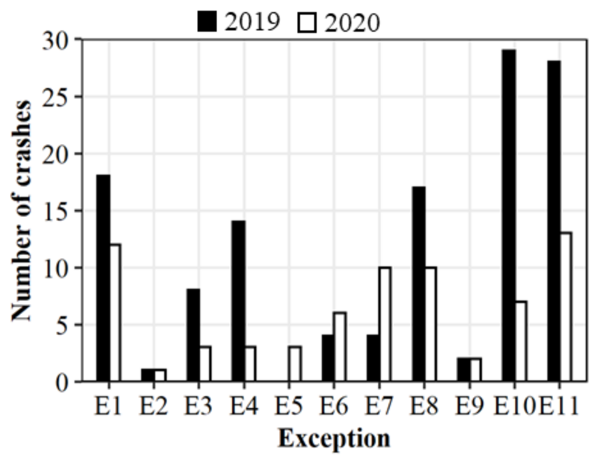

Figure 4. Year-over-year crash count comparison for 11 exceptions

2.1.7.2 Crash Counts by Manner of Collision

Figure 5 shows crash counts by exception, and further categorized by crash type. Same direction sideswipe crashes increased by 7 in 2020 for exception E7. A review of crash report narratives showed that improper merging before lane shifts and trailer involvement were frequent factors in these crashes. Rear end crashes, one of the detrimental outcomes and telling indicators of long queuing on interstates, were observed to have decreased across the board on all exceptions.

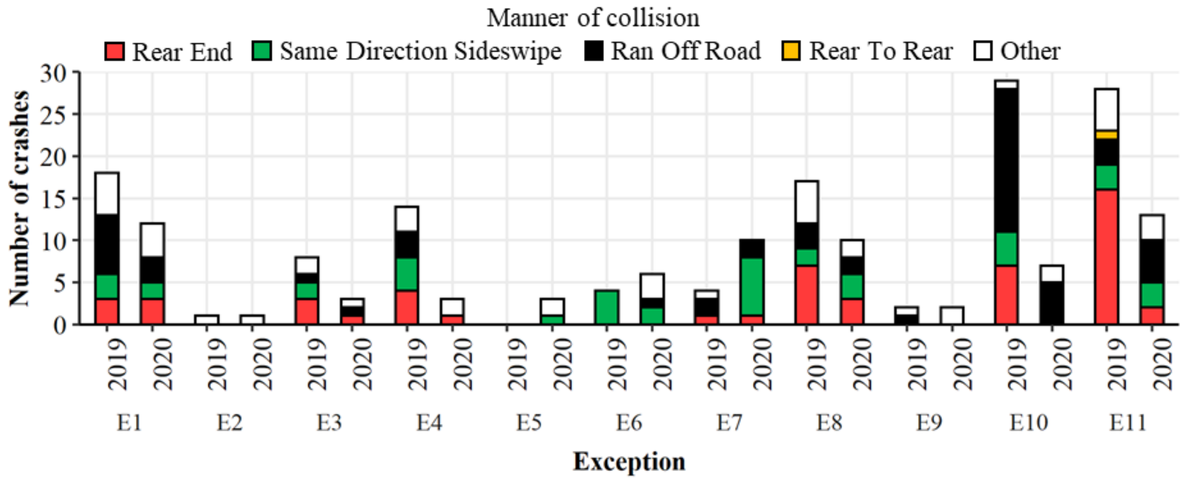

Figure 5. Year-over-year crash count comparisons for 11 exceptions by Manner of Collision

2.1.7.3 Visualizing Congestion using Speed Profile Heatmaps

Spatial and temporal heatmaps of traffic speeds for the period of April 2 through May 13 in 2019 and 2020 were used to visualize differences in recurring and non-recurring congestion and queuing on the exception evaluation areas in this study. These heatmaps were generated using commercially available CV data consisting of average vehicle speeds for 1-mile interstate segments at 1-minute frequency. Traffic speed data was binned into 15-minute intervals, colored from green to purple as average speeds decreased from above 65 mph to below 14 mph.

Figure 6 shows these speed profile heatmaps for 2019 (a) and 2020 (b) for exception E3 in the eastbound direction of travel on interstate 70. Recorded crash incidents for this evaluation area are overlaid on the heatmaps in Figure 6a and b. A rise in congestion is observed beginning May 4, 2020 (callout i) which corresponds to the first phase of the state's commercial businesses reopening during COVID-19.

Figure 7 shows the same speed profile heat maps for 2019 (a) and 2020 (b) for exception E11 in the eastbound direction of travel on interstate 265. Recorded crash incidents for this evaluation area are overlaid on the heatmaps in Figure 7a and b. While Figure 7a clearly shows recurring weekday congestion throughout the observation area in 2019, the same trends were not observed in 2020 except for non-recurring congestion attributable to a personal injury crash in May 2020.

While the heatmaps shown in this section present an after-action review of lane closure exception impacts on traffic, the availability of speed profile data with only a few minutes of delay makes it possible for agencies to track ongoing exceptions in real-time and affords them the flexibility to make modifications to closures timings and/or locations as and when they notice impact on roadways and motorists.

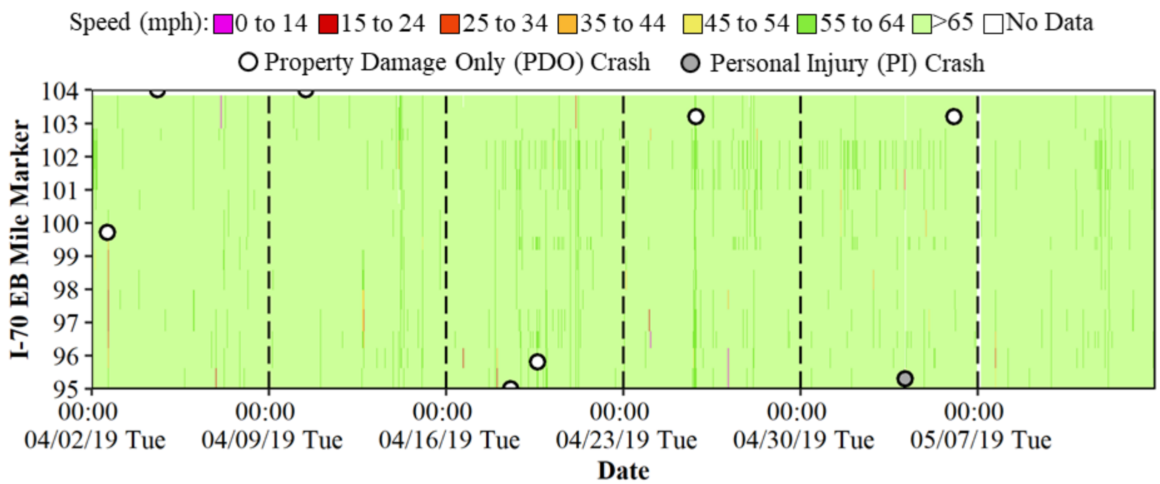

(a) 2019 Speed Profile Heatmap by Mile Marker and Day

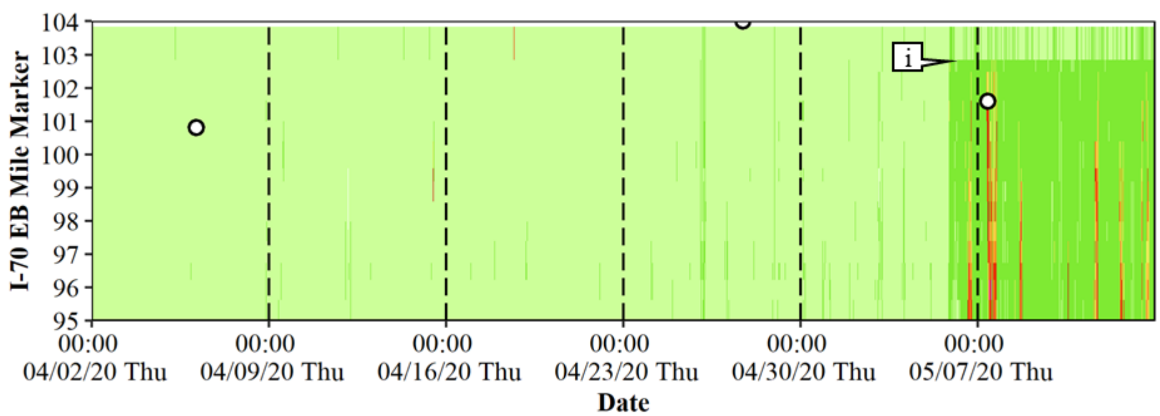

(b) 2020 Speed Profile Heatmap by Mile Marker and Day

Figure 6. Exception E3: I-70 Eastbound (EB) MM 95-104

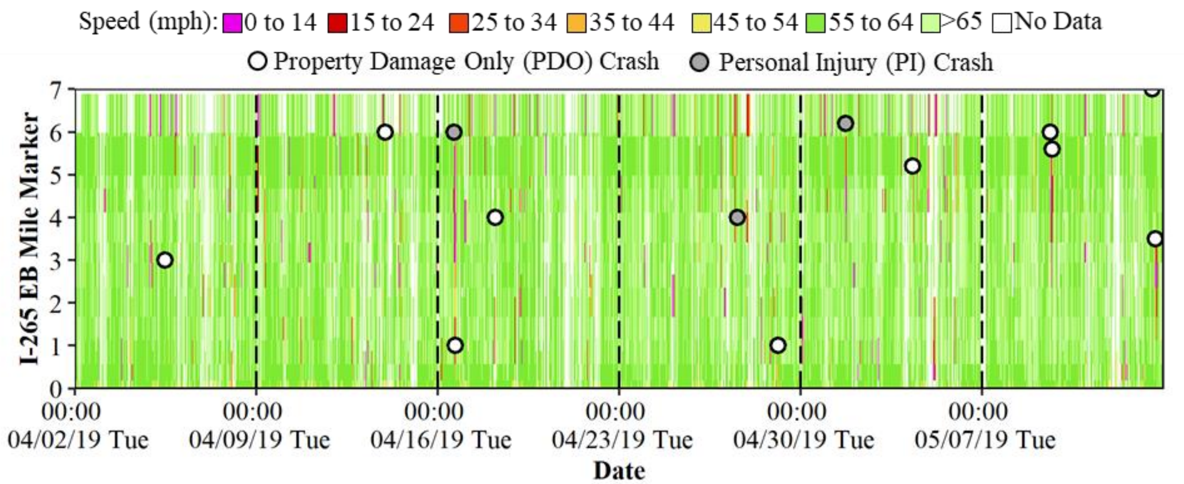

(a) 2019 Speed Profile Heatmap by Mile Marker and Day

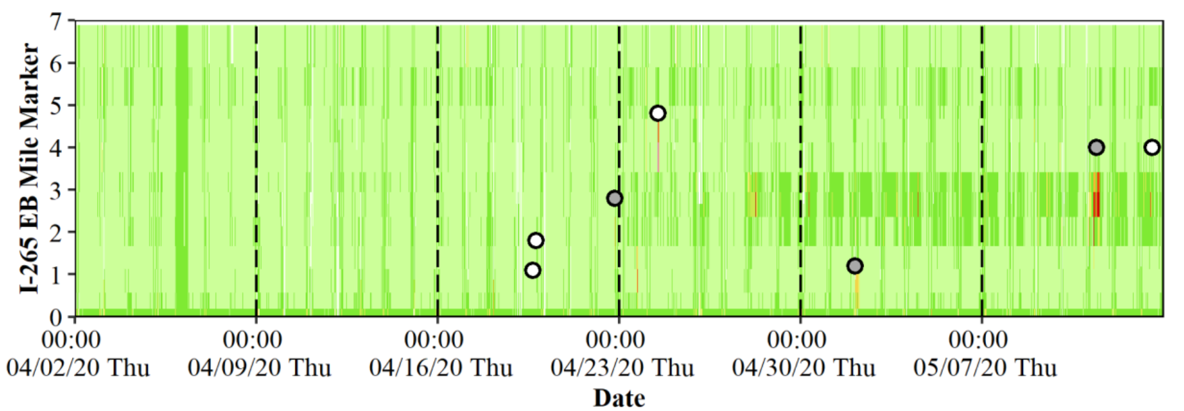

(b) 2020 Speed Profile Heatmap by Mile Marker and Day

Figure 7. Exception E11: I-265 Eastbound (EB) MM 0-7

2.1.8 Summary

This study analyzed congestion trends and crash activity for 11 lane closure exceptions granted by INDOT on 4 interstate roadways over a 6-week period in 2020. The same 6-week period from 2019 was analyzed for base level comparison. This study observed an overall 81% decrease in congestion and 44% decrease in crashes in 2020 compared to 2019. Although the traffic volume changes were unprecedented, these results support the use of agile data-driven tools for agencies to be flexible in their lane closure policies in conjunction with close monitoring of the impact of those exceptions.

While the exceptions analyzed in this study only constituted 139 miles of a total of nearly 2500 centerline miles of interstate roadways in Indiana, their successful implementation makes a strong case for adopting agile work zone project management practices on a larger scale in conjunction with close monitoring made possible by access to real-time connected vehicle speeds, hard-braking and hard-acceleration data. Exceptions analyzed for this research were the first 11 instances of INDOT utilizing agile lane closure procedures in 2020. Agile lane closure policies were subsequently implemented at an additional 25 locations across the state. In addition to including crash date and time information in the dashboards, INDOT is now incorporating hard-braking events reported by connected vehicles to provide even faster assessment on system operation [29].

This section of chapter 2 demonstrated how real-time CV data can aid in monitoring work zone's (or even a freeway segment not under construction) mobility performance, and allow transportation agencies to make dynamic adjustments to roadway maintenance strategies based on observed volumes rather than historical forecasts or models. As of this writing, INDOT is actively leveraging real-time CV dashboards as those presented by this study to monitor freeway traffic for daily operational use.

2.2 Methodology for Applying Connected Vehicle Data to Evaluate Impact of Interstate Construction Work Zone Diversions

2.2.1 Overview

Diversion of Interstate traffic can significantly impact the surrounding road network with increased volumes and congestion. This paper uses commercially available connected vehicle data to examine the impact of a construction zone on Indiana I-70 with 7 days of reduced interstate capacity that resulted in significant diversion onto US-40, an adjacent signalized arterial east of Indianapolis. Approximately 12 million connected vehicle GPS points, collected at nominal 3 second intervals were analyzed over an eight-week period for an 11-mile section of I-70 and similar length parallel section of US-40. Congestion peaked at approximately 5 PM on August 10th, 2020 and resulted in a 115% increase in sampled vehicle volumes using the adjacent US-40. Critical intersections along US-40 experienced an increase of approximately 1175% in split failures. Travel time on the US-40 corridor increased by 16% during the peak hour. The framework presented in this paper will serve as a valuable tool for agencies to deploy connected vehicle performance measures for both Interstate and Arterial routes, without significant investment in traditional intelligent transportation system (ITS) sensors. Since these techniques are based upon emerging commercially available connected vehicle data, they can be readily scaled to any interstate construction project in the United States.

2.2.2 Introduction

Interstate construction activity and peak period lane closures can lead to significant delays, congestion and adversely impact the adjoining road network due to diverting traffic. Work zones account for about 10% of overall congestion and approximately 24% of non-recurring congestion, as reported by the FHWA [30], [31]. Additional data from state departments of transportation observed that nearly 20% of the National Highway System experiences construction activity during summer [31]. Assessing and subsequently mitigating the impact of interstate construction diversions on overall network performance is thus essential for state agencies.

2.2.3 Literature Review

There are multiple route guidance models [32]–[36] and Advanced Traveler Information Systems (ATIS) [37], [38] that offer motorists alternate diversion route information during congestion. Studies have also looked at the factors that affect the route choice during network disruptions and found that provision of real-time information was an important factor that affected traveler decision [39], [40].

Understanding the impact of traffic on alternate routes is critical for agencies during detours. Several studies have used stated surveys and modelling approaches for this purpose [41]–[45]. Only a few studies have used real-world probe vehicle data to investigate the impact of diversions. Traditional intelligent transportation system (ITS) sensors including Bluetooth sensors and dynamic message signs have been used in the past decade to evaluate work zone diversions [46]–[49] and traffic management strategies during special events [50]. Bluetooth sensors were also deployed to estimate the distribution of diverted traffic on four alternate routes during an unexpected bridge closure [51]. The study found that relatively few drivers took the official detour compared to the other routes. During an unplanned closure of a 37-mile stretch of interstate in Indiana, agencies used traffic impact dashboards generated using real-time commercial probe vehicle data to monitor mobility and queuing on diverted routes [52]. A study in Japan also used probe data from a commercial vehicle to evaluate the detour rate by analyzing trip origin-destination (OD) during a heavy rain disaster [53].

Recent advancements in capturing anonymized trajectory-based data from connected vehicles can provide detailed information on the alternate routes and their traffic impact during diversions. A recent study using trajectory data was able to highlight the number of vehicles that diverted during a crash incident on an interstate [54]. However, there are very limited studies that use this emerging data to evaluate work zone diversions. This study uses commercially available CV trajectory data to examine the impact of a construction zone on Indiana I-70 that resulted in significant diversion on the adjacent US-40, a signalized arterial.

2.2.4 Objectives

The objective of this study is to propose a methodology by which CV data can be applied by practitioners to assess the impact of diversions caused by interstate work zones on freeway mobility as well as arterial traffic signal performance. Using emerging CV data, agencies can deploy interstate and arterial performance measures without having to put in a substantial long-term investment in cost prohibitive and labor intensive ITS sensor infrastructure.

2.2.5 Study Location

In this study, the impact of a construction work zone on the eastbound (EB) direction of an 11-mile section of I-70, located east of Indianapolis (Figure 8a), and its effects on a parallel 12-intersection stretch of the alternative route US-40 are analyzed. Variation in vehicle speeds, travel-time, and mile-hours of congestion caused by the construction on I-70, between mile markers (MM) 88 and 99 (Figure 8b), are examined in the following sections. There are exit and entry ramps that lead to and from US-40 at I-70 MM 91 and MM 96.

The consequences of increased volumes on traffic signal performance on US-40 intersections are estimated from connected vehicle (CV) data. Figure 8b shows the signalized intersections analyzed on US-40: Post Rd. (I1), Washington Village Shoppes (I2), Cherry Tree Plaza (I3), Mitthoeffer Rd. (I4), Washington Square (I5), Kroger (I6), Wal-Mart (I7), German Church Rd. (I8), Hugo St. (I9), Muessing St. (I10), S 700 W (I11), and S 600 W (I12).

(a) Indiana, United States

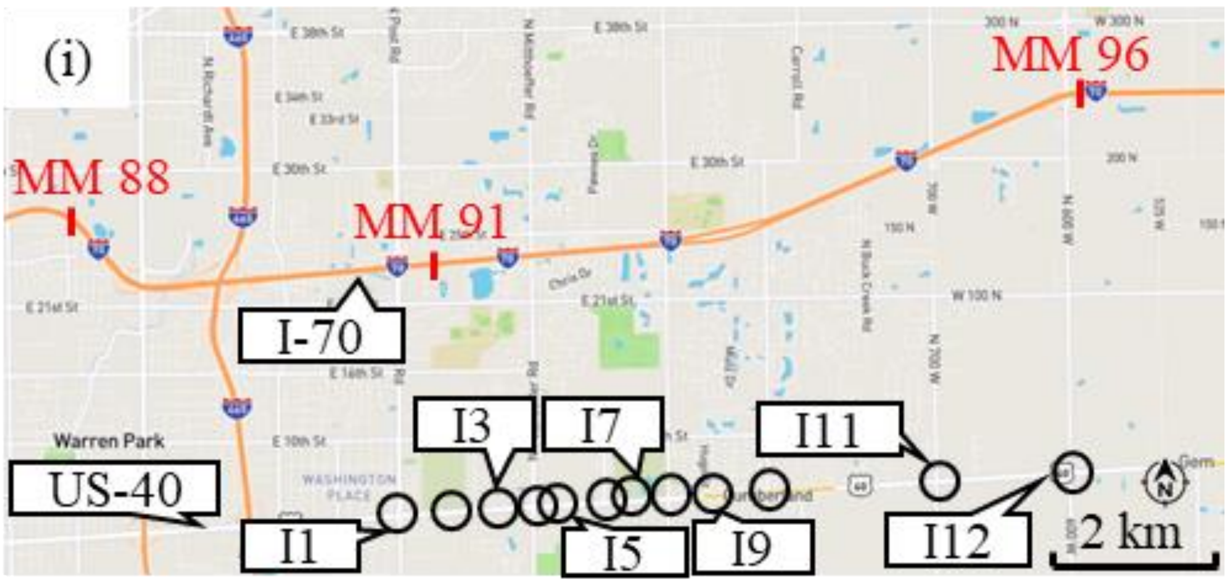

(b) East Indianapolis, IN

Figure 8. Study Location

2.2.6 Data Description

Third-party crowdsourced CV data with an estimated penetration rate of 5.0% on state and US roads [55], crash data obtained from the state repository and traffic images acquired from a fixed ITS camera in the study location, for the months of July and August 2020, were used in this study. Two different CV datasets are analyzed: trajectory data and event data. Geofences were defined to capture trajectory and event data points within the study location as shown in [29].

2.2.6.1 Trajectory Data

The CV trajectory data utilized by this study consists of individual vehicle waypoints with a reporting interval of 3 seconds and a 1.5-meter fidelity radius. Every waypoint has the following information attached: GPS location, timestamp, speed, heading, and an anonymized unique trajectory identifier. By linking individual waypoints using their trajectory identification number, a vehicle's trajectory can be obtained.

2.2.6.2 Event Data

The CV event data consists of individual hard-braking events, each of which has the following information: GPS location, timestamp, and speed. A hard-braking event is classified by the occurrence of a deceleration greater than 2.67 m/s^2 (defined by OEM).

2.2.7 Interstate Congestion: I-70

Reduced interstate capacity due to construction on I-70 resulted in a significant rise in congestion in the EB direction of travel, specifically in the region of MM 91-96, for weekdays in the 9-day period beginning August 10^{th}, 2020. Figure 9a shows a series of speed profile heat maps for the weekdays beginning August 3^{rd} and ending August 14^{th}. Hard-braking events are indicated by red circles while crash incidents by white circles. Recurring congestion with hard-braking events at the back-of-queue can be observed beginning August 10^{th}. Figure 9c depicts traffic conditions captured by an ITS camera situated at I-70 MM 93.1. Free flow conditions are observed the week before congestion (i), followed by substantial queuing during the construction period (ii-iii), followed by traffic returning to free flow conditions once construction terminates (iv).

Figure 10a shows a map of the study area east of Indianapolis, IN. A 5-mile stretch of interstate I-70 between exits 91 and 96 highlighted in red shows the region that observed recurring congestion beginning August 10^{th}. Due to this interstate congestion, a number of vehicles likely diverted away from I-70 to the parallel US-40 (indicated by the southbound translucent grey arrowhead). Additionally, motorists on I-465 who may have seen ITS messages warning of conditions on I-70, may have chosen to divert onto US-40 and then merge onto I-70 (indicated by the eastbound translucent grey arrowhead).

2.2.7.1 Trajectory-based Interstate Performance Measures

2.2.7.1.1 Travel Times and Diversion Rates

Using the anonymized trajectory identifier mentioned earlier, a vehicle's entire trajectory could be tracked as it passed through the region of congestion on I-70. This enables the computation of diversion rates and travel times (Figure 9b). Trajectories were captured just before exit 91 so as to only capture travel times over a consistent stretch of I-70 EB starting at MM 90 and ending at MM 99. For all the analyzed trajectories on I-70 EB, average travel time increased by over 102% between the week before (August 3rd – 7th: 10.7 minutes) and during the congestion (August 10th – 14th: 21.7 minutes). 3% of all analyzed trajectories were observed to have taken an alternative route by diverting off of I-70 and rejoining the interstate using the entry ramp at MM 96 during the week of congestion. These CV trajectories showed 8% lower travel times on average than those that stayed on I-70.

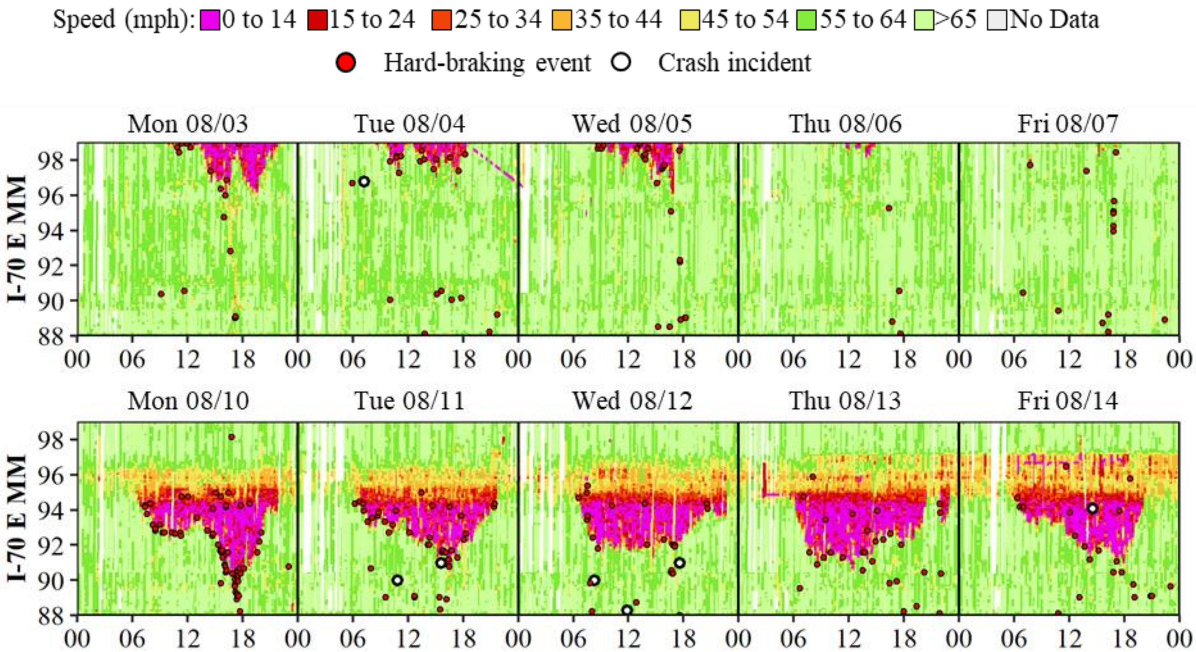

(a) I-70 EB MM 88-99 speed profile heat maps for the week before and during congestion: August 3 – August 14, 2020

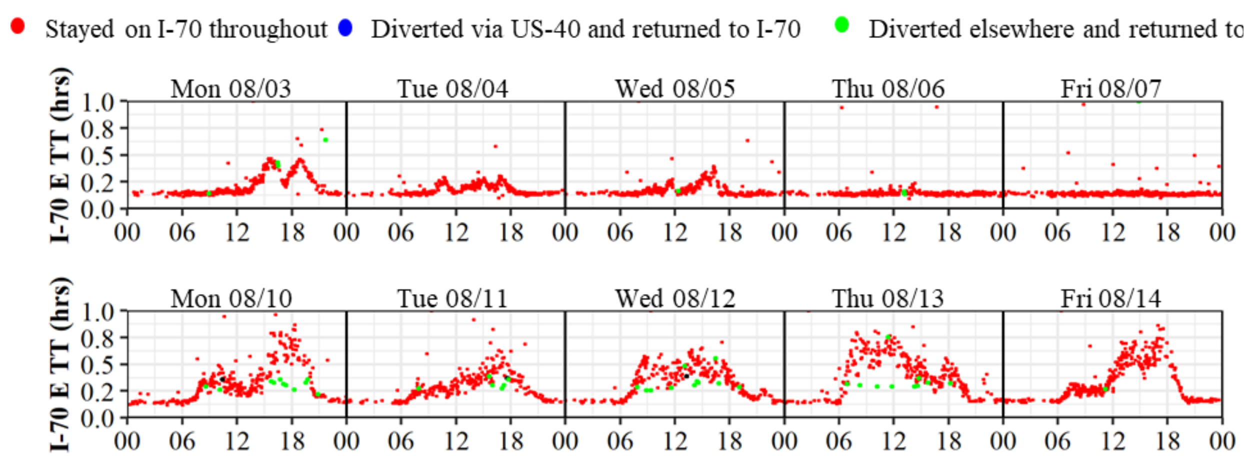

(b) I-70 EB travel times for MM 90-99 for the week before and during congestion: August 3 – 14, 2020

(c) I-70 EB Congestion as seen on INDOT Traffic Camera at MM 93.1 at noon on (i) August 3 (ii) August 13 (iii) August 17 and (iv) August 24, 2020

Figure 9. Interstate Congestion and Travel Times on I-70

2.2.7.1.2 Mile-hours of congestion

Previous studies have defined congested conditions as lengths of interstate roadway operating below a speed threshold of 45 miles per hour (mph) [56], [57]. Figure 10b shows a stacked bar representation of the mile-hours of congestion on I-70 EB by hour of day, computed by summing lengths of quarter-mile segments where median speed of trajectory data points over an hour dipped below 45 mph. An increase of 437% in average mile-hours of congestion per day was observed from the week before (August 3^{rd} – 7^{th}) to the week during the congestion (August 10^{th} – August 14^{th}) on I-70.

Figure 10c shows the number of unique trajectories that traversed US-40 from Post Road (I1) to S 600 W (I12) during the same time period. While the pre-construction period from July 6 – August 8 observed an average of 96 trajectories per weekday on US-40, the period of I-70 congestion from August 10 – August 18 showed an average of 182 trajectories per weekday on the same stretch of US-40. This clearly points to diverting trajectories from I-70 resulting in an increase in sampled volumes on US-40. It is visually discernible from Figure 10b and Figure 10c, that during the week of congestion, peak mile-hours of congestion observed on I-70 in the evening hours of 15:00 to 19:00 show a corresponding rise and thus a direct impact in sampled vehicle volumes on US-40.

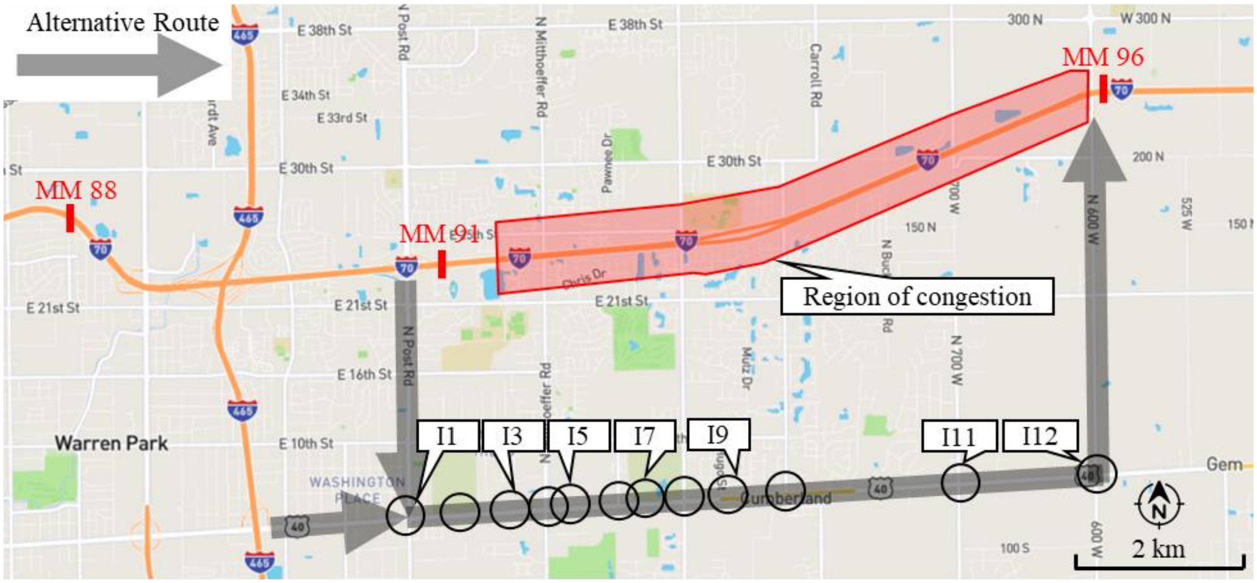

(a) Study location showing region of congestion on I-70 and alternative routes on US-40

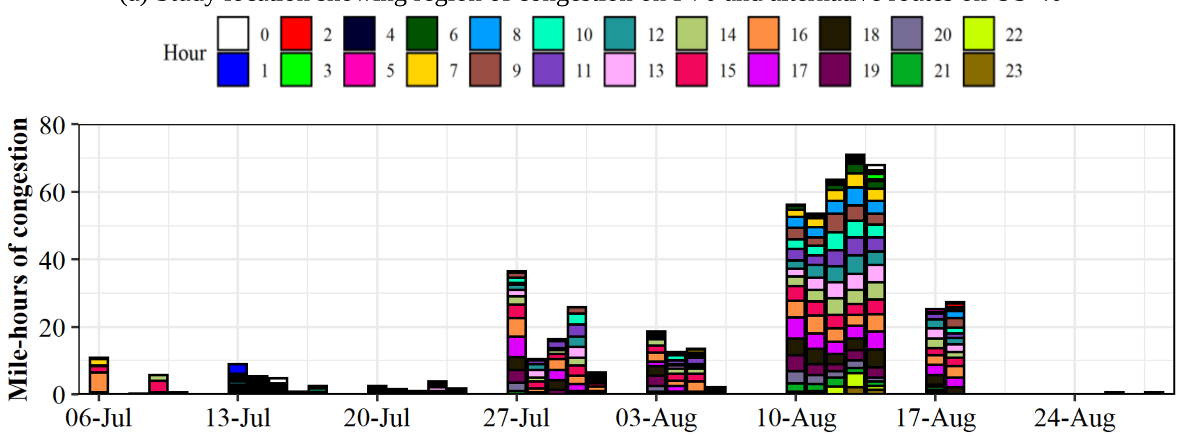

(b) Mile-hours of congestion on I-70 EB MM 88-99 by hour of day for weekdays in July 6 – August 28 2020

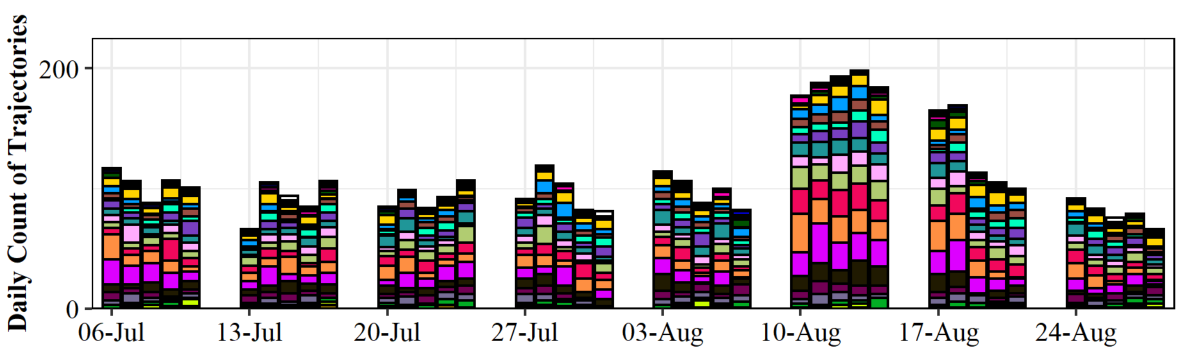

(c) Unique trajectory counts on US-40 EB (Post Road to S 600 W) by hour of day for weekdays in July 6 – August 28 2020

Figure 10. Region of congestion and impact on alternative route sampled volumes

2.2.8 Alternative Route: US-40

Increased volumes on US-40 due to diversions have the potential to negatively impact traffic signal operations. The week before congestion on I-70 (August 3rd – 7th) there were only 490 unique CV trajectories traveling EB from Post Rd. (I1) to S 600 W (I12). In contrast, during the week of congestion (August 10th – 14th) 940 unique CV trajectories completed the same trip, which represents a 92% increase in sampled connected vehicle volume. During the peak of congestion, which occurred on August 8 between 17:00 and 18:00, there was a 115% increase on sampled CV EB volume on US-40 when compared to the previous week. Additionally, for the same period, travel time on the corridor increased by 16%, and critical intersections along US-40 experienced an increase of approximately 1175% in split failures. The following sub-sections analyze the impact that the increased sampled volumes had on traffic signal operations.

2.2.8.1 Trajectory-based Traffic Signal Performance Measures

The methods used in this study to estimate traffic signal performance for the EB through movements on US-40 are based on [58], [59]. Four different metrics are analyzed: split failures (SF), arrivals on green (AOG), downstream blockage (DSB), and the traditional Highway Capacity Manual level of service (LOS) categories based upon control delay [60].

2.2.8.1.1 Split Failures

A split failure is an indication of an approach operating at over capacity. It occurs when a traffic signal does not provide enough green time to discharge the current queue, resulting in vehicles having to wait for longer than one cycle-length. Split failures are identified from CV trajectory data when a vehicle stops more than once before crossing through the intersection.

Figure 11a and Figure 11b graphically show the percentage of vehicles experiencing split failures, for the different analyzed intersections, by time-of-day, when traveling EB through on US-40 for the week before and during the congestion on I-70. It can be appreciated that German Church Rd. (I8) had the highest increase in the percentage of vehicles experiencing split failures (31%) between 16:00 and 18:00 (callouts i and ii). To further analyze the operational state at this location, Purdue Probe Diagrams (PPDs) for the same periods are shown on Figure 11c and Figure 11d [58], [59]. Additionally, Figure 12 shows the percentage of trajectories, by number of stops, for vehicles traveling EB through at German Church Rd. for the weekdays between July 6th and August 28th, where the daily increase on split failures due to congestion can be appreciated.

For all the analyzed intersections on US-40, there were over 430 additional split failures (872% increase) between the week before (August 3rd – 7th) and during the congestion (August 10th – 14th) on I-70.

2.2.8.1.2 Arrivals on Green

AOG has been traditionally utilized to assess the level of progression. A CV trajectory is characterized as AOG when the vehicle does not stop when crossing through the intersection.

By comparing Figure 11c and Figure 11d, it can be appreciated how the percentage of vehicles arriving at the intersection during green (no stops) drops from 71% to 33% at German Church Rd. between the 16:00 and 18:00 hrs. The variation on AOG for this location, for all weekdays between July 6th and August 28th, can be seen on Figure 12.

For all the analyzed intersections on US-40, there was a 2% decrease on AOG between the week before (August 3rd – 7th) and during the congestion (August 10th – 14th) on I-70.

2.2.8.1.3 Downstream Blockage

As defined in [58], [59], downstream blockage helps identify locations where adjacent intersections obstruct the progression of vehicles. A CV trajectory can be attributed as having downstream blockage by calculating the experienced delay after crossing the far side of the intersection.

For all the analyzed intersections on US-40, there were over 240 additional trajectories with downstream blockage (220% increase) between the week before (August 3rd – 7th) and during the congestion (August 10th – 14th) on I-70.

2.2.8.1.4 Level of Service

LOS provides a description of the operating conditions at an intersection based on control delay [58]–[60]. For German Church Rd. between the 16:00 and 18:00 hrs. (Figure 11c and Figure 11d), it can be seen how trajectories start with a longer time to the intersection's far side during the week of congestion on I-70 compared to the week before. This is an indication of vehicles experiencing longer delays. There was a 40 second weighted average increase on control delay between Figure 11c and Figure 11d, resulting in a change on LOS from B to E.

For all the analyzed intersections on US-40, there was a change on the corridor LOS from A to B between the week before (August 3rd – 7th) and during the congestion (August 10th – 14th) on I-70.

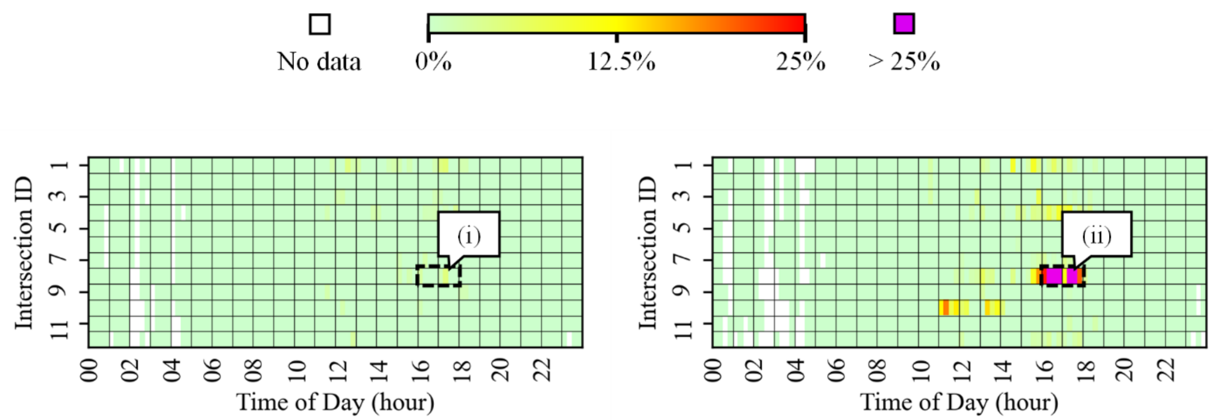

(a) Percentage of vehicles experiencing split failures before the week of congestion: August 3-7, 2020

(b) Percentage of vehicles experiencing split failures during the week of congestion: August 10-14, 2020

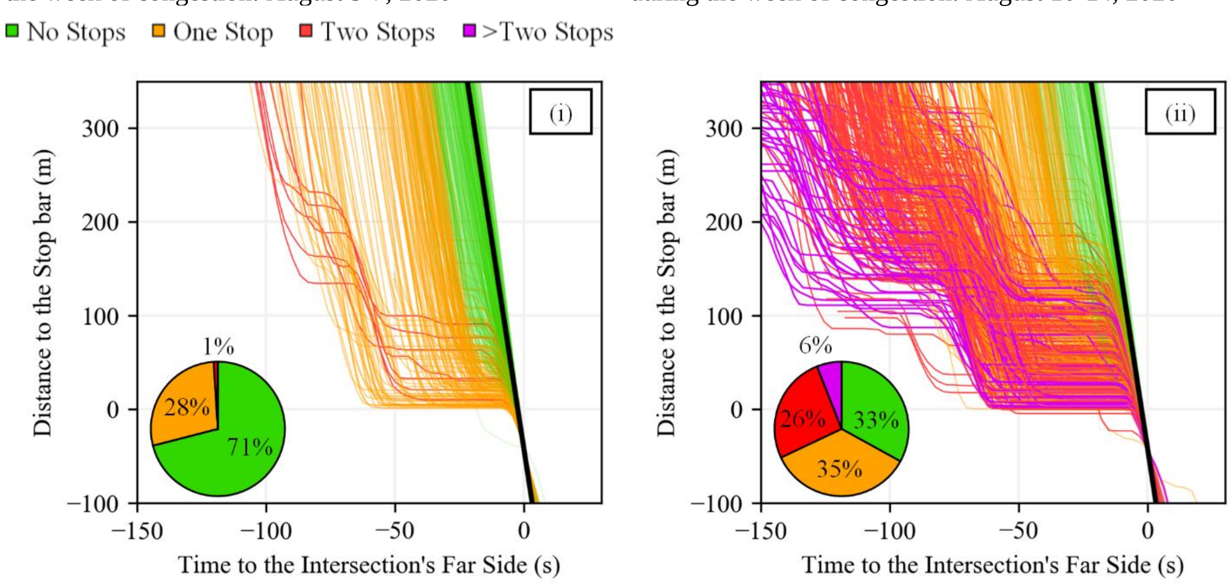

(c) German Church Rd. PPD before the week of congestion: August 3-7, 2020 between 16:00 and 18:00

(d) German Church Rd. PPD during the week of congestion: August 10-14, 2020 between 16:00 and 18:00

Figure 11. Corridor-wide split failures and PPDs at German Church Rd. (I8) longitudinal comparisons for vehicles traveling EB through on US-40

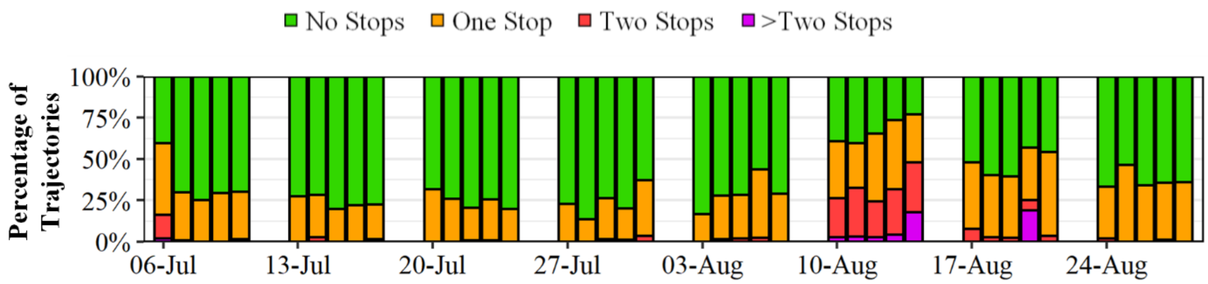

Figure 12. Percentage of trajectories by number of stops for vehicles traveling EB through at German Church Rd. (I8)

2.2.9 Summary

This study analyzed CV trajectory and event data for weekdays in a two-month period spanning July 6th to August 28th, 2020, to understand the impact of interstate construction work zone diversions on traffic signal performance measures on an adjoining 12-intersection arterial corridor.

CV trajectory data with waypoints available every 3 seconds enabled travel time and diversion rate analysis on I-70, showing a 102% increase in travel times and 3% diversion rate during the week of congestion. Correspondingly, the adjoining US-40 corridor observed a 92% increase in sampled volumes with travel times increasing by as much as 16% during peak congestion on I-70. Analysis of traffic signal operations on the 12-intersection corridor with trajectory-based traffic signal performance measures showed the impact the interstate construction diversions had on the adjoining arterial, namely, an 872% increase in trajectories experiencing split failures, 2% decrease in AOG, 220% increase in trajectories experiencing downstream blockage and a degradation of the corridor LOS from A to B.

The analysis, methodology, and results discussed in this study can potentially assist agencies and contractors when planning future construction activity and recommending alternative routes to the traveling public. With increasing penetration rates and widespread availability, the use of connected vehicle data provides a viable path forward for agencies by removing any spatial constraints that may be imposed by traditional ITS sensors and affords them the freedom to scale these methodologies to any interstate construction project in the United States.

The methods presented in this chapter for using CV trajectory or segment-based data at-scale towards monitoring freeway and arterial mobility in near real-time will provide agencies with valuable ground-level feedback and operational insights into traffic behavior, without any additional investment in fixed ITS sensor infrastructure.

3. IMPACT OF SECONDARY CRASHES ON INTERSTATE MOBILITY IN INDIANA

The details presented in this chapter have been published in “Using Connected Vehicle Data to Evaluate Impact of Secondary Crashes on Indiana Interstates” [61].

This chapter discusses the application of CV data for quantifying the mobility impact of secondary crashes on interstate roadways in Indiana for the year 2019. These methodologies developed in this work provided the foundation for the Indiana Criminal Justice Institute to invest in the Indiana Unmanned Aerial System (UAS) training program that helps agencies reduce crash clearance time. The USDOT Federal Highway Administration identified this as an EDC-5 initiative to promote nationally [62].

3.1 Overview

Interstate crashes often result in significant queuing, which can lead to secondary crashes in or at the back of the queue. These secondary crashes are of national concern and their occurrence and duration of traffic impact can now be assessed at-scale with CV data. This chapter describes in detail a study that evaluated 195 unique incidents in 2019 that involved one or more secondary crashes. Approximately 84% of the secondary crashes led to property damage only (PDO) whereas 15% and 1% of the secondary crashes led to personal injuries (PI) and fatalities (F) respectively. This study uses commercially available connected vehicle data to assess the impact of these secondary crashes on Interstate mobility using metrics such as event duration time and road closure time. The connected vehicle data for events longer than 2 hours showed that 29% of evaluated incidents had a total road closure and 30% of incidents over 2 hours had event duration longer than 5 hours. This study summarizes the mobility impacts of secondary crashes on Indiana Interstates and provides foundational data for agencies to invest in public safety training to accelerate incident clearance to reduce secondary crashes.

3.2 Introduction

More than 36,000 fatal crash incidents occurred in the United States in 2019 according to estimates from the National Highway Traffic Safety Administration (NHTSA) [63]. Crash incidents often result in reduced speeds of traffic flow, closure of a lane or entire road for incident clearance and queueing in some cases. These queuing conditions often lead to secondary crashes. The Federal Highway Administration (FHWA) termed secondary crashes as crashes that would not have occurred unless preceded by an earlier one in close proximity [64]. Possible causes of secondary crashes include rapidly growing queues caused by the primary crash and rubbernecking by motorists. These secondary crashes pose a serious safety hazard on roadways and are a growing safety concern for agencies nationwide. Additionally, secondary crashes may also prevent first responders from reaching the scene of the primary crash. This study utilizes statewide connected vehicle data and crash data to evaluate the impact of secondary crashes on Indiana Interstates during 2019.

3.3 Literature Review

Freeway congestion delays can be of recurrent or nonrecurrent type. The latter are caused by accidents, breakdowns, weather effects or road debris among other causes. It is estimated that 40%-60% of nonrecurrent freeway delays are caused by crash incidents [65]–[66]. These nonrecurrent congestion instances can lead to impacts on safety and mobility by reducing freeway capacity and adding to travel time uncertainty. In some instances, it can lead to a secondary crash in or at the back of the queue [67]. A three-year study of interstate crashes showed that the congested crash rate on Indiana's interstates was 24 times higher than the crash rate under uncongested conditions [68]. While existing literature on the impact of secondary crashes is sparse, multiple attempts have been made in the past to identify secondary crashes occurring as a direct result of one or more primary crash incidents. Sensor data have been employed in the past on designated sections of freeways to identify secondary crashes [69]. An analysis of crash reports on urban arterial roadways in a metropolitan region in Illinois postulated that a primary and subsequent secondary crash may be related if the incidents occurred within 15 minutes and 1 mile of each other [70]. More advanced dynamic methods including spatiotemporal crash impact analysis, incident filtering, loop detector data among others, were also developed to identify freeway sections affected by crashes and the likelihood of secondary crash occurrence within that region [71]–[72].

Emerging connected vehicle data presents practitioners with a unique opportunity to accurately assess system-wide performance [73]–[74] without the need for extensive intelligent transportation system (ITS) sensor infrastructure. Recent studies have shown how connected vehicle data can be used by state agencies for independent validation of interstate queues, analyzing traffic impacts [75] and determining speed limit compliance in work zones [76]. Research analyzing hard-braking behavior in interstate work zones observed a crash incident occurring for every 150 hard-braking events per mile of interstate roadway, a majority of which would naturally be expected to occur within or at the back of a queue [77].

The FHWA's Traffic Incident Management (TIM) performance measurement initiative reported that for every minute that a primary crash scene is not cleared, the likelihood of a secondary crash occurring, increases by 2.8% [78]. Logistic regression models developed using a five-year incident database from the Borman Expressway showed that the clearance time of a primary crash is statistically significant in determining the likelihood of occurrence of a secondary crash [67]. However, there are very limited studies that use connected vehicle data to quantify incident clearance and road closure times on a macroscopic scale rather than on designated sections of freeway that may be bound by spatiotemporal sensor or data constraints.

3.4 Objectives

The objective of this study is to propose a methodology by which CV data can be leveraged to assess the impact of secondary crashes on interstate mobility. This study used commercially available CV data to examine the year-round impact of secondary crashes on interstate routes in the state of Indiana. The quantitative data produced from this study can then be used by state transportation agencies to make a case to invest in public safety training to accelerate incident clearance to reduce secondary crashes.

3.5 Study Location

Seven primary interstate routes operating north-south (I-65, I-69) and east-west (I-64, I-70, I-74, I-90, I-94) in addition to three auxiliary interstate routes operating as beltways and bypasses (I-465 around Indianapolis, I-469 around Fort Wayne and I-265 around Louisville) together comprise the study area as shown in Figure 13. This study looked at connected vehicle speeds and crash incidents on over 2500 centerline miles (4023 kilometers) of the aforementioned routes over 2019. Interstate 275 (I-275) was not included due to its limited 3-mile length in Indiana.

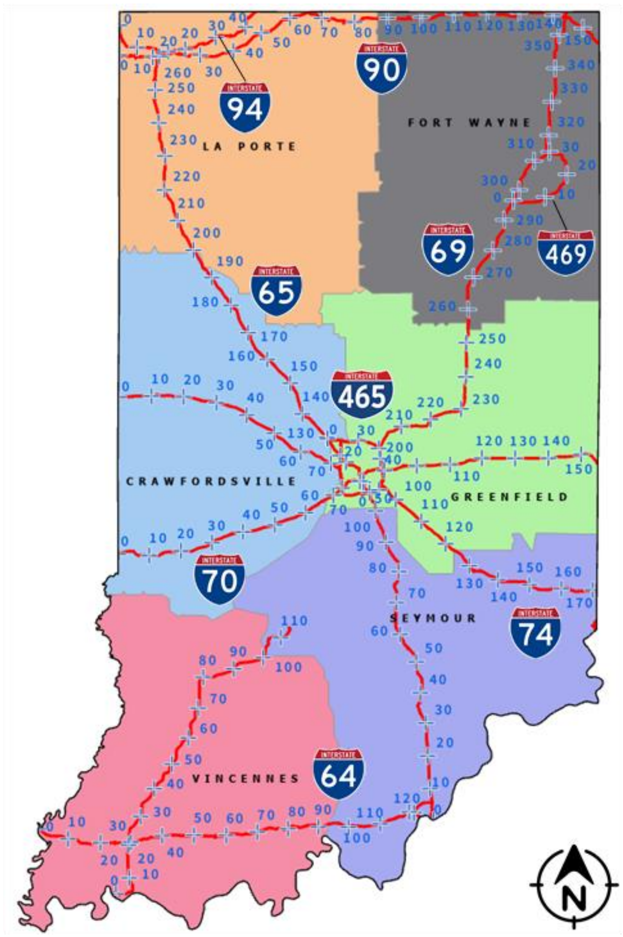

Figure 13. Study Location

3.6 Data Description

High fidelity CV speed data coupled with crash data were utilized for this study. This section describes the data sources and attributes in detail.

3.6.1 Speed Data

Commercially available CV data [79][80] was analyzed during this study. CV data provides speed records at one-minute intervals for a roughly 1-mile stretch of interstate segments by direction of travel. The speed data is categorized into 7 different speed bins to isolate congested conditions from uncongested. This categorized speed data is subsequently used to generate spatiotemporal speed profiles, alternatively known as speed profile heatmaps, an example of which is shown in Figure 14. The horizontal axis represents the hour of the day whereas the vertical axis represents the mile marker along Interstate 65 (I-65) in the southbound (SB) direction. An arrow is shown on the figure indicating direction of travel for vehicles represented in the figure. These speed profile heatmaps were used as the primary screening tool to assess and document the impact of secondary crashes on Indiana's interstates.

3.6.2 Crash Data

Crash data classified by its severity type i.e. property damage only (PDO), personal injury (PI) and fatality (F) were extracted from the state of Indiana's online repository [68]. Any personal or identifying information was omitted from the crash data. The timestamp and geolocation of a crash record were utilized to analyze them in conjunction with speed data. An additional layer of crashes was overlaid on the speed profile heatmaps, pointed to by callouts P, i and ii on Figure 14.

3.7 Methodology

A comprehensive evaluation of all crashes during 2019 was followed by segregating incidents that had impacts longer than 2 hours and had one or more secondary crashes. If a crash had occurred within the congested influence region of another preceding crash upstream, it was flagged for additional human confirmation using the speed profile heatmap. If confirmed by human inspection, the primary and secondary crashes were entered into our analysis data set. For all identified incidents, event metrics were computed as described below.

3.7.1 Event Metrics

3.7.1.1 Event Duration Time

The total duration for which traffic was impacted starting from the time of the primary crash and lasting until congestion dissipates was defined as the Event Duration Time (Figure 14, dimension a). A section of interstate was considered to be congested if it was operating at speeds below 45 mph, a common threshold established in existing literature [80], [81].

3.7.1.2 Road Closure Time

The duration for which no speed data was recorded by the heatmap due to a total road closure in effect was defined as the Road Closure Time. It generally starts after the primary or secondary crash has occurred and around the crash location, identified as a no data block on the speed profile heatmap. The road closure duration is determined by computing the duration of time that no connected vehicles were traversing the segment (Figure 14, dimension b).

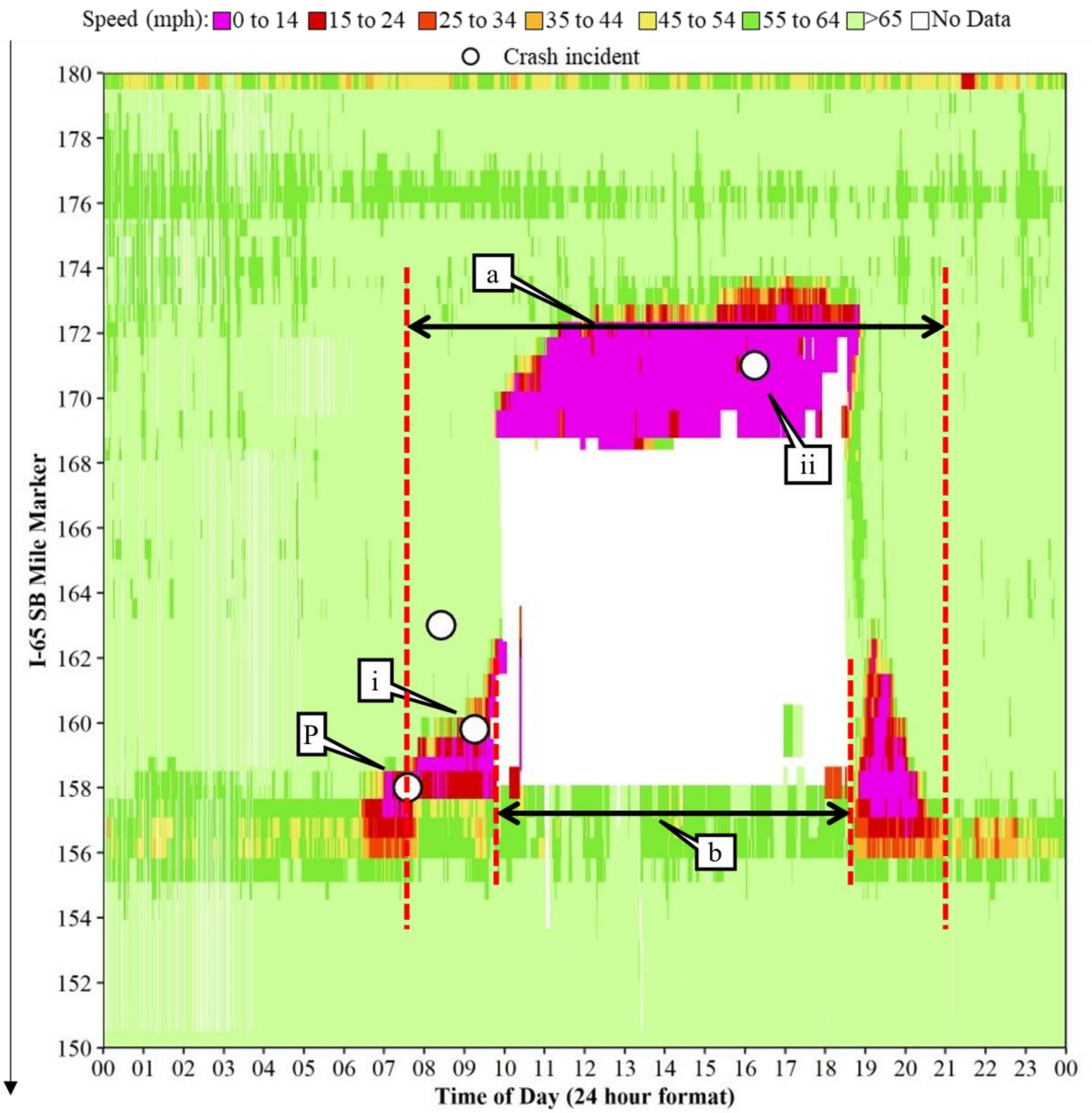

Figure 14. Speed Profile Heatmap for I-65 Southbound on September 12, 2019 showing 24 hours of average segment speed over 30 miles as well as crash time and locations

3.7.2 Incident Example

A primary crash and two secondary crashes occurring on I-65 on Thursday, September 12, 2019 are depicted as a representative sample incident in Figure 14. A 30-mile section of I-65 in the southbound (SB) direction of travel from mile marker (MM) 150 to MM 180 is shown. Callout P shows the primary crash that occurred in the vicinity of MM 158 at 7:35 AM. The primary crash led to downstream traffic congestion resulting in the formation of a queue. The first of two secondary crashes occurred at 9:15 AM at the back of the queue (callout i), followed by another secondary crash occurring inside the queue forming behind the total road closure at 4:15 PM (callout ii). This incident resulted in a total Event Duration Time of 13 hours and 25 minutes (callout a) and a total Road Closure Time of 8 hours and 45 minutes (callout b).

3.8 Mobility Impact Analysis

A systematic review of all interstate crashes in 2019 resulted in the identification of 195 unique incidents that satisfied the pre-defined criteria of exhibiting at least one secondary crash and an impact on traffic of 2 hours or more. A comprehensive analysis of these 195 incidents (involving 203 primary crashes and 358 secondary crashes) using the prescribed event metrics, further revealed the mobility impact that secondary crashes had on the ten interstate routes under consideration.

Figure 15 shows primary and secondary crash counts categorized by their severity levels as well as the time of day. 68% of all primary crashes resulted in property damage while 29% and 3% resulted in personal injuries and fatalities, respectively. Correspondingly, 84% of all secondary crashes resulted in property damage with 15% and 1% resulting in personal injuries and fatalities, respectively. The evening hours of 16:00 to 18:00 showed a high concentration (25%) of secondary crashes over the entire year.

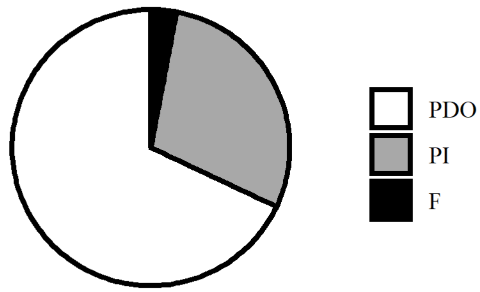

(a) 203 Primary Crashes categorized by severity

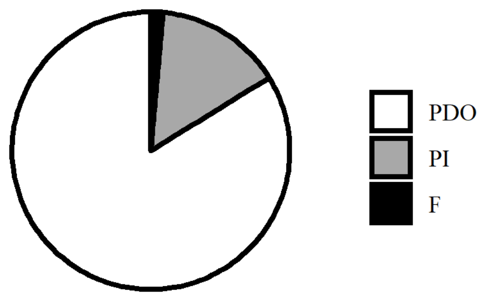

(b) 358 Secondary Crashes categorized by severity

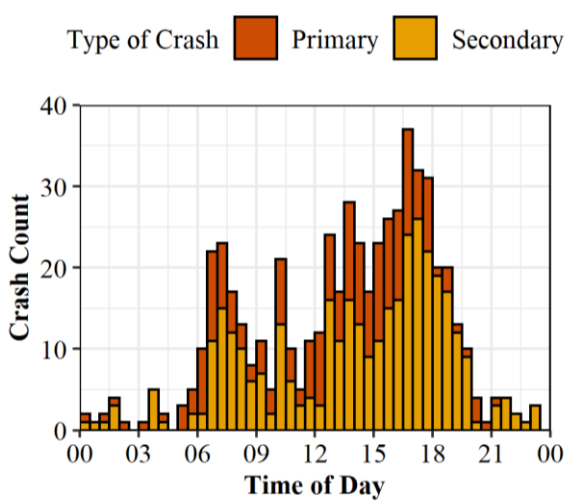

(c) Primary and Secondary Crashes by Time of Day

Figure 15. Crash Data by Severity and Time of Day

As a means of spatially visualizing crash incident hotspots around the state, the entire study location was split into 10-mile segments by interstate route and direction of travel. Figure 16 highlights each such segment with the radius of the circular blue marker scaled by the total crash count (primary and secondary) observed at the location. Five locations that observed greater than 10 secondary crashes during 2019 were I-94 westbound (WB) MM 0-20, I-465 outer loop (OL) MM 0-10, I-69 northbound (NB) MM 300-310, and I-94 EB MM 0-10. A number of these hotspots were located on urban interstates and near the Indiana-Illinois state borderline. This spatial map can potentially provide agencies with valuable input in allocating queue management and scene clearance resources.

Figure 16. Crash locations on Indiana Interstates (10-mile segments by direction of travel)

With road closure times ranging from zero to 8 hours 45 minutes as shown by the cumulative frequency diagram in Figure 17a, it was seen that 29% of incidents observed a non-zero duration of road closure (callout i). Correspondingly, event duration times ranged from a lower limit set at

2 hours to 13 hours 53 minutes, with 30% of all incidents showing event duration times longer than 5 hours (callout ii). It naturally follows that the range of event duration times would be significantly higher than the road closure times.

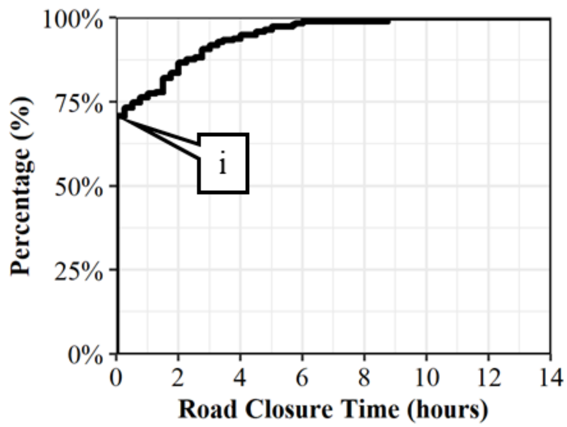

(a) Cumulative Frequency Diagram of Road Closure Time (hours)

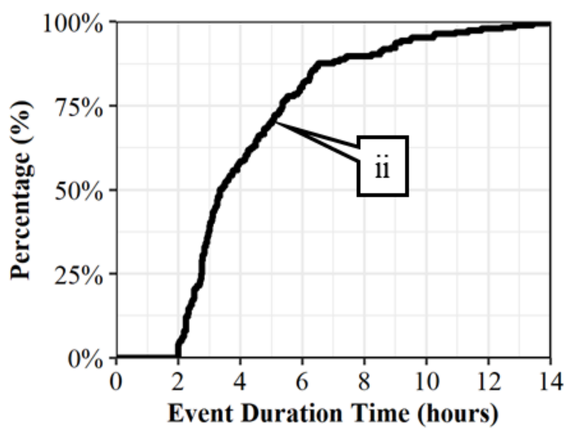

(b) Cumulative Frequency Diagram of Event Duration Time (hours)

Figure 17. Event metrics summary

Table 2 shows an overall summary of the mobility impacts of secondary crashes categorized by the 10 interstate routes analyzed in this study. I-65 experienced the highest average total road closure time of 3 hours and 27 mins while I-94 observed the highest average event duration time of 5 hours and 31 minutes. 57 incidents involved a total road closure with closures being in effect for an average of 2 hours and 33 minutes.

Table 2. Summary of 2019 Incidents by interstate route

Interstate	**Length (mi)**	**Total Number of Primary Crashes**	**Total Number of Secondary Crashes**	**Number of Incidents with Road Closure**	**Average Road Closure Time (when closed)**	**Average Event Duration Time**
I-94	46	63	133	8	1h 17m	5h 31m
I-65	262	35	64	13	3h 27m	4h 46m
I-69	271	33	45	13	2h 13m	3h 46m
I-465	53	28	59	4	2h 38m	3h 21m
I-70	157	21	28	9	2h 37m	3h 53m
I-74	171	9	11	6	2h 02m	3h 43m
I-90	156	5	9	4	3h 38m	4h 16m
I-64	124	4	4	0	-	2h 40m
I-265	13	3	3	0	-	3h 05m
I-469	31	2	2	0	-	3h 21m
Statistics for all Interstates	1264	203	358	57	2h 33m	3h 50m

3.9 Summary

This study used connected vehicle data to evaluate the impact of 358 secondary crashes occurring over 195 unique incidents, on interstate mobility in the state of Indiana during 2019. Interstate route-level analysis of secondary crash mobility impacts presented in Table 1 showed an average road closure time of 2 hours and 33 minutes with an average event duration time of 3 hours and 50 minutes. The analysis presented depicts the significant impact that secondary crashes have on interstate travel both in terms of safety and reduced mobility. This data thus provides quantitative evidence useful for state agencies to allocate resources to public safety agencies towards accelerating incident clearance [82]. In fact, approximately 33 public safety agencies have been trained on using Unmanned Aircraft Systems (UAS) to rapidly map crash scenes. Two of the early adopting agencies have mapped nearly 50 crash scenes in the past 2 years, and together the participating agencies have mapped nearly 200 crash scenes so far.

A potential next step for this research is replacing visual inspection of speed profile heatmaps with an automated process of detecting queues building up in real-time thus enabling the generation of advance warnings to motorists as well as state agencies. The ability of connected vehicle data to identify spatial and temporal hot spots of interstate queues on a near real-time basis provides agencies with the necessary tools to actively mitigate the detrimental safety and mobility impacts of back of queue crashes.

4. CORRELATING HARD-BRAKING ACTIVITY WITH CRASH OCCURRENCES ON INTERSTATE CONSTRUCTION PROJECTS IN INDIANA

The information presented in this chapter was published in “Correlating hard-braking activity with crash occurrences on interstate construction projects in Indiana” [83].

Crash data has historically been used to identify emerging safety concerns in work zones. This chapter discusses the use of hard-braking events in place of crash incident reporting for evaluating the safety performance of interstate construction work zones. This work has resulted in INDOT institutionalizing practices to monitor week to week changes in CV hard-braking to data to identify emerging safety concerns so they can be addressed quickly [84].

4.1 Overview

The Federal Highway Administration (FHWA) reported between 2016 and 2017, fatal crashes in work zones increased by 3%, while fatal crashes outside of work zones decreased by 1.5%. The FHWA also reported that work zones account for approximately 10% of the nation’s overall congestion and 24% of unexpected interstate delays. This paper reports on a study of 23 construction work zones that covered approximately 150 centerline miles of Indiana interstate roadway in the summer of 2019. Approximately 50% of all interstate crashes for the period of May through September 2019 occurred within or in an approach upstream or downstream of one of these work zones. Commercially-available vehicle hard-braking event data is used for the study and geofenced to the work zone approaches and limits. This research examined 196,215 hard-braking events over a 2-month period in the summer of 2019 and 3,132 crashes over the same 2-month period in 2018 and 2019 for the 23 interstate work zones. The study found there were approximately 1 crash/mile for every 147 hard-braking events in and around a construction site. The R^2 was approximately 0.85. The paper concludes by recommending that hard-braking event data be used by agencies to quickly identify emerging work zone locations that show relatively large number of hard-braking events for further evaluation.

4.2 Introduction

There are approximately 800 fatal work zone crashes in the US annually, most of which occur in the summer and fall, and over 25% of those crashes involve large trucks or buses [30]. The Federal Highway Administration (FHWA) reported between 2016 and 2017 [30] fatal crashes in work zones increased by 3%, while fatal crashes outside of work zones decreased by 1.5%. The FHWA also reported that work zones account for approximately 10% of the nation's overall congestion and 24% of unexpected interstate delays [30]. Historically, crash report data has been used to identify opportunities to improve the design of future construction zones. However, the infrequency of crashes and the time it takes for personnel to read crash narratives makes it difficult and infeasible to use crash data for tactical monitoring of work zones. Furthermore, crash reports are often reported with a time delay due to associated investigation time, and the exact location and time reported in the crash reports varies by investigating agency. In contrast, hard-braking event data can be obtained daily from commercial providers with a precise timestamp and geo-location information. This paper investigates the feasibility of using hard-braking event data to identify opportunities to improve the safety and operating efficiency of construction work zones.

4.3 Literature Review

Work zone safety and mobility have been measured in the past using a variety of metrics, including number of injury crashes, motorist complaints, safety inspection scores, closure and delay times [85] and crash severity indexes [86]. Probe vehicle data has been effectively leveraged to measure travel time delays in work zones and establish correlations among crashes and queue times [87], [88]. However, crashes are often reported with a time lag and underreported due to a variety of reasons [89]–[91], including unwillingness of involved drivers to report a crash [92], or reporting delays due to ongoing investigations that may lead to a change in the documented crash severity. This can potentially hamper or render unreliable any near real-time measurement of safety performance in work zones. Moreover, not all locations with safety challenges have crashes early in the construction season to help identify problem areas. Drivers making evasive maneuvers to avoid conflicts, such as decelerating in advance of stopped traffic, have been well studied and modeled [93], [94]. Finding a way to detect near-misses before crashes accumulate can be useful to proactively develop operating strategies.

Multiple studies in the past have analyzed braking behavior and reaction times at the individual driver level in a variety of hazardous driving situations. Using simulated driving environments, hard-braking by distracted motorists was found to have significant impacts on following vehicles in traffic, increasing the risk of a rear-end collision [95]. Investigations into the use of harsh braking incidents as a surrogate for truck crash counts using truck telematics data have shown promise in identifying potential hot spots with high crash risk [96]. A 6-month study of drivers in Georgia traveling on freeways, arterials and local roads found that those involved in a crash incident tend to more frequently hard brake (8.8 ft/s^2) than those not involved in crashes [97]. An analysis of undesirable driving events such as hard braking, sharp turning and sudden lane changes showed that looking at the frequency of occurrence of such events could prove to be a valuable surrogate for determining driver behavior and accident risk [98]. Others have reported the linkages between hard-braking and driver performance, crash severity and driver fatigue [99], [100]. While existing literature has focused on driver behavior and its correlation to crash risk, we propose using aggregate hard-braking event counts as a surrogate safety measure instead of crash counts, for transportation system elements. Although this study focuses on hard-braking activity within work zones on interstate roadways, the relationship established here between hard-braking and crash incident counts encourages future research into using hard-braking as a surrogate safety measure for other elements of transportation systems as well (arterials, local roads, roundabouts).

4.4 Enhanced Probe Data

Commercial probe data that provides real time average segment speeds every minute at approximately 1-mile fidelity has been available for several years. In fact, in Indiana, the state ingests approximately 32 billion records per year and uses that data for a number of historical and real-time dashboards [57].

Enhanced probe data that contains vehicle acceleration attributes has become available in the past two years. One example of enhanced probe data generated by anonymized passenger vehicles includes the time and the latitude and longitude attribute of a hard-braking event experienced with a deceleration greater than 8.76 ft/s^2 (defined by original equipment manufacturer). As a surrogate safety measure, and when considered in aggregate form, hard-braking activity has the potential to provide timely information to agencies in evaluating the safety performance of a work zone by quantifying near-misses. However, there are no reports in existing literature of agencies using information such as hard-braking for operations-oriented management of roadways.

4.5 Objectives

The objectives of this study are:

1. To evaluate the relationship between hard-braking activity and crashes in and around Interstate construction projects in Indiana

2. To investigate causal factors for increased hard-braking activity

4.6 Data Description

4.6.1 Study Locations

The study evaluated 23 construction zones spanning 6 different interstate routes across the state of Indiana. Construction on these work zones was carried out in the summer of 2019, however crash incidents in these zones were recorded for 2018 as well as 2019 for comparing the impact of construction activity on crash frequency. Table 3 summarizes the approach start and end mile markers (MM) for each of these 23 work zones and assigns them a unique label that is used as a reference in the graphics that follow. Figure 18 shows statewide spatial distribution of 11 interstate work zones, while Figure 19 shows a distribution of the remaining 12 interstate work zones that were concentrated in the Indianapolis metro area.

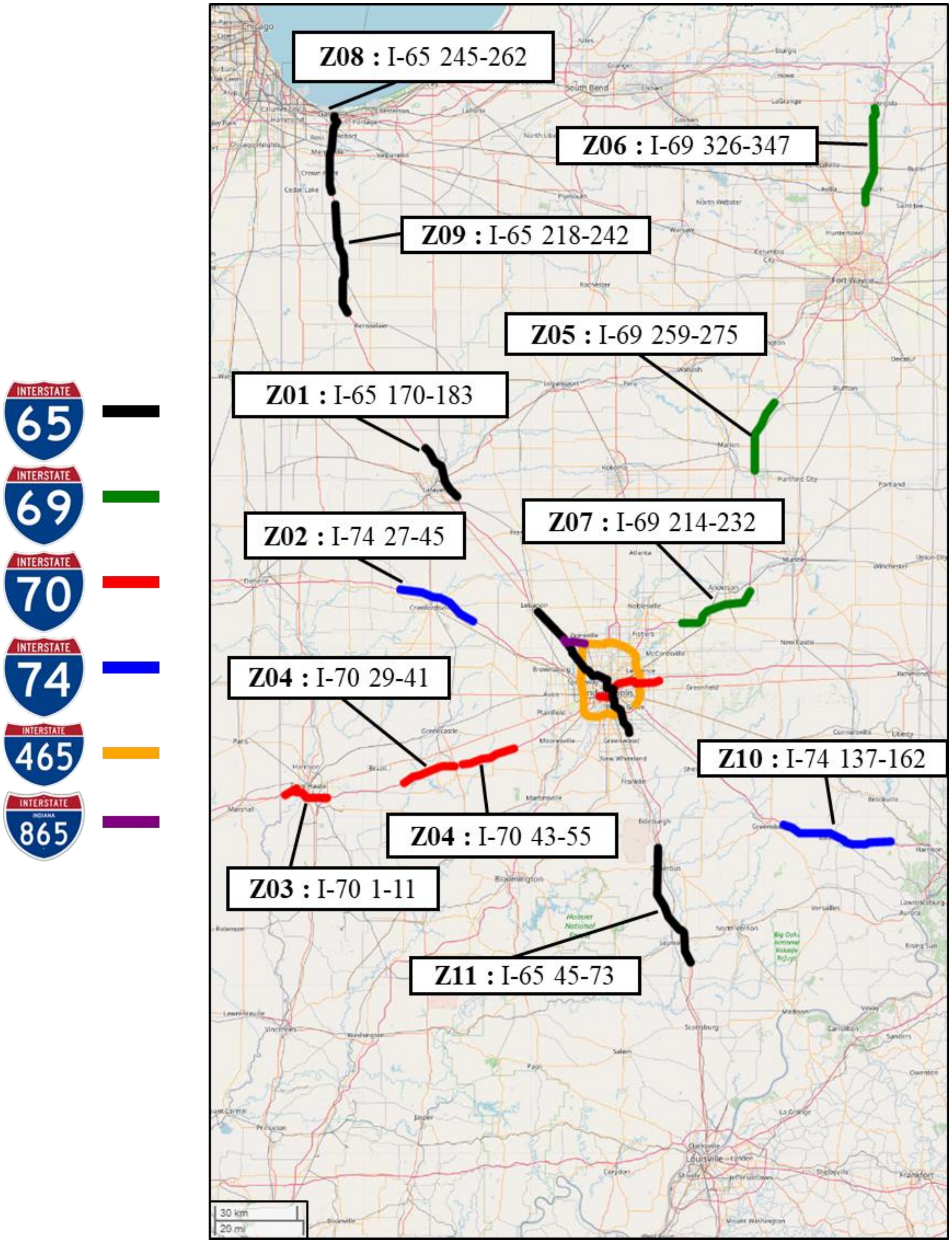

Figure 18. Statewide view of interstate work zone projects with approaches

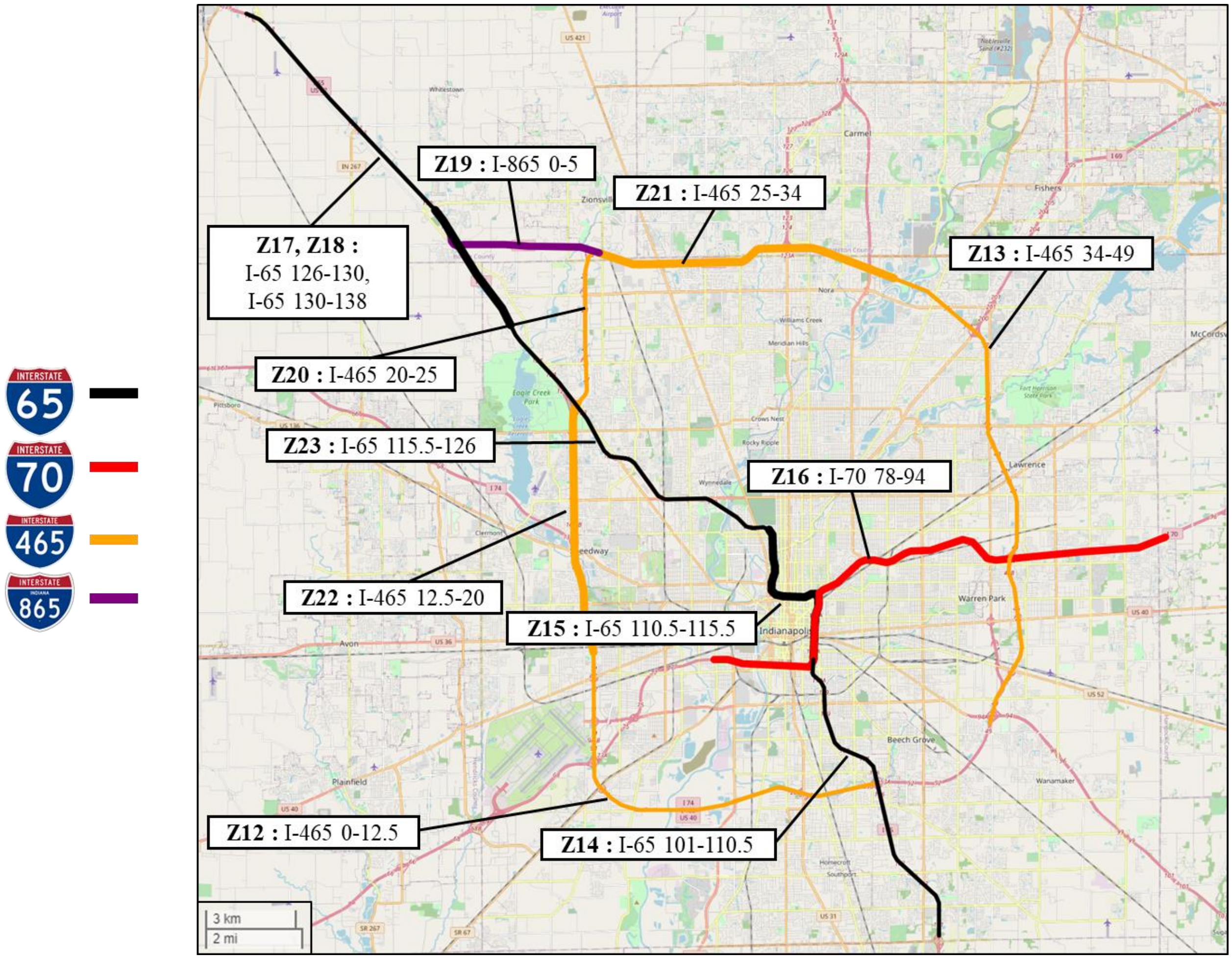

Figure 19. Indianapolis metro area view of interstate work zone projects with approaches

4.6.2 Statewide Crash Data

Crash data was aggregated from a review of all crashes in the study area. 5-mile approaches to each work zone wherever possible (both upstream and downstream) were also included in our analysis to account for tapers, transition areas and merging resulting in crashes. In addition, impact on traffic from queuing resulting from construction activity in a work zone may potentially extend well beyond a work zone's extent thus underlining the need for including approaches in such an analysis. Owing to close proximity of work zones on interstate 465, it was not feasible to include 5-mile approaches for the Z12, Z13, Z20, Z21 and Z22 work zones. To account for this, any gap (if existing) between pairs of adjacent work zones was split equally to create a lesser than 5-mile approach for both work zones. To prevent double counting of crashes on overlapping work zone approach extents, an open limit on the mile marker location for one work zone and a closed limit for the subsequent work zone were chosen. For example, hard-braking events and crash counts for Z12 were captured for MM >= 0 and MM < 12.5 while for Z22 were captured by MM >= 12.5 and MM < 20. This procedure was then applied to all cases on I-465 and I-65 where work zone limits overlapped at a mile marker location to arrive at the crash counts shown in Table 3. Table 3 shows total crash counts for both directions of each of the 23 construction work zones for the months of July and August in 2018 and 2019, along with percentage change in crash counts. Construction activities occurred in 2019 and crash data from the same two months in 2018 was used to visualize if a change in crash counts was seen between the two years owing to construction activity. An overall decrease of 2.4% in crash counts was seen over the 23 work zones for the 2-month analysis period. Comparing changes in crash counts for individual zones between 2018 and 2019, 13 work zones showed an increase in crash counts, 1 zone showed no change, and 9 zones showed a decrease in crash counts.

One of the major hurdles with using crash data as a performance measure for work zone safety is that crash reports often do not get filed in real-time, some agencies still use paper-based reporting methods, and serious crashes often require several days of investigation before reports are available online. On average, only 80% of the crash reports are available in a statewide database within one week of the crash and some crash reports take as long as 6 months to appear in the database. Thus, any real-time road safety analysis using aggregate collision counts will have an underrepresentation of crash data.

Table 3. Summary details and crash counts for areas studied from July 1 through August 31 for 2018 and 2019

Work Zone	Route	Approach Start MM	Approach End MM	July and August 2018 Crashes	July and August 2019 Crashes	% Change
Z01	I-65	170	183	32	32	0%
Z02	I-74	27	45	13	9	-31%
Z03	I-70	1	11	16	17	6%
Z04	I-70	29 – 41 & 43 - 55		25	23	-8%
Z05	I-69	259	275	14	30	114%
Z06	I-69	326	347	26	30	15%
Z07	I-69	214	232	67	81	21%
Z08	I-65	245	262	116	88	-24%
Z09	I-65	218	242	78	35	-55%
Z10	I-74	137	162	22	19	-14%
Z11	I-65	45	73	71	91	28%
Z12	I-465	0	12.5	156	129	-17%
Z13	I-465	34	49	214	217	1%
Z14	I-65	101	110.5	107	121	13%
Z15	I-65	110.5	115.5	123	125	2%
Z16	I-70	78	94	165	169	2%
Z17	I-65	126	130	5	13	160%
Z18	I-65	130	138	19	23	21%
Z19	I-865	0	5	20	16	-20%
Z20	I-465	20	25	52	54	4%
Z21	I-465	25	34	148	105	-29%
Z22	I-465	12.5	20	74	58	-22%
Z23	I-65	115.5	126	22	62	182%
			Total	1585	1547	-2.4%

4.6.3 Crash Count Comparisons

For the period of July 1 through August 31 in 2018 and 2019, crash reports were obtained and individually mapped to the 23 work zones under consideration. Across all 23 work zones for the analysis period, 2018 saw 1585 crash incidents while 1547 crashes were seen for the corresponding period in 2019. Crash counts were normalized across work zones by dividing the total number of crashes occurring in a zone by the length of the zone calculated as the difference between the approach start and end mile markers as listed in Table 3. Figure 20 shows a sorted stacked column chart of normalized crash counts for the 23 work zones compared for the period of July 1 through August 31 for 2018 and 2019. Work zones are ordered from left to right in descending order of number of crashes per mile for 2019. Each column shows crash counts per mile categorized by severity between property damage only (PDO) and personal injury (PI). Due to small numbers of fatal crashes on interstates and for privacy reasons, personal injury and fatality data in this study is combined into and referenced by the PI category. In addition, it was observed that PI crashes only account for approximately 14% of the total number of observed crashes in this study. Segregating the analysis by crash severity category would not have resulted in a good sample for the PI category to arrive at reliable results. Hence, crashes from both categories (PDO and PI) were combined and the aggregate crash count per mile was used for each work zone for the analysis described in the sections that follow.

The work zone labelled Z15 which shows the highest crash per mile value for both years, covers a 5-mile stretch of I-65 that overlaps with I-70 near downtown Indianapolis. An average percentage change of 15.24% in crash counts from 2018 to 2019 was observed across all 23 work zones. Three work zones in particular showed far higher percentage change in crash counts than this average, namely Z23 (182%), Z17 (160%) and Z05 (114%). Figure 20 highlights how the peak of the construction season resulted in an increase in crashes in most of the work zones. However, it is worth noting that 7 out of the 23 work zones (Z01, Z03, Z04, Z07, Z08, Z09 and Z11) witnessed construction activity in both years for the months of July and August. While the comparison drawn here is not a direct comparison of active and inactive work zone periods, it is instrumental in underlining the need for an efficient safety performance analysis of work zones. The underlying assumption in making this assertion is that all other external factors (such as traffic volumes, weather conditions) remained the same from 2018 to 2019. Annual growth rate of Annual Average Daily Traffic (AADT) from 2018 to 2019 averaged over all 23 work zones in both directions of travel was found to be -0.2%. The months of July and August in total observed precipitation greater than 0.01 inches on 20 out of 62 days (32%) in Central Indiana (home to 12 out of the 23 work zones) in both years [101]. Overall crash counts decreased by 2.4% for the 2-month period from 2018 to 2019. This decrease can be attributed to a number of factors including: improved early warning systems implemented by agencies and contractors for motorists, reduced vehicle volumes, underreporting and delayed reporting of crash incidents, a number of work zones that observed construction activity for both years may have resulted in learnings from 2018 contributing to better decision making and work zone design in 2019 resulting in lower crash counts.

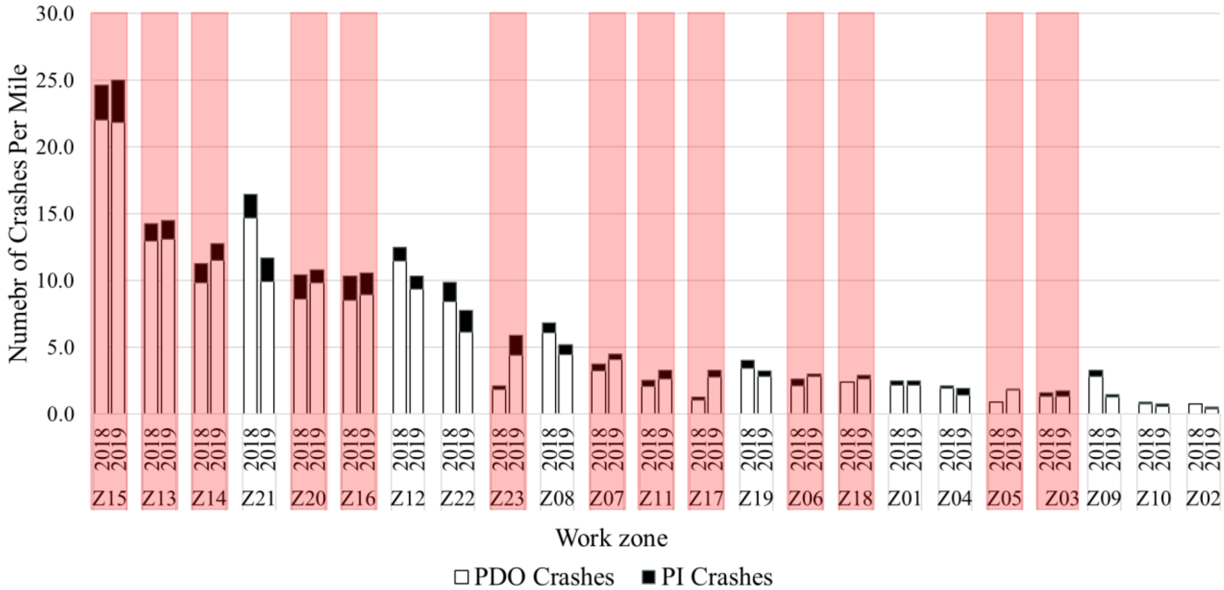

Figure 20. Crash counts normalized by work zone length and categorized by severity for 23 work zones for July 1 to August 31 for 2018 and 2019 (highlighted work zones in red indicate work zones that showed an increase in crash count from 2018 to 2019)

4.6.4 Statewide Hard-braking Data

As indicated in previous sections, there is considerable variation in the time and location of reported crashes, as well as delay in that data being available in a database. In contrast, modern connected vehicles can provide GPS location and accurate time stamps of hard-braking events. Hard-braking is an event in which a driver applies more force than is typically needed to slow or stop a vehicle using the vehicle's brake system. For this study, crowdsourced hard-braking event data for the state of Indiana was made available wherein any deceleration of 8.76 ft/s^2 or greater occurred.

For every hard-braking event, a geolocation, timestamp and speed value were provided to spatially and temporally map these events. Approximately 12.7 million unique hard-braking events were recorded throughout the state of Indiana for the period of July 1 to August 31, 2019. Figure 21 shows a statewide map summarizing spatial distribution of hard-braking event activity seen in Indiana during the months of July and August in 2019. Among these, more than 196,000 hard-braking events in total were found to have occurred over the 23 work zones as a result of spatial joins performed on the dataset to zero in on events occurring in 46 created geofences (one per direction of travel per work zone). AADT values for 2019 were compared with trip counts in each work zone for July 2019 to arrive at an average penetration of 4.7%. The third-party crowdsourced hard-braking event data showed highest penetration rates for urban interstate work zones.

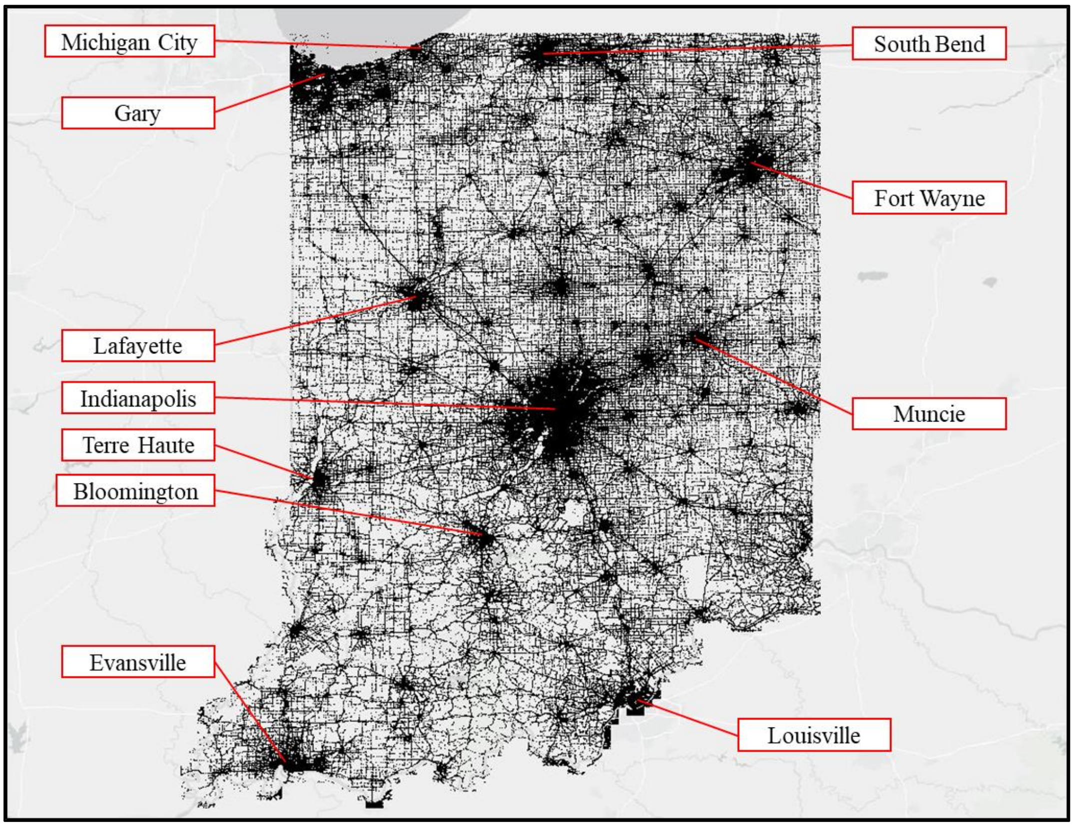

Figure 21. Plot of 12.7 million hard-braking events in Indiana for July 1 to August 31 2019

4.7 Methodology

4.7.1 Capturing Hard-braking Event Counts by Work Zone and Direction of Travel

Owing to the computational complexities involving in handling this large hard-braking dataset of 12.7 million events, matching each event individually to its nearest interstate location was infeasible. Similar hard-braking event counts available for the month of August 2020 for 11 states

– California (25,441,595), Connecticut (2,048,510), Georgia (8,704,155), Indiana (6,683,366), Minnesota (3,254,094), North Carolina (6,546,877), Ohio (10,012,453), Pennsylvania (9,831,815), Texas (26,300,993), Utah (948,931) and Wisconsin (4,049,073), underlined the need for a quicker procedure for capturing hard-braking activity at specific locations on roadways of interest. Owing to this, an alternate approach was developed wherein 46 separate geofences were created to spatially outline the area for every work zone analyzed in this study in two directions of travel. From the statewide dataset of hard-braking events shown in Figure 21, spatial joins were then used to effectively narrow down the hard-braking dataset to events that occurred within the virtual perimeter defined by any of the 46 geofences mentioned earlier. A temporal join was next applied to this dataset to further narrow down the events to those that occurred within the period from July 1 through August 31, 2019. Callout (i) on Figure 22 shows such a set of geofenced polygons capturing hard-braking events on I-65 in the northbound direction of travel in the vicinity of mile marker 102. Each hard-braking event represented by a colored dot on Figure 22 has been colorized by the initial speed recorded in miles per hour at the time of hard-braking. When this procedure was repeated individually 46 times for each work zone by direction, the dataset of 12.7 million hard-braking events was narrowed down to the 196,215 hard-braking events used for the analysis in this study.

Figure 22. Geofenced polygons showing hard-braking events colorized by initial speed in miles per hour on I-65 in the northbound direction of travel in the vicinity of mile marker 102

4.7.2 Visualizing Relationship between congestion, crashes and hard-braking events

Figure 23 (a) shows a spatial and temporal heatmap of traffic speeds for the period of July 1 through August 31, 2019 for a nine and a half mile stretch of I-65 northbound from MM 101 – 110.5. Work zone Z14 makes up the stretch of I-65 depicted in the heatmap in Figure 23 (a).

The legend at the top shows the color for speeds ranging from greater than 65mph (green) to less than 14 mph (purple). The heatmap is generated from commercially available probe data consisting of average vehicle speeds for 1-mile interstate segments at 1 minute fidelity [102]. This visualization easily helps segregate recurring congestion from non-recurring events as highlighted by red dashed lines in Figure 23 (a). For the 2-week period beginning August 12, 2019, significant weekday recurring congestion can be seen between mile marker 106 and 110 (Work zone Z14) in the northbound direction of travel.

Crashes are shown on the heat map in Figure 23 (a) as circles. Property damage (PDO) crashes are indicated by hollow circles, while personal injury (PI) crashes are indicated by gray circles. Figure 23 (b) shows a stacked bar graph tabulation of the number of crashes occurring each day using the same color grey shading as the circles in Figure 23 (a), with elevated crash counts for the 2-week period starting August 12, 2019 highlighted by red dashed lines.

Hard-braking event counts by day for this stretch of I-65 northbound are shown in Figure 23 (c) with the corresponding region of elevated crash counts and congestion highlighted by red dashed lines. It can clearly be seen from Figure 23 (a), (b) and (c) how hard-braking activity clusters correspond to regions of elevated crash counts and congestion.

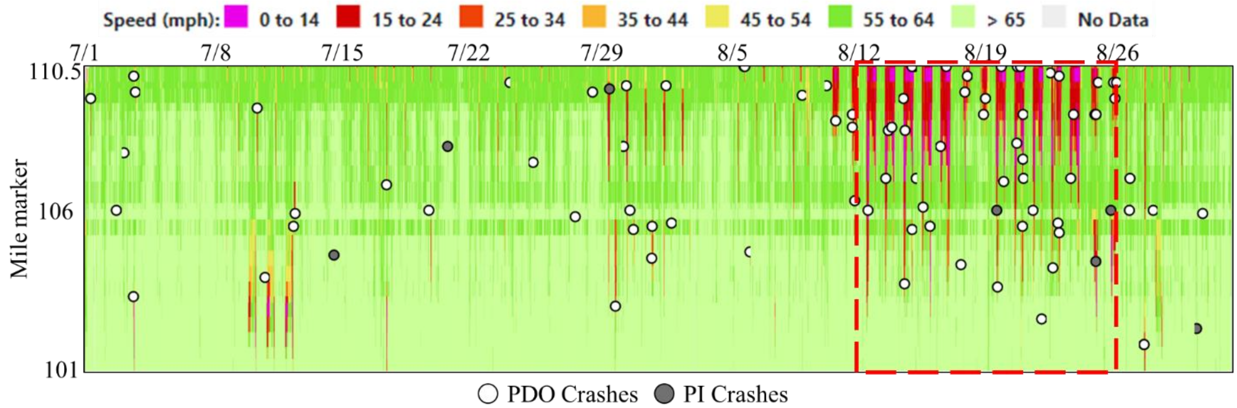

(a) Spatial-temporal heat map showing speed profiles by mile marker and day

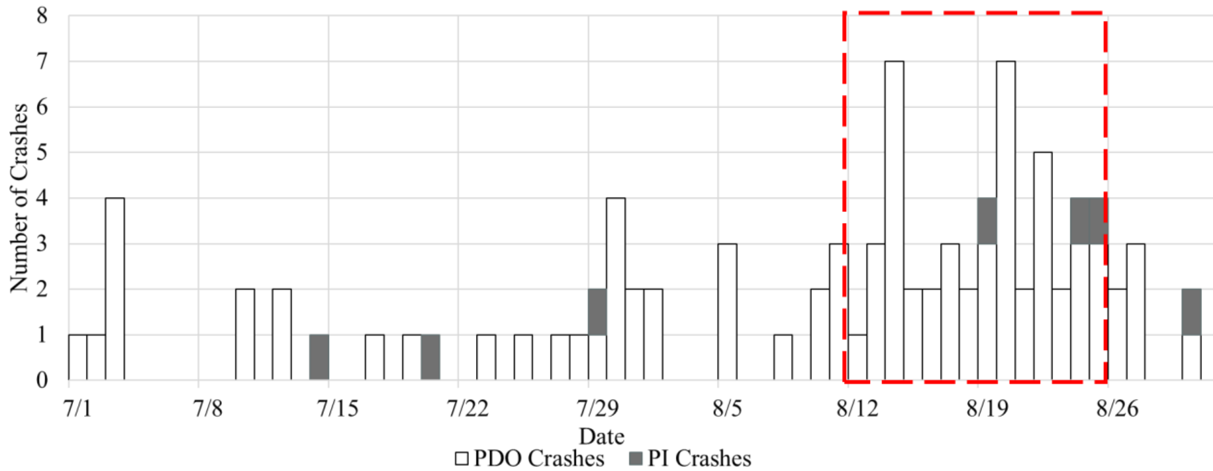

(b) Crash count column plots stacked by severity

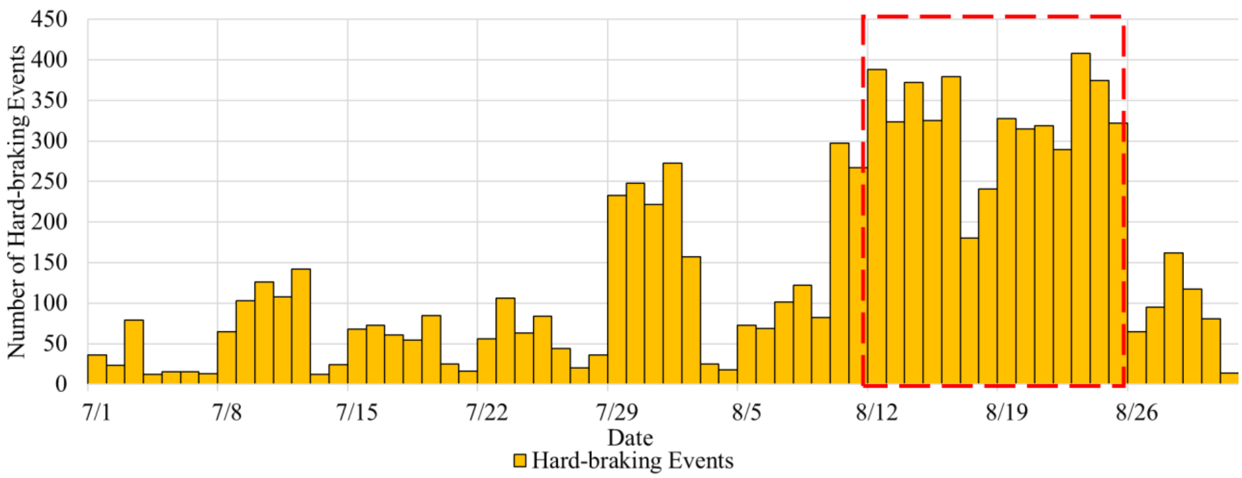

(c) Hard-braking events by day

Figure 23. I-65 MM 101 – 110.5 in the northbound direction of travel for July 1 through August 31, 2019

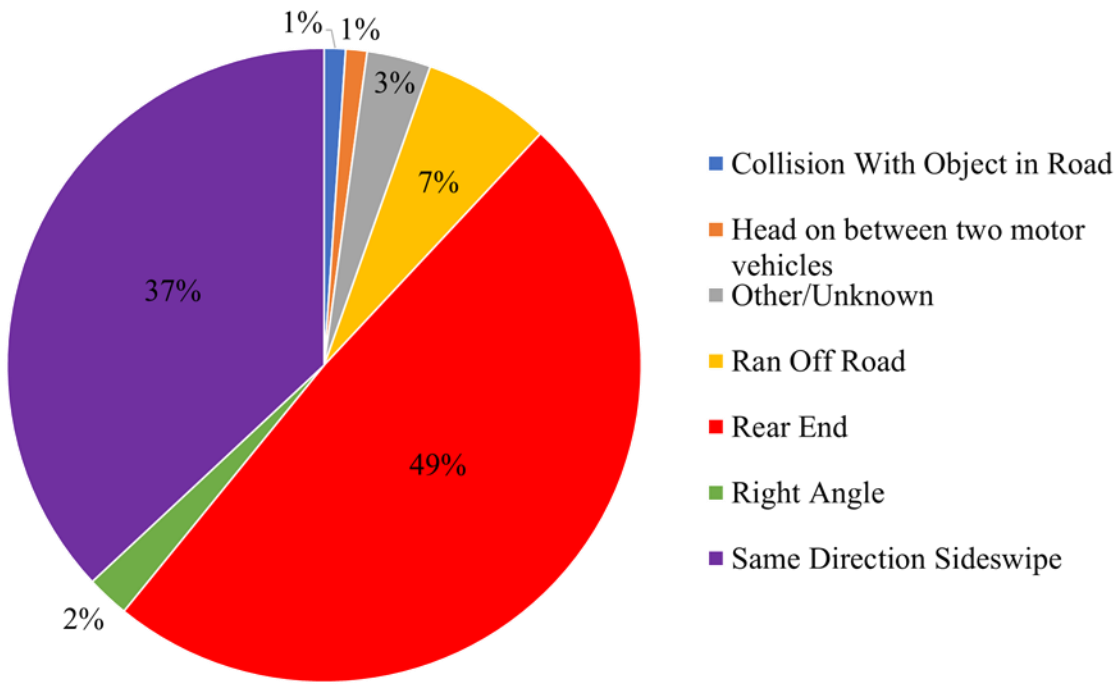

Figure 24. Crashes by manner of collision percentages for Z14 in the northbound direction of travel, for July 1 through August 31, 2019

In this study, congested conditions are defined as lengths of interstate roadway that are operating below a speed threshold of 45 miles per hour [57], [103]. Long queues that often build up on interstate work zones, such as those highlighted by red dashed lines in Figure 23 (a), would result in motorists having to swiftly slow down or hard-brake which increases the risk of a rear-end collision. Figure 24 shows the manner of collision percentages for the 92 crashes recorded for this work zone in Figure 23 (b). From the congestion seen in the region of MM 106 - 110 in Figure 23 (a), significant hard-braking activity is seen to have occurred in this same region shown in Figure 23 (c), some of which may have contributed to back-of-queue collisions. This is validated by the 49% of crashes occurring in the two month period being rear end collisions shown in Figure 24. Lane closures, lane shifts, crashes, sweeping and painting in work zones, and inclement weather are some of the leading causes that are expected to result in hard-braking activity as motorists adjust to changing roadway conditions.

In this particular instance, the region of heavy congestion and elevated crash counts was only able to be identified in an after-action review once crash reports were filed. Using hard-braking events as a surrogate for crash counts could have pinpointed this region of concern within 24 hours instead of having to wait for a crash history to develop. This is visibly verifiable by the strong relationship observed between crash activity and hard-braking events in Figure 23 (b) and Figure 23 (c).

4.7.3 Evaluating Relationship between Hard-braking and Crashes Within Work Zones

Hard-braking events for each work zone occurring during July 1 through August 31, 2019 were totaled and divided by the extent of the work zone in miles (including approaches) to arrive at a value of hard-braking events per mile as shown below:

$$\frac{\text{Hard-braking Events}}{\text{mile}} = \frac{\text{Hard-braking Events}_{\text{July 2019}} + \text{Hard-braking Events}_{\text{August 2019}}}{\text{Approach End MM - Approach Start MM}} \tag{1}$$

Mile-markers and directional information were used from statewide crash reports to spatially determine if a crash occurred within any of the 23 work zones' boundaries. The total 2-month crash count was then calculated and divided by the extent of the work zone in miles (including approaches) to similarly arrive at the crashes per mile value defined as:

$$\frac{\text{Crashes}}{\text{mile}} = \frac{\text{Crashes}_{\text{July 2019}} + \text{Crashes}_{\text{August 2019}}}{\text{Approach End MM - Approach Start MM}} \tag{2}$$

These numerical quantities together form the basis for evaluating the relationship between hard-braking activity and crash occurrences.

Figure 25 shows a scatter plot of crashes per mile against hard-braking events per mile for each of the 23 work zones, calculated separately for each direction of travel, for data totaled over the 2 months of July and August in 2019. A linear trendline is plotted over the data points which returned an R^2 value of 0.85. The plot shows that in general, 1 crash per mile is to be expected for approximately every 147 hard-braking events per mile within a work zone. With the exception of a few outliers visible in Figure 25, it can be safely said that crashes per mile increase at a steady rate with respect to hard-braking events per mile. Our approach to determining the correlation between hard-braking event and crash incident counts involved the use of the linear regression method. The regression resulted in an adjusted R^2 value of 0.845 with a p-value of 0.000(rounded to three decimal places) reinforcing the statistical significance of obtained results.

Using this established relationship between crashes per mile and hard-braking events per mile and having accomplished the first objective of this study, one of the 23 work zones needed to be chosen for a case study in order to look at causal factors for increased hard-braking activity, the second objective of this study. The availability of an independent dataset, namely a mobile LiDAR map of the pavement profiles in work zone Z11 made it an ideal candidate for further analysis. Secondly, work zone Z11 was an area that had observed construction activity both in 2018 and 2019 and saw a 28% increase in crash count in 2019 pointing to a cause of concern for INDOT. This led to a case study analysis of crashes and hard-braking activity in this work zone described in detail in the following section.

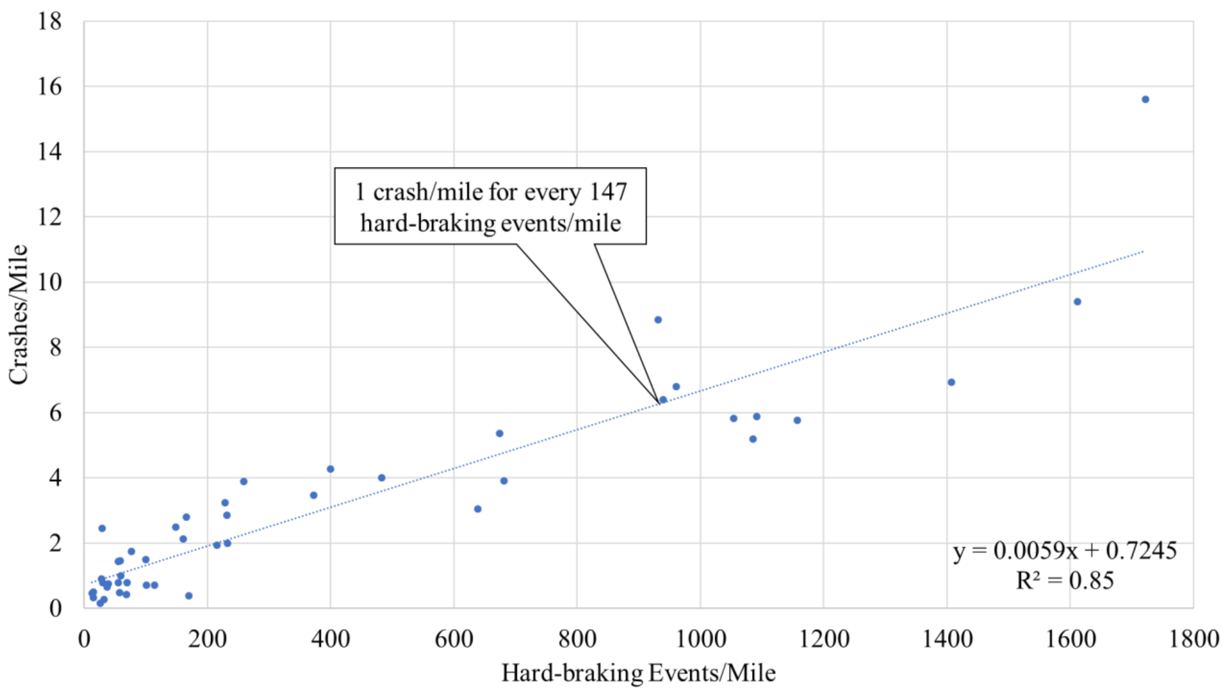

Figure 25. Scatter plot showing crashes and hard-braking events per mile across all 23 work zones for July 1 through August 31, 2019 with a linear trendline

4.8 Results

As seen in Figure 20 and Table 3, Zone 11 (Z11) experienced a modest increase in crashes and was representative of a common rural interstate construction work zone and there was a mobile LiDAR map available for detailed analysis during the time period. The northbound direction experienced approximately 70 hard-braking events/mile and 1.57 crashes per mile for the 2-month analysis period of July and August 2019. Figure 26 shows hard-braking event counts and crash counts for work zone Z11, categorized by severity and manner of collision, in the northbound direction of travel. Callouts (i) in Figure 26 (a) and (b) indicate an elevated frequency of crashes were in the vicinity of MM 61, the same region that exhibited an elevated number of hard-braking event counts. In fact, almost 60 hard-braking events within a 0.1-mile section of road in two months suggested an opportunity for further investigation.

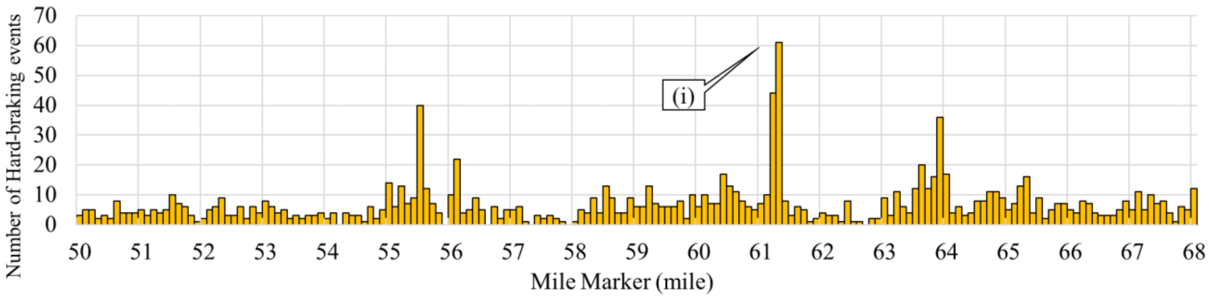

(a) Hard-braking events by tenth of a mile for July 1 through August 31, 2019

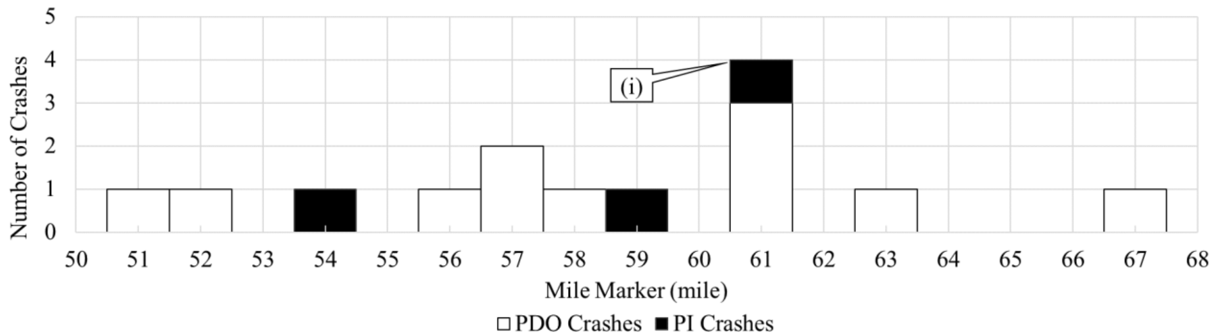

(b) Crashes by mile and severity, for July 1 through August 31, 2019

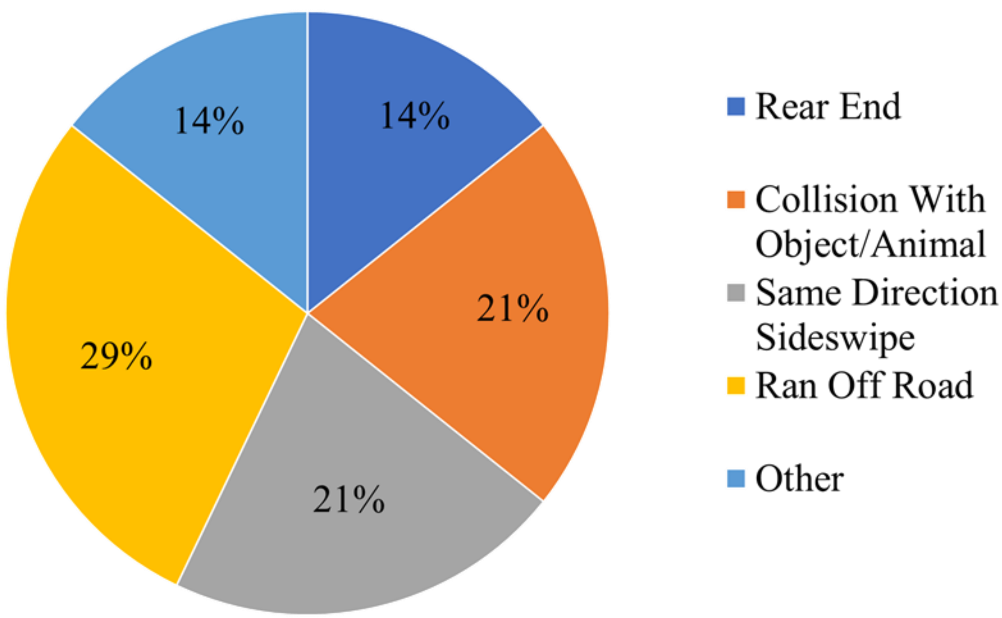

(c) Crashes by manner of collision percentages, for July 1 through August 31, 2019

Figure 26. Northbound I65 Work zone Z11 (MM 50 – 68)

To safely conduct this evaluation, a wheel-based mobile mapping system was used to capture images and lane width data in the vicinity of mile marker 61 on I-65 in the northbound direction on July 17, 2019 [104]. Figure 27 (a) and Figure 28 (a) show images collected using the mobile mapping system with cross sections of interest highlighted. Callouts (i), (ii) and (iii) in Figure 27 and Figure 28 correspond to the left, middle and right edges of traveling lanes used as reference points for lane width computations. Callout (i) has not been marked on Figure 27 (a) as the left edge line of the roadway was not visible in this particular image. Figure 27 (b) and Figure 28 (b) show cross sectional pavement profiles colored by the intensity of LiDAR data aiding in feature visualization and specifically lane width measurement. A single cross-sectional pavement profile has been used in Figure 27 to depict narrow lane widths. Two different cross-sectional pavement profiles are used in Figure 28 to depict narrow lane widths (cross section 1) and edge drop-offs (cross section 2) separately. Figure 27 (b) shows that at MM 61.196 the left lane and right lane have widths of 11.6 ft and 10.6 ft respectively. Figure 28 (b) similarly shows that at MM 61.262 the left and right lanes have lane widths of 11.8 ft and 10.7 ft respectively. The skid marks pointed to by callout (v) in Figure 27 (a) provide additional evidence of hard-braking events in this area. 14 crashes were observed on I-65 northbound between mile marker 50 and 68 for July 1 through August 31, 2019. Figure 26 (c) shows the manner of collision for those crashes split into five distinct categories based on obtained crash reports namely – rear end, collision with object/animal, same direction sideswipe, ran off road and other. 29% of the 14 crashes involved vehicles that ran off the road which points to a validation of the assertion that pavement edge drop-offs were a causal factor for crash incidents and hard-braking activity. Same direction sideswipes were the second leading manner of collision which points to narrow lane widths being a potential explanation as motorists would be forced to maintain far lesser lateral spacing when driving through the work zone resulting in a risk of sideswipes. While the skid marks pointed to by callout (v) in Figure 27 (a) provide visual evidence of hard-braking activity, the 14% of crashes caused by a rear end collision provide further confirmation of the same.

Slightly further North, callout (vi) in Figure 28 (a) depicts broken pavement which results in the right edge line being 11.02 inches from the edge of pavement. Measurements in Figure 28 (c) using LiDAR data indicate an edge drop-off of 2.36 inches at the pavement boundary identified with callout (vi). Freeway design standards established by the American Association of State Highway and Transportation Officials (AASHTO) in 'A Policy on Geometric Design of Highways and

Streets', more commonly referred to as the Green Book, state that through-traffic lanes on freeways must be 12 ft wide (AASHTO, 2001). This leads to the conclusion that observed lane widths in Figure 27 (b) and Figure 28 (b) are narrow lane widths. The combination of these narrow lanes and close proximity of a lane to the pavement edge provide a potential explanation for the high number of hard-braking events seen in this region on Figure 26.

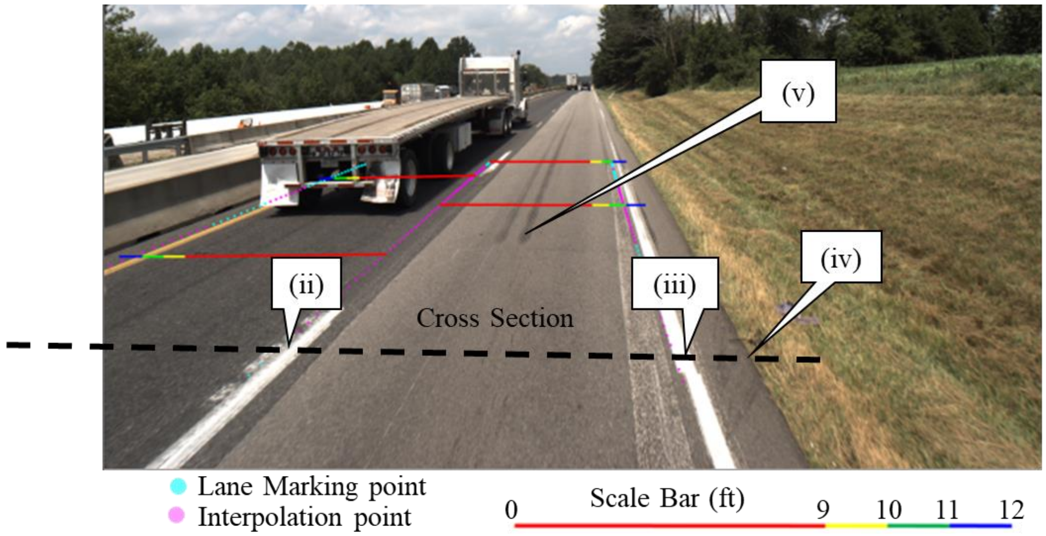

(a) Skid marks indicative of hard-braking activity

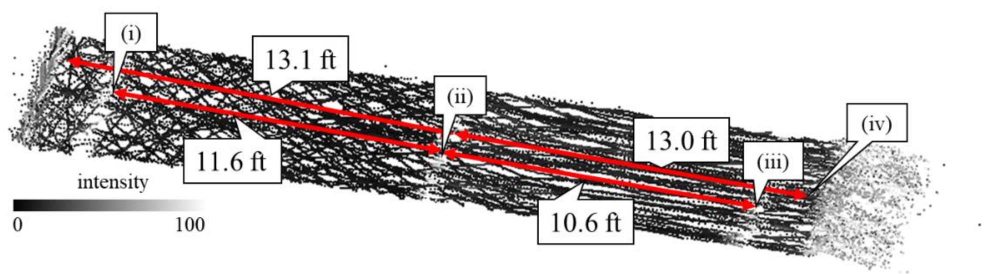

(b) Pavement profile at cross section colored by intensity showing lane widths

(c) Pavement profile at cross section colored by height

Figure 27. I-65 northbound MM 61.196 as seen on July 17, 2019

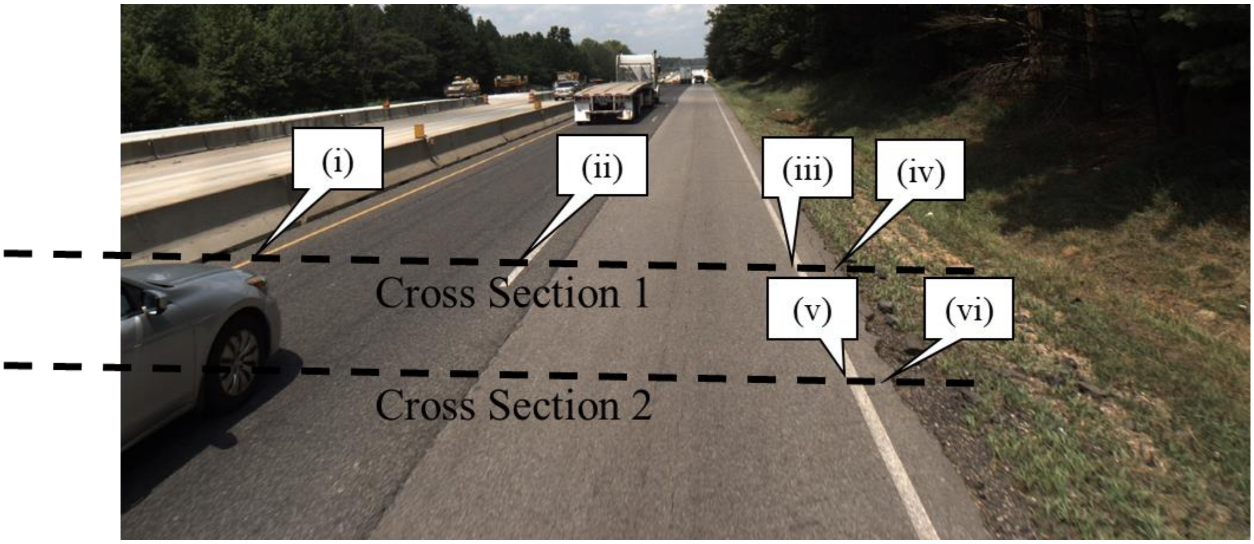

(a) Cross sections used to observe lane widths and edge drop-off

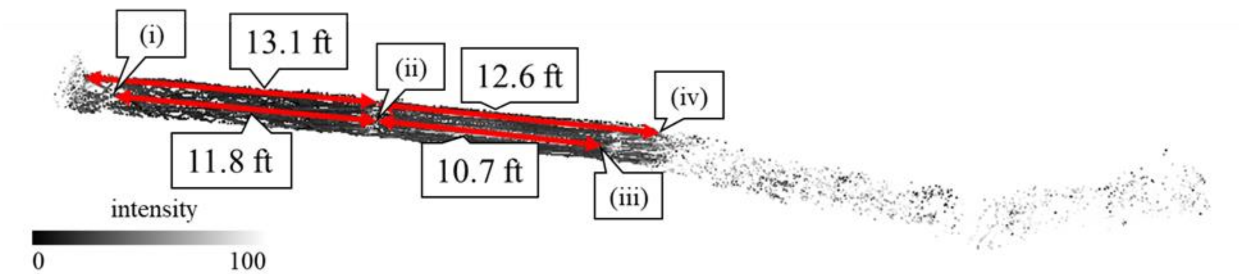

(b) Pavement profile at cross section 1 colored by intensity showing lane widths

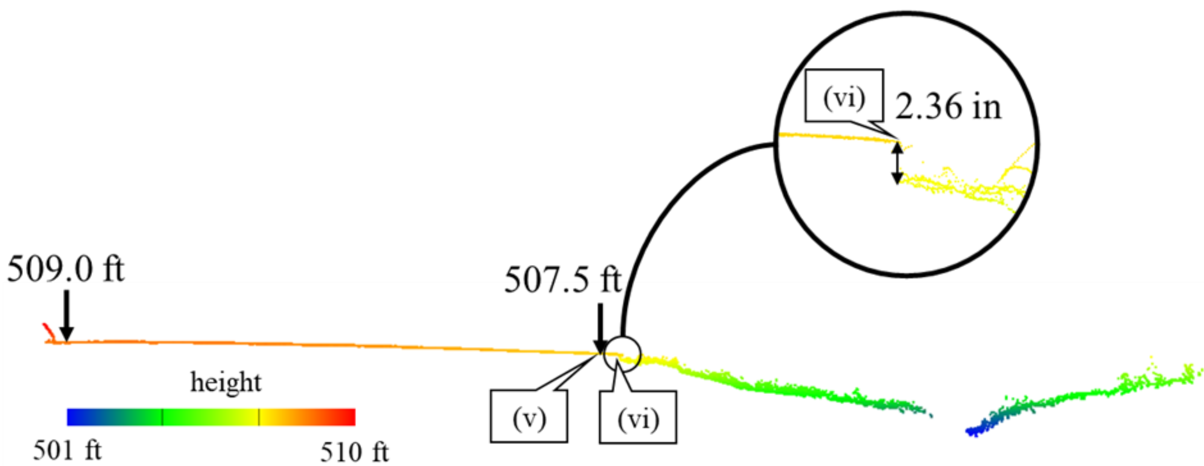

(c) Pavement profile at cross section 2 colored by height showing edge drop-off

Figure 28. I-65 northbound MM 61.262 as seen on July 17, 2019

4.9 Summary

This paper presented a quantitative analysis of hard-braking events and crash incidents conducted on 23 work zones across the state for a 2-month period that demonstrates the observed near-linear relationship between the two quantities. Image captures of skid marks, ambiguous lane markings and broken pavement resulting in edge drop-offs on one of the I-65 work zones in addition to LiDAR data were used to help validate high density of hard-braking events. This correlation helps to make the case for tracking hard-braking events in real-time which, when fused with traffic speeds, can aid in identifying opportunities for improvements in and around work zones. Use of hard-braking data can potentially help prioritize safety investments for agencies, without having to wait for crash history to develop over time on a stretch of road that is under evaluation. The study found that approximately 1 crash occurred for every 147 hard-braking events per mile with an average probe penetration of 4.7%. Due to the challenge in accessing construction work zones for detailed measurements, mobile mapping technology is important for safely conducting measurement of lane widths and/or edge drop offs.

Some of the limitations of this analysis include the assumption of construction activities taking place in both directions of travel, inconsistencies with the reporting of crash incident locations and times, aggregate analysis conducted owing to unavailability of exact construction schedules and crash incident timestamps. Although this study only observed a set of 23 work zones to demonstrate feasibility, the methodology described herein can be easily scaled to a statewide or even nationwide level to monitor multiple work zones at a time due to the now widespread availability of hard-braking event data coupled with the high penetration levels of connected vehicles in the current automobile market.

The results from this chapter thus show the effectiveness and statistical evidence needed to incorporate the use of connected vehicle events such as hard-braking into an agency's daily safety monitoring workflow, thus allowing real-time proactive safety monitoring on roadways as opposed to reactive monitoring that has historically relied on crash reports.

5. USING CV DATA TOWARDS ASSESSING ELECTRIC VEHICLE CHARGING INFRASTRUCTURE USAGE AND IDENTIFYING INVESTMENT OPPORTUNITIES

The information presented in this chapter has been published in “Analysis of Electric and Hybrid Vehicle Usage in Proximity to Charging Infrastructure in Indiana” [106] and in “Using Connected Vehicle Data for Assessing Electric Vehicle Charging Infrastructure Usage and Investment Opportunities” [107].

This chapter discusses visualizations, methodologies and performance measures for assessing electric vehicle charging infrastructure usage using CV data and leveraging the same towards allocation of future infrastructure investment. The first section (5.1) of this chapter presents a study that utilized a one-week CV dataset from July 2021 for the state of Indiana to analyze EV and HV usage as well as prototype methodologies that assess charging infrastructure usage. The second section (5.2) of the chapter builds on this Indiana analysis to demonstrate scalability and comparative analyses among 10 additional states (California, Connecticut, Georgia, Ohio, Pennsylvania, Minnesota, North Carolina, Utah, Texas and Wisconsin) in the US using over 185 billion CV records for the month of August 2021.

5.1 Analysis of Electric and Hybrid Vehicle Usage in Proximity to Charging Infrastructure in Indiana

5.1.1 Overview

This study explores the movement of connected vehicles in Indiana for vehicles classified by the NHTSA Product Information Catalog Vehicle listing as being either electric (EV) or hybrid electric (HV). Analysis of trajectories from July 12-18, 2021 for the state of Indiana observed nearly 33,300 trips and 267,000 vehicle miles travelled (VMT) for the combination of EV and HV. Approximately 53% of the VMT occurred in just 10 counties. For just EVs, there were 9814 unique trips and 64,700 Electric Vehicle Miles Traveled (EVMTs) in total. A further categorization of this revealed that 18% of these EVMTs were on Interstate roadways and 82% on non-interstate roads. A proximity analysis of existing DC Fast charging stations in relation to interstate roadways revealed multiple charging deserts that would be most benefited by additional charging capacity. Eleven roadway sections among the 9 interstates were found to have a gap in available DC fast chargers of 50 miles or more. Although the connected vehicle data set analyzed did not include all EV's the methodology presented in this paper provides a technique that can be scaled as additional EV connected vehicle data becomes available to agencies. Furthermore, it emphasizes the need for transportation agencies and automotive vendors to strengthen their data sharing partnerships to help accelerate adoption of EV and reduce consumer range anxiety with EV. Graphics are included that illustrate examples of counties that are both overserved and underserved by charging infrastructure.

5.1.2 Introduction

An estimated 10 million electric vehicles (EV) were on roads in 2020, an increase of 41% for the calendar year. Eighteen of the world's top 20 vehicle manufacturers in 2020 have announced plans to scale up the production of electric vehicles in their fleets [108]. Fifteen countries have publicly announced plans to phase out sales of internal combustion engine (ICE) vehicles in support of zero emissions vehicles [109]. The United States recently set forth a national target for EVs to make up half of all new vehicle sales by the end of this decade [110]. While EVs only account for 4% of vehicles in the US, their penetration rate has continued to increase approximately 1% annually since 2017 [111]. It is estimated that EVs will come close to reaching cost parity with ICE vehicles around 2025 that will result in an accelerated transition from ICE to EV [112].

In addition to cost, range anxiety and availability of public charging stations [113], [114] are two of the major barriers currently cited for inhibiting growth of EVs. Furthermore, it is unclear to transportation agencies, consumers, and the private sector where infrastructure usage and charging demand will grow or how fast it will grow. The motivation of this paper is to explore using connected EV data to:

- characterize differences (or lack of a difference) in EV and ICE operating speeds on Interstates in Indiana;
- characterize vehicle miles traveled by counties;
- identify counties that are underserved by charging infrastructure (and perhaps overserved);
- identify "charging deserts" on major interstates;

- propose a methodology for evaluating candidate Interstate exits for installing new charging stations.

5.1.3 Literature Review

A study utilized questionnaire surveys to understand the reasons behind EV and hybrid vehicle (HV) owners in California reverting from an EV purchase and found convenience of charging and limited access to level 2 charging at home as contributing factors to discontinuance [115]. A survey of plug-in electric vehicle (PEV) owners in California in 2016 and 2017 indicated over half of respondents prefer home charging, while results indicated that the use of home, work and public charging locations is an interdependent relationship of charging capacity [116].

Past research has studied the impact of driving characteristics (driving style and speeds) on EV usage and energy consumption using test vehicles in both rural and urban areas indicating aggressive driving of EVs increases cost to the user by 30% and causes a marked difference in energy consumption [117]. Multiple energy consumption studies have looked at various factors that may detrimentally impact EV efficiency and range including road type, auxiliary loads (such as HVAC systems), driving at higher speeds, acceleration profiles, increased vehicle cross-sectional area and ambient environment [118]–[120]. Research has established that battery electric vehicles have significant energy savings for low speed drives with frequent stops, and observe substantial energy consumption at highway speeds [121].

An EV usage and planning study completed on six EVs deployed in Athens, GA found most EVs were charged continuously within 3 hours and 80% of all trips were less than 10 miles [122]. EV charging infrastructure planning research has utilized long-term traffic flow predictions and public transportation datasets to estimate optimal future charging infrastructure plans [123]. A study looked at spot traffic counts in Western Australia coupled with an assumed EV penetration rate of 1% to select sites for future DC Fast charging stations using the criterion of reliability, accessibility and availability of amenities and services [124]. Various simulation-based approaches have been employed in the past for EV fast charging infrastructure planning using simulated trajectories and charging behavior assumptions [125], urban mobility simulations that minimize EV energy consumption [126], as well as mathematical programming models factoring in user convenience and grid connections for low penetration levels of 5% [127]. Data obtained from fast charging stations in Ireland observed 0.18 charges per day per EV user at home and 0.06 charges per day per EV user in public charging locations, thus reinforcing the need for more strategically placed fast charging stations to incentivize more usage in non-peak grid demand times [128].

Past research has heavily focused on factors affecting EV range and charging behavior and patterns on a user level. While most of the above studies utilized floating car data, spot traffic counts, mathematical programming or simulation modeling, very few studies have looked at real world connected vehicle data collected from EVs and HVs to evaluate driver behavior and usage as it relates to charging infrastructure on a macroscopic, statewide level. Our study aims to bridge this gap by using connected vehicle data for a 1-week period in Indiana for EVs and HVs.

5.1.4 Connected Vehicle Data

Indiana ingests over 10 billion connected vehicle records per month from a combination of EV and ICE, with a penetration of roughly 4% of all vehicles [129]. The charging standard for the EV vehicles analyzed is the SAE J1772 and Combined Charging System (CCS) standard. This study looked at a one-week period from July 12-18, 2021 to evaluate EV and HV usage patterns as they relate to existing charging infrastructure.

Connected vehicle data utilized in this study is made up of individual journey waypoints recorded at a 3-second fidelity. Each data record contains the following attributes: geolocation, speed, heading, timestamp, an anonymized unique trajectory identification number and a vehicle classification code. This vehicle classification code was then cross referenced with the National Highway Traffic Safety Administration's (NHTSA) Product Information Catalog Vehicle Listing (vPIC) Application Programming Interface (API) [130] to obtain the electrification level associated with it. If the electrification level obtained is 'BEV (Battery Electric Vehicle)', the vehicle classification code and subsequently the associated waypoint is flagged as belonging to an electric vehicle. A similar classification process is followed for Hybrid Vehicles as well (Figure 29).

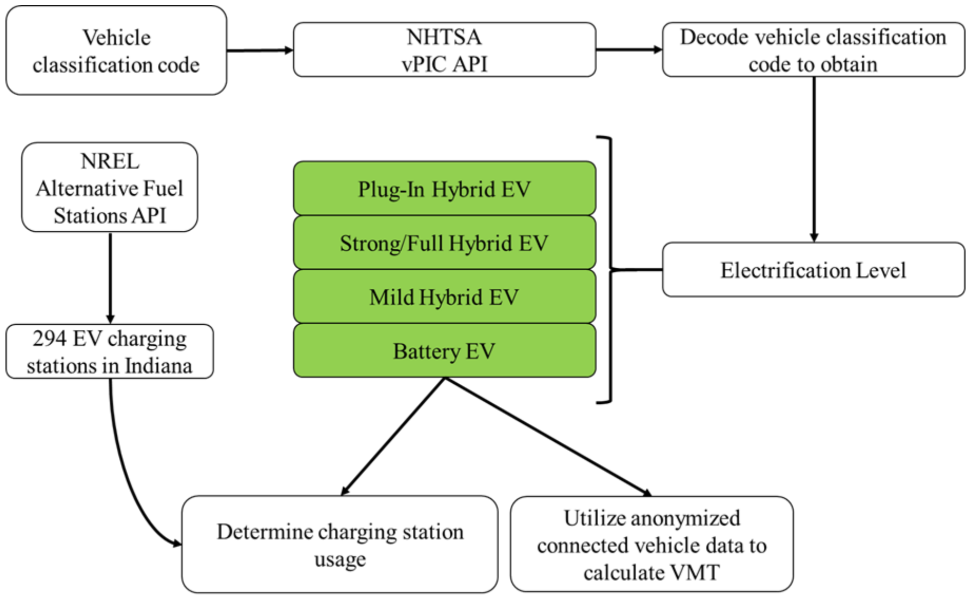

Figure 29. Methodology for Decoding Vehicle Classification Code to isolate EV and HV Connected Vehicle Data

Nearly 2.65 million waypoints were thus found for EVs for the week of July 12-18, 2021 spread over 9,800 unique trips for the state of Indiana. Correspondingly, 7.74 million waypoints were obtained for HVs for the same week spread over 23,000 unique trips. A spatial representation of these EV and HV waypoints has been shown in Figure 30 a and b respectively. In comparison, over 7.54 million unique trips were found for ICE vehicles (ICEV) for the same period. The majority of the EV and HV coverage is concentrated in metropolitan areas.

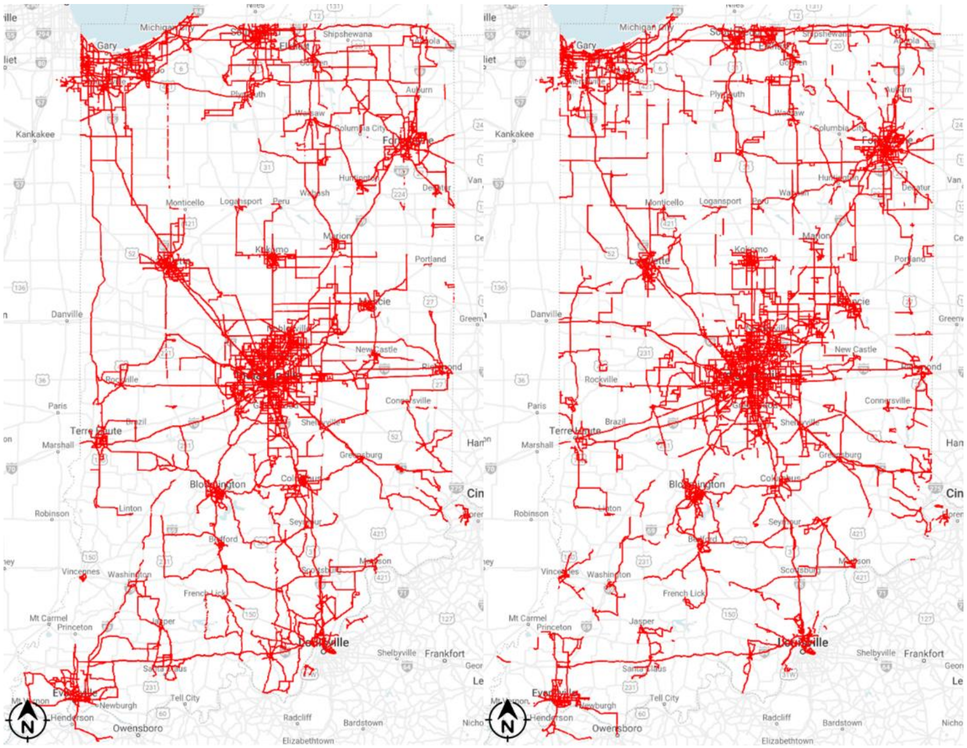

(a) ~64,700 EVMTs in Indiana (b) ~202,000 HVMTs in Indiana

Figure 30. Electric and Hybrid Vehicle Trails in Indiana (July 12-18, 2021)

Of the 92 counties in the state of Indiana, vehicle miles traveled (VMT) totals were computed for both EVs and HVs by matching each individual waypoint to the county it was recorded in. A spatial representation of these EVMTs and HVMTs in terms of percentage of the total VMT (EVMT + HVMT) by county have been shown in Figure 31 a and b. A tabular representation of the top 10 counties with highest combined totals of EVMT and HVMT is shown in Table 4. Marion (callout i), Hamilton (callout ii) and Lake (callout iii) counties account for the highest EVMTs while Marion, Hamilton and Allen (callout iv) counties observed the highest HVMTs. Marion county had the highest vehicle miles traveled for EVs and HVs overall.

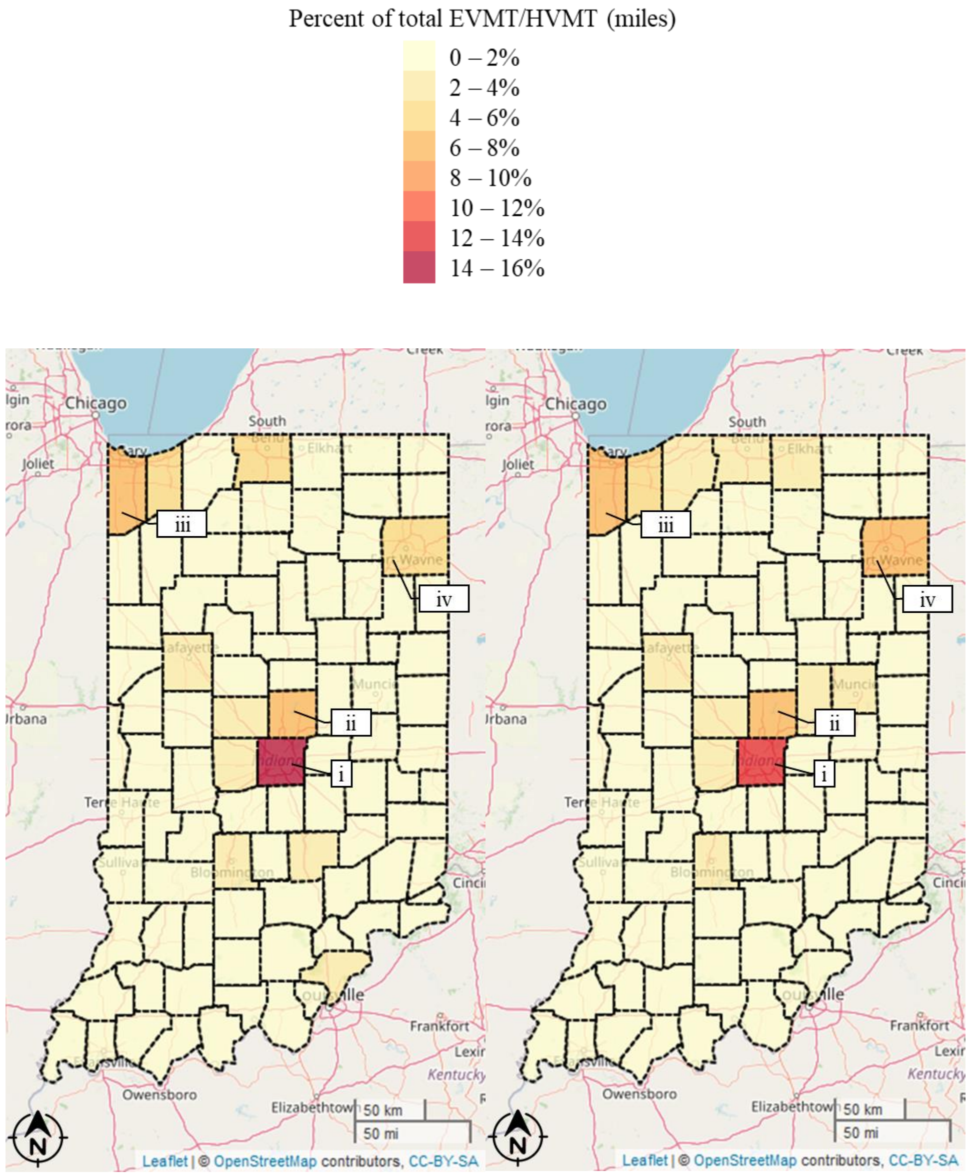

(a) EVMTs aggregated by County (b) HVMTs aggregated by County

Figure 31. EVMTs and HVMTs aggregated by Indiana County (July 12-18, 2021)

Table 4. Top 10 Indiana Counties with highest totals of EVMT and HVMT (July 12-18, 2021)

County	EVMT (miles)	HVMT (miles)	Total (miles)
Marion	9557	27980	37537
Hamilton	4625	15994	20619
Allen	3067	15085	18152
Lake	4294	12862	17156
Porter	2693	8223	10916
St. Joseph	2899	5820	8719
Hendricks	1865	5447	7312
Tippecanoe	2274	4910	7184
Monroe	1983	5010	6993
Madison	916	5353	6269

5.1.5 Electric and Hybrid Vehicle Miles Traveled by Roadway

Using linear referenced sections of the roadway on all Indiana interstates at approximately 0.1-mile fidelity, each EV and HV waypoint was cross-referenced and matched to an interstate route with a direction of travel. This enabled the computation of summary statistics for EVs and HVs in terms of percent of vehicle miles traveled (VMT) on interstate corridors and non-interstate roadways (Figure 32). Approximately 18% of EVMTs occur on interstate roadways and 24% of HVMTs occur on interstates. A further categorization of EVMTs and HVMTs was performed for individual routes for 11 interstate corridors around the state. A stacked bar representation shown in Figure 32c clearly illustrates the north-south interstate route I-65 and I-69 seeing the most EV and HV traffic in addition to substantial EV and HVMT on the I-465 loop around Indianapolis.

Using the route-by-route breakdown of EVMTs for Indiana Interstates obtained earlier, the top ten 1-mile interstate segments with highest EVMTs are shown graphically and on an Indiana map in Figure 33 a and b respectively. Eight of the top 10 segments were found to be in urban areas primarily on or near the I-465 beltway around Indianapolis which observes daily commuter traffic. Additional segments on I-94 in northwest Indiana see significant usage potentially owed to traffic commuting to and from Illinois. These high usage sections could be potential early deployment sites for additional charging stations and/or in-pavement wireless charging [131].

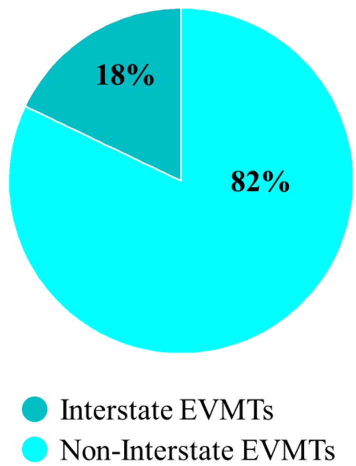

(a) EVMTs categorized by roadway

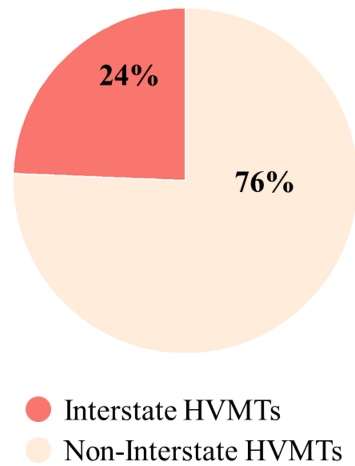

(b) HVMTs categorized by roadway

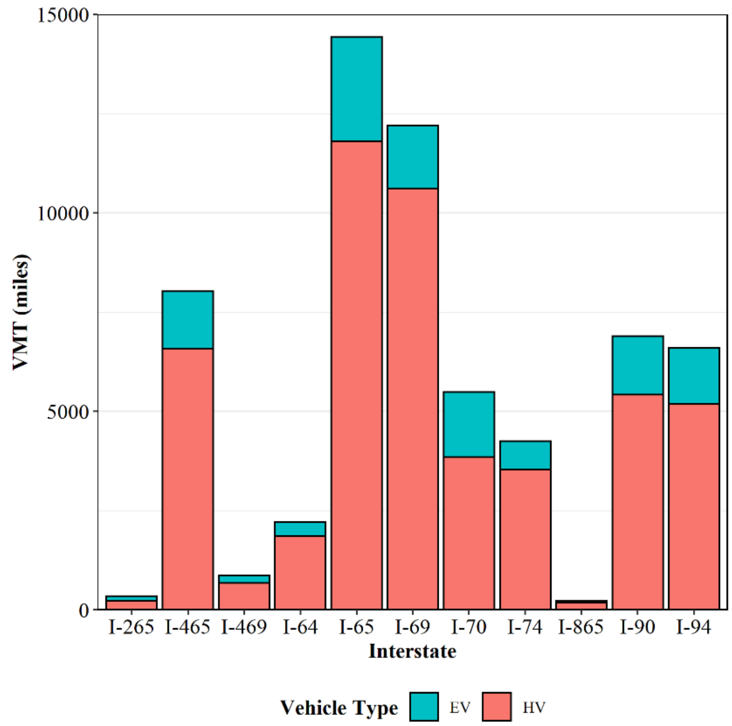

(c) Interstate VMTs categorized by EVs and HVs

Figure 32. VMTs categorized by roadway, interstate routes (July 12-18, 2021)

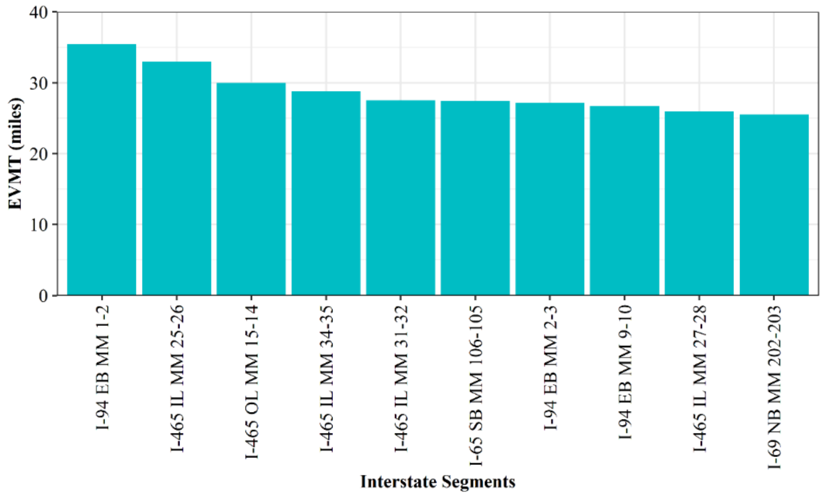

(a) Top 10 Interstate Segments with Highest EVMTs

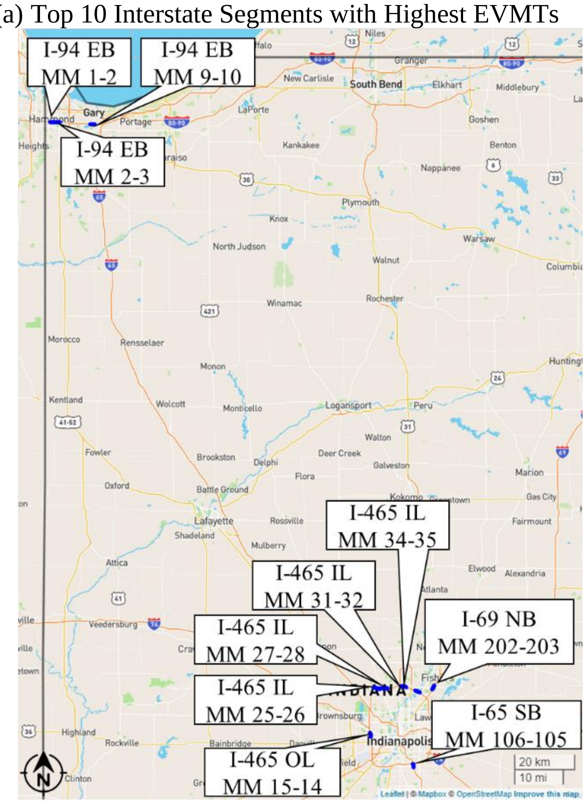

(b) Statewide Map of Top 10 Interstate Segments with Highest EVMTs

Figure 33. Interstate segments with highest EVMTs (July 12-18, 2021)

5.1.6 Interstate Operating Speeds of Electric and Hybrid Vehicles

Average Speeds of EVs and HVs, and ICEVs that traversed on I-65 (chosen due to highest EVMTs and HVMTs recorded among all interstates) were evaluated for the week of July 12-18, 2021.

Median EV and HV speeds were found to be 68.7 and 71.6 mph respectively, with ICEVs operating at a median speed of 72.3 mph.

Figure 34 shows a cumulative frequency distribution plot of uncongested vehicle speeds (speeds above 45 mph) for I-65. A separate frequency line has been used for each of the EV, HV and ICEV vehicle classes for ease of comparison.

From Figure 34, one can see that the distribution of ICE vehicle speeds is higher than both HV and EV. In fact, there is approximately a 3mph difference in median speeds between ICE and EV. Some of this may be due to range anxiety concerns by EV operators resulting in them driving at lower speeds to conserve battery charge and/or different driving styles of ICE and EV consumers.

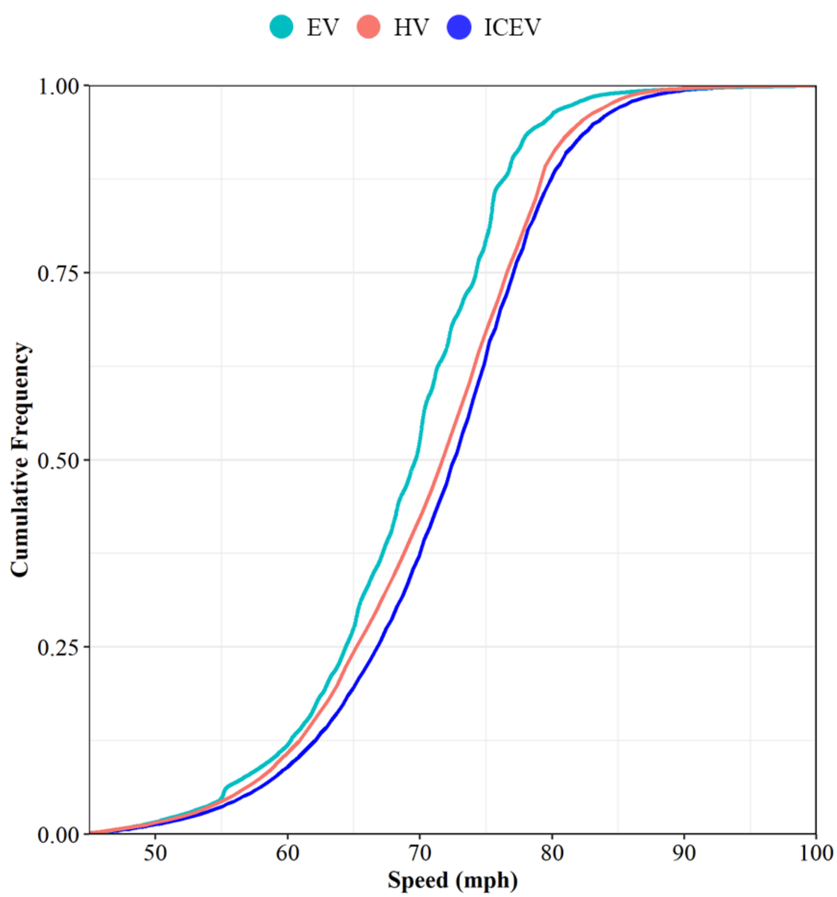

Figure 34. Cumulative Frequency Distributions of EV, HV and ICEV Uncongested Speeds for I-65 (July 12-18, 2021)

5.1.7 Evaluating EV Charging Infrastructure

Using the National Renewable Energy Laboratory’s (NREL) alternative fuel stations API [132], geolocation data and multiple other pertinent attributes including number of charge points were obtained for 294 electric charging stations in Indiana. Among these, 270 were found to be level 2 capable (Figure 35a) and 24 stations were found to be capable of providing DC Fast Charging (Figure 35b). Fast charging is a critical need for long-distance driving, especially for travel on long stretches of limited access roadways such as interstate corridors. Level 2 charging was observed to be spread out across the state with clusters in the Gary, South Bend, Fort Wayne and Indianapolis regions. DC Fast charging is however more sparsely distributed with few in the north-central and southwest region.

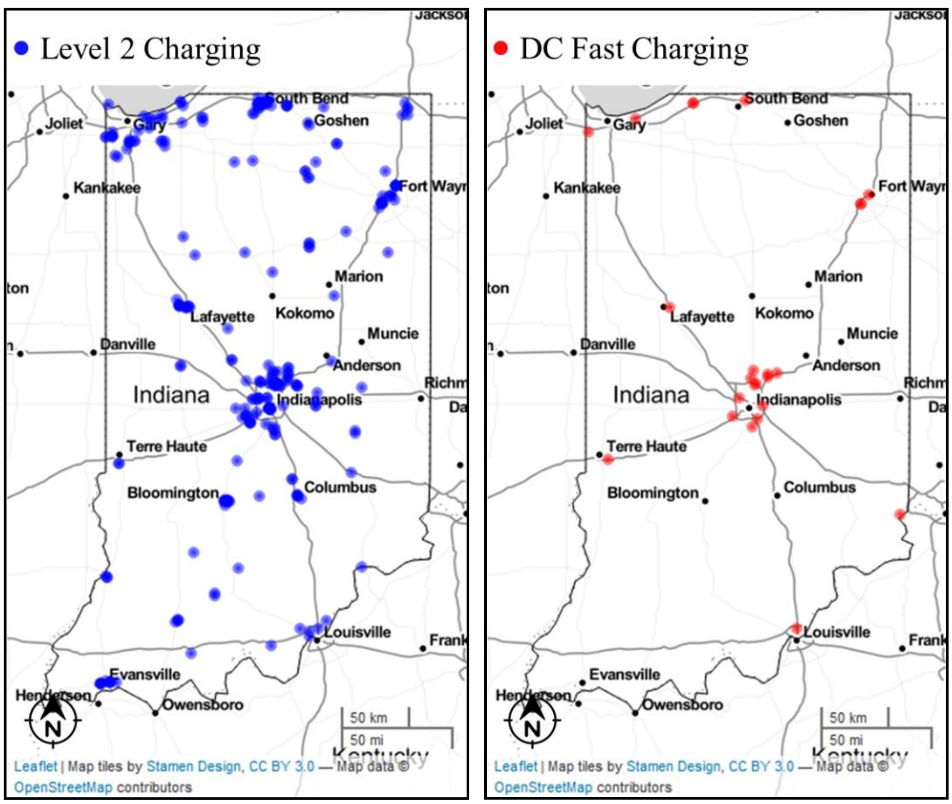

(a) 270 Level 2 Charging Stations (b) 24 DC Fast Charging Stations

Figure 35. Level 2 and DC Fast Charging Infrastructure in Indiana [132]

5.1.7.1 Charging Station Usage

With rising adoption rates of EV and HV, a clear and present concern for EV owners as well as the private sector is charging station capacity. With limited charging infrastructure and charging spots at each station, the adoption rate of EVs could soon possibly surpass the ability of existing infrastructure to serve all EV owners if the growth of infrastructure does not keep pace. Owing to this, an analysis of charging station usage is needed to compute number of unique uses per day to look at charging patterns. A DC Fast charging station in South Bend, Indiana was utilized for this analysis as shown in Figure 36a.

A spatial polygon was drawn around all of the charging spots at this station. EV waypoint geolocations for a nearly 2-month period of June 1 – July 27, 2021 were then cross-referenced with this polygon to detect those waypoints that coincided directly with either of the charging spots. Using the obtained intersection of data, a temporal profile of unique EV trips visiting this charging station has been shown by the illustration in Figure 36b categorized by day of week and hour of day. The hours of 2 PM and 8 PM specifically show up as peak charge times with the weekend period of Friday, Saturday and Sunday appearing to be the preferred time to charge. While this analysis only provides an initial look at charging patterns at one station, this methodology is easily scalable to any charging station irrespective of location which makes it a valuable tool for EV stakeholders.

(a) DC Fast Charging Station (South Bend, Indiana)

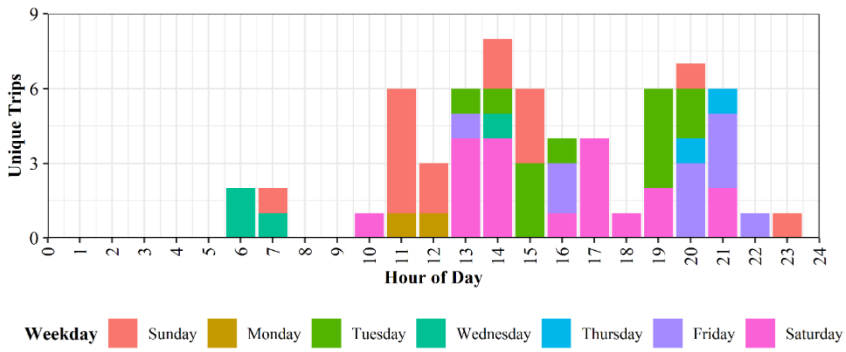

(b) Usage by Hour of Day and Day of Week

Figure 36. Charging Station Usage (June 1 – July 27, 2021)

Using a similar methodology as shown above, the top ten most utilized EV charging stations were found for the state of Indiana, 9 of which were level 2 capable and 1 provided DC fast charging capability (ranked 7). A majority of these stations were found to be in urban areas near Indianapolis, South Bend and Columbus and have also been shown on an Indiana county map along with their ranks called out in Figure 37.

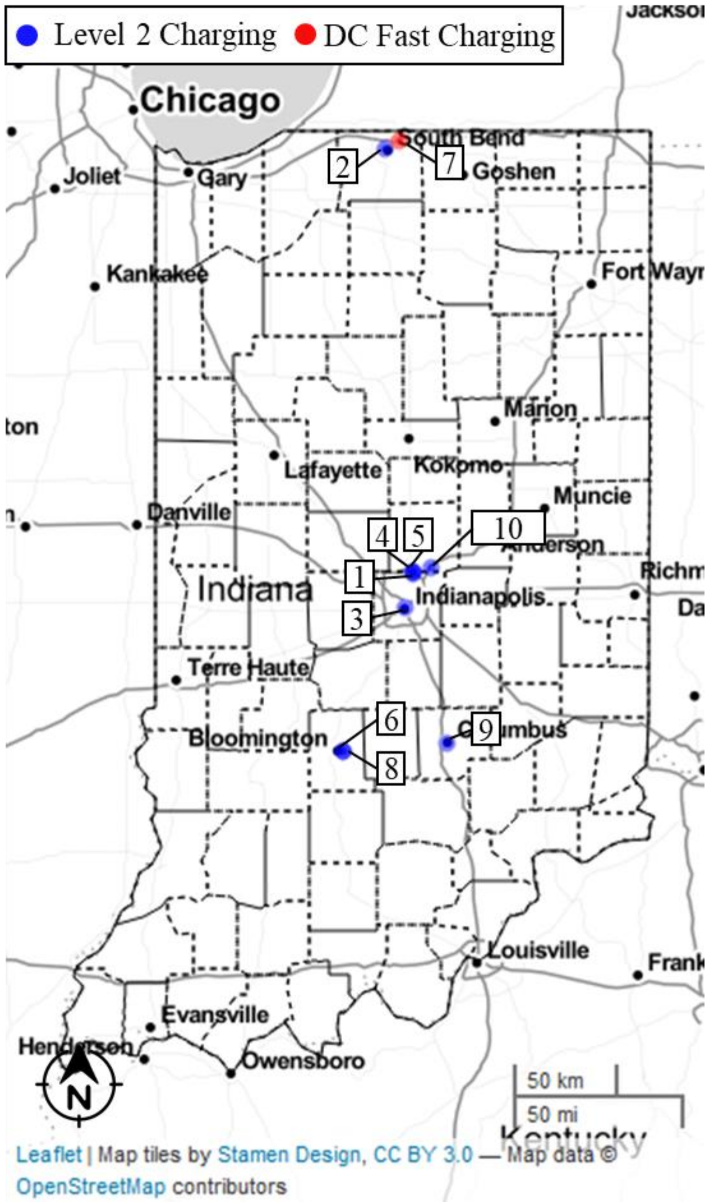

Figure 37. Top 10 Utilized EV Charging Stations in Indiana called out by rank (July 12-18, 2021)

For all 92 counties in Indiana, the number of charging stations and the number of charge points at all stations were obtained. A linear relationship was established between VMTs for EVs and HVs versus the number of charge stations as well as the number of charge points available per county. This distinction between charge points and charge stations is needed as the number of charge stations in a county alone may not reflect the true charging capacity owing to multiple charge points available at each station. A scatter plot along with a predicted linear relationship line between number of charge stations, EVMTs and HVMTs by Indiana county has been shown in Figure 38a. A similar plot showing a relationship with number of charge points is depicted in Figure 38b.

- Clusters near the y-axis pointed to by callouts i on Figure 38a and b indicate overserved counties in the state where a high number of charging stations and charge points are available however minimal EVMTs and HVMTs are observed.

- Clusters near the x-axis pointed to by callouts ii on Figure 38a and b indicate underserved counties in the state where there is a high EVMT or HVMT, but little charging infrastructure.

These visualizations may be helpful to government and private sector planners in providing a first look at determining which geographical locations in particular are over or underserved and allocating resources and investment accordingly.

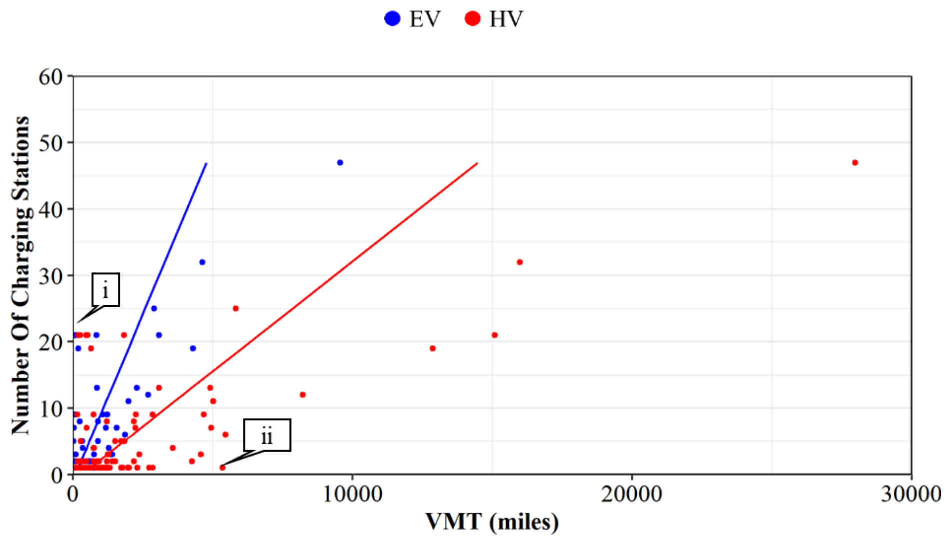

(a) Count of EV charging stations vs. EVMT and HVMT by Indiana County

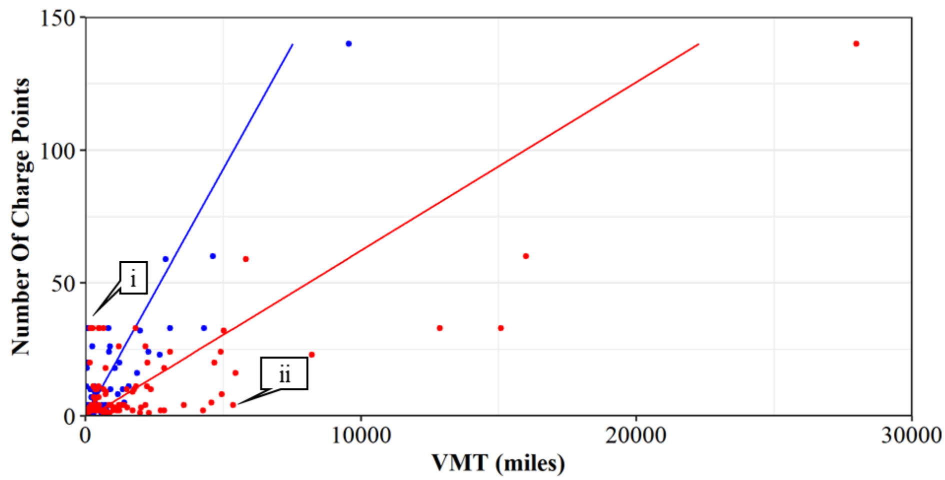

(b) Count of EV charging points vs. EVMT and HVMT by Indiana County

Figure 38. Relationship between charging locations and VMT by Indiana county (July 12-18, 2021)

5.1.7.2 Sensitivity Analysis for DC Fast Charging Station Proximity to Interstates

As fast charging is essential for planning long distance routes, availability of fast charging stations near high-speed interstate corridors is essential to assuage range anxiety. Using the geolocations of the 24 DC Fast charging stations in Indiana [132], a proximity analysis was conducted to determine the closest interstate roadway to each station within a specified radius. The results of a sensitivity analysis wherein the specified radius was increased in 1-mile steps are shown in Table

5. 75% of all DC Fast charging stations were found to be within 1-mile of an interstate corridor while 96% of all DC Fast charging stations were within 6 miles of an interstate.

Table 5. Proximity of DC Fast Charging Stations to Indiana Interstates

Radius (mi)	Number of DC Fast Charging Stations within the radius	Percentage of DC Fast Charging Stations within the radius
1	18	75%
2	20	83%
3	21	88%
4	22	92%
5	22	92%
6	23	96%
7	23	96%
8	23	96%
9	23	96%
State of Indiana	24	100%

5.1.8 Charging Deserts on Interstate Routes

Using the results of the sensitivity analysis from above, the closest interstate roadways were found within 1-mile of each of the 18 stations. These limits were subsequently utilized to introduce the concept of a fast "charging desert," which indicates long segments of interstate without a DC Fast charging station available within a 1-mile threshold. A statewide summary of charging segments and deserts on nine interstate routes is shown in Figure 39a. Each interstate is broken up into segments at either end of which is either a charging station, route endpoint, or the state boundary line, however a fast-charging station is not found in the interior of the segment. It was assumed that a 50-mile length threshold for a fast charging desert would be significant enough to add to range anxiety concerns, as the average late-model production EV can travel about 3.4 miles per kilowatt-hour [133] and a typical level 2 charger outputting 6.6 kilowatts, thereby potentially adding up to about one hour to a trip if resorted to a level 2 charger. Each such 50-mile or longer segment is termed a desert and has been illustrated in Figure 39b highlighting multiple long fast charge gaps on Indiana's interstates, from Lafayette to Gary on I-65, Evansville to Indianapolis on I-69 and Terre Haute to Indianapolis on I-70 to name a few.

To spatially visualize the sensitivity of the 1-mile threshold, a corresponding desert map has been shown in Figure 39c with a 5-mile threshold where the I-65 desert south of Indianapolis is shorter owing to a DC fast charging station found within a 5-mile radius. Callout (i) on Figure 39b shows the original longer desert on I-65 which reduces in length when the proximity threshold for charging stations is changed from 1 mile to 5 miles.

For a detailed look at each interstate, start and end mile markers (mm) for each charging segment and whether it is a potential desert or not are provided in Table 6. For example, I-65 consists of three charging deserts, one between MM 4 and MM 120, the second between MM 120 and MM 172 and the third between MM 172 and MM 262. Eleven fast charging deserts in total were found across 9 interstate routes in Indiana.

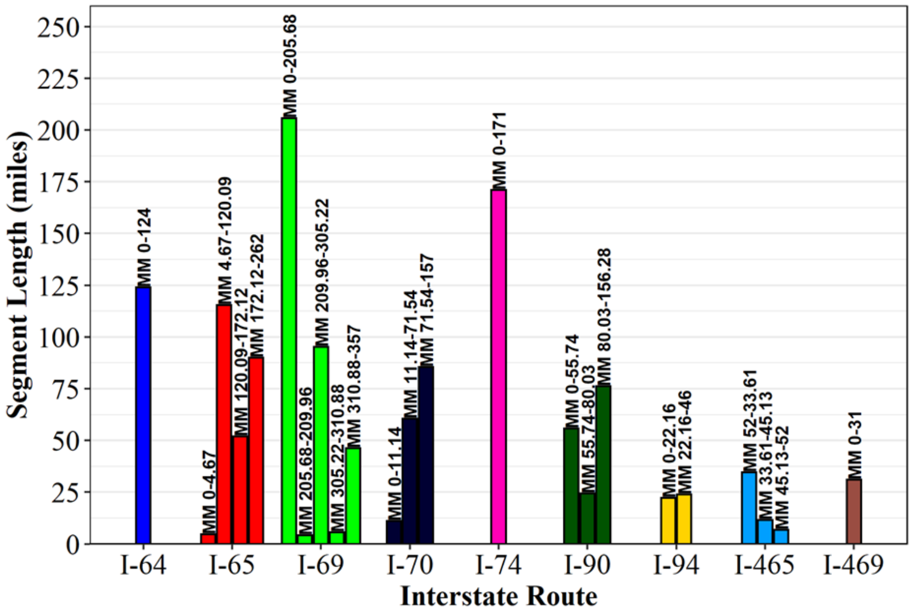

(a) DC Fast Charging Availability Segments on Indiana Interstates

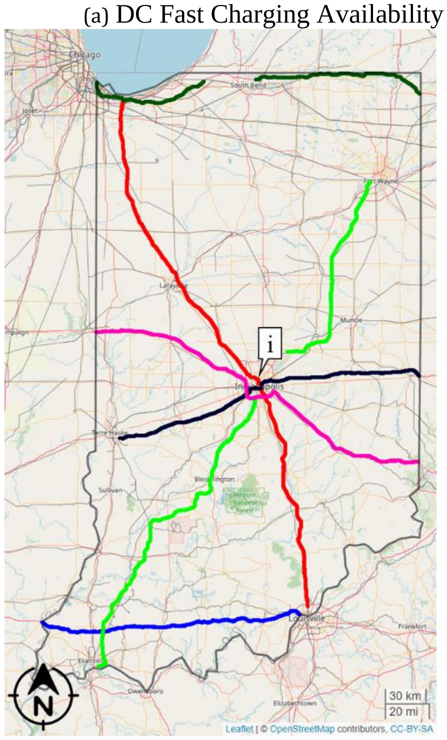

(b) DC Fast Charging Deserts longer than 50 miles (no station within 1 mile of interstate)

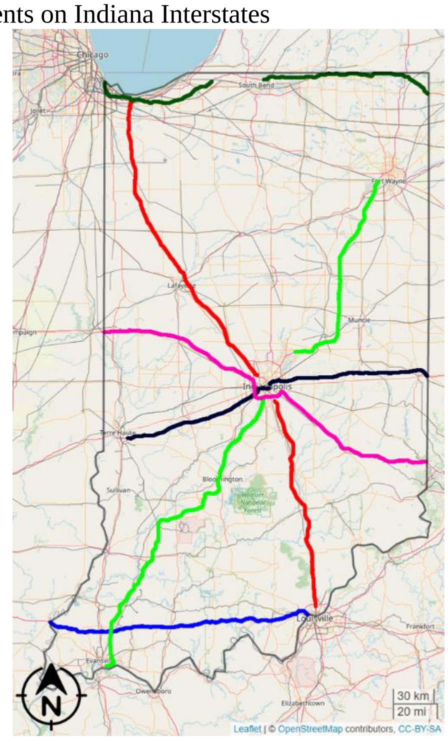

(c) DC Fast Charging Deserts longer than 50 miles (no station within 5 miles of interstate)

Figure 39. Segment lengths on Indiana Interstates without a DC Fast Charging Station (Fast Charge Deserts)

Table 6. Summary of charging segments and deserts on Indiana Interstates (no station within 1 mile of interstate)

Interstate	Total Length (mi)	Fast Charging Availability Segments			Potential Desert
		Start MM	End MM	Length (mi)	
I-465	53	52.0	33.6	34.6	
		33.6	45.1	11.5	
		45.1	52.0	6.9	
I-469	31	0.0	31.0	31.0	
I-64	124	0.0	124.0	124.0	**Yes**
I-65	262	0.0	4.7	4.7	
		4.7	120.1	115.4	**Yes**
		120.1	172.1	52.0	**Yes**
		172.1	262.0	89.9	**Yes**
I-69	357	0.0	205.7	205.7	**Yes**
		205.7	210.0	4.3	
		210.0	305.2	95.2	**Yes**
		305.2	310.9	5.7	
		310.9	357.0	46.1	
I-70	157	0.0	11.1	11.1	
		11.1	71.5	60.4	**Yes**
		71.5	157.0	85.5	**Yes**
I-74	171	0.0	171.0	171.0	**Yes**
I-94	46	0.0	22.2	22.2	
		22.2	46.0	23.8	
I-90	156.28	0.0	55.7	55.7	**Yes**
		55.7	80.0	24.3	
		80.0	156.3	76.3	**Yes**

5.1.9 Evaluating EV Usage of Interstate Exits for Charging Locations

Having identified the significant fast charge gaps on interstates as shown in earlier sections, the opportunity provided to planners would be to decide which interstate exits to place additional charging infrastructure. It can be assumed that the most heavily utilized exits, irrespective of vehicle class, would serve as the ideal locations to reinforce with charging capacity.

Without tracking user activity patterns over an entire trip, our methodology makes use of the vehicle classification code which represents the make and model of a vehicle in order to look at outflows and inflows on the exit and entry ramps respectively at a chosen interstate location by defining a time threshold ranging from 30 to 90 minutes. We thus ensure anonymity by not capturing any stopping patterns from the connected vehicle data.

Figure 40 shows exit 68 on I-65 NB (near the midway point on I-65 charging desert MM 4-120 from Table 6) near Columbus, Indiana to illustrate this analysis technique. Connected vehicle waypoints shown in blue indicate those trips traveling through on I-65 without taking the exit, red indicate those exiting (callout ii) and green indicate trips entering I-65 NB (callout i) at the same location using one of two entry ramps. All EV, HV, and ICEV waypoints were used for this analysis.

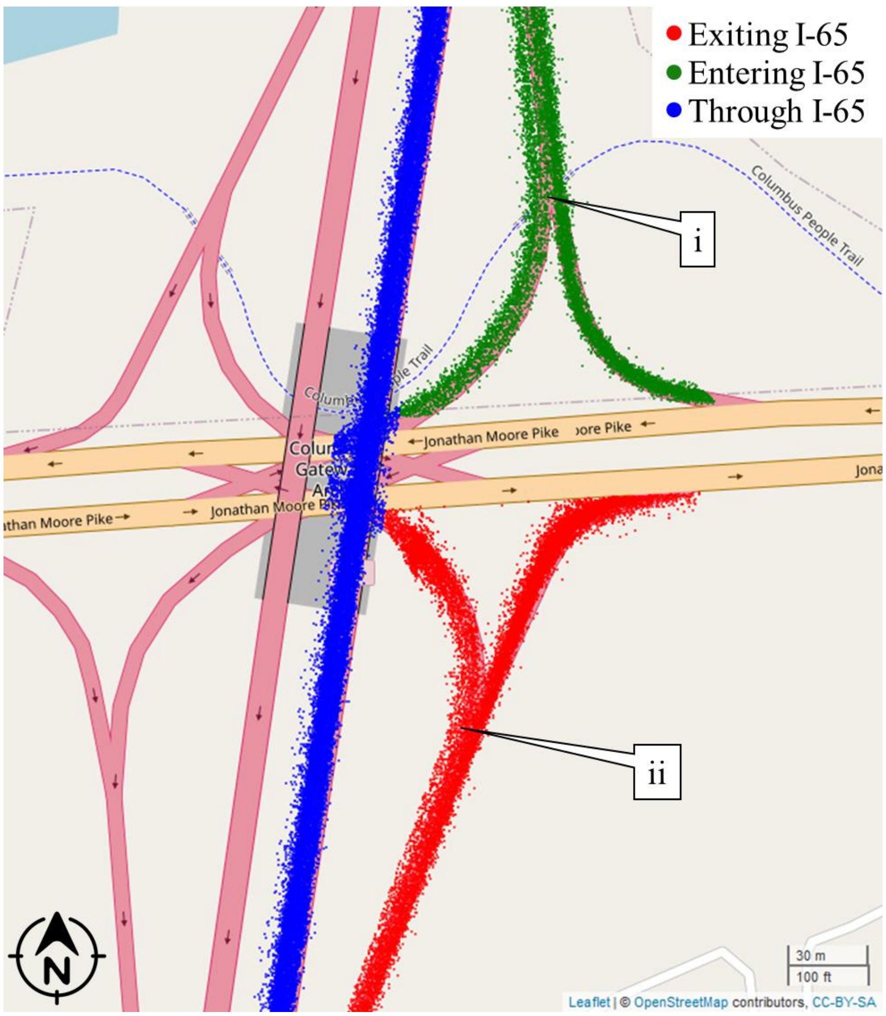

Figure 40. I-65 NB through, exiting and entering trajectory samples at I-65 Exit 68 (July 12-18, 2021)

Once trips have been categorized as exiting, entering and through, each vehicle classification code from an exiting trip is matched with all vehicle classification codes from entering trips that are seen on the entry ramps within 30-minutes of the exiting trip. If a match is found, that particular trip is flagged as one that took a short break at the exit under consideration.

Using the methodology defined above, the analysis was conducted for a 1-week period from July 12-18, 2021 for MM 68 exclusively for the northbound direction of travel. Nearly 8.5 million connected vehicle records from over 61,000 unique trips were observed near this exit. Out of these, approximately 1.5 million records were found to be traveling northbound on I-65 spread over 11,800 unique trips. The results of the analysis conducted on these records have been shown in Table 7.

Table 7. Summary Table of Time Threshold Sensitivity and Number of Journeys Taking a Short Break at I-65 Exit 68 Categorized by Vehicle Type (July 12-18, 2021)

Time Threshold (minutes)	Journeys taking a short break		
	EV	HV	ICEV
30	0	2	260
60	0	2	364
90	0	2	414

We thus see 262 trips (30-min threshold), 366 trips (60-min threshold) and 416 trips (90-min threshold) taking a short break at exit 68 over a 1-week period. This represents at the very least nearly 2% of trips taking a short break at this exit. The scalable nature of this methodology allows practitioners and researchers to apply similar techniques throughout an interstate to find the most utilized exits on a corridor and subsequently plan the placement of additional EV charging infrastructure accordingly so as to provide a good charging level of service to the EV and HV motoring public.

5.1.10 Summary

This study used one week of connected vehicle trajectory data in Indiana to analyze EV and HV usage patterns. Nearly half of all VMTs for EVs and HVs were seen in just the top 10 counties. A spatial analysis highlighted multiple Indiana counties near Indianapolis with highest EV ownership and usage, followed by Allen County in Northeast Indiana and Lake County in Northwest Indiana. (Figure 31,Table 4). Out of nearly 11,600 EVMTs and 49,200 HVMTs on Indiana interstates, I-65 had the largest EV traffic with 2,631 EVMTs (Figure 32c). In general, the average speeds of the EVs were close, but slightly less than HV and ICE, indicated by the left shift on the EV speed distributions (Figure 34).

A graphic of charge stations and charge points versus VMTs for EVs and HVs on a county-by-county basis was used to identify underserved and overserved counties where the charging infrastructure does not match travel demand and vice versa (Figure 38).

Subsequently, a methodology was presented to evaluate percent of EV, HV and Non-EV trips exiting for short breaks at interstate exits. This methodology can be used to obtain most commonly utilized Interstate exits by EVs to further aid in decisions involving the deployment of charging infrastructure to address any under or overserving issues.

There are 24 DC Fast charging stations spread around the state, and the majority of them (75%) are accessible within 1 mile of interstate roadways in Indiana (Table 5). The concept of a "fast charging desert" was introduced to identify long interstate segments that lacked DC Fast charging stations within 1 mile of the Interstate. The study found 11 interstate segments, over 50 miles in length that lacked adjacent DC Fast charging stations. These segments have been shown in Figure 39 and Table 6. Methods to analyze charging station usage (Figure 36) coupled with this analysis of charge gaps can together provide a good overview of existing charging infrastructure performance for stakeholders.

In addition to examining opportunities for fast charging stations, it is also important to look at locations that might be viable for wireless EV charging. This study identified ten 1-mile interstate segments observing highest EVMTs (Figure 33) as an early screening for further evaluation [131]. Not surprisingly, they were near urban areas.

In conclusion, an important question all EV stakeholders are currently facing is balancing investment in areas that have growing EV usage versus investing in underserved areas in an effort to stimulate demand. The performance measures and visualizations put forth in this paper will be important tools for public agencies and private sector partners to use to help inform future policies and investments.

5.2 Scaling Connected Vehicle Data Analytics for Assessing EV Charging Infrastructure Usage and Investment Opportunities in 11 states

5.2.1 Overview

With the projected growth of electric vehicles, there is a need for well-planned and equitable investment in the charging infrastructure. Connected vehicle data holds immense promise to understand the usage of electric and hybrid vehicles and thus inform policy. This paper discusses the use of connected vehicle data to inform decision makers on those investments. Approximately 218 billion connected vehicle records across 1,014 counties in 11 states in the continental United States were analyzed to develop an aggregated dataset of 51 million vehicle miles traveled by battery electric and hybrid electric vehicles over a one-month period in 2021. This dataset was used to assess the current usage of existing electric vehicle charging infrastructure and also suggest metrics for prioritizing investments at the statewide, city and county level. This dataset and companion methodologies illustrate the need for policy makers and automotive OEMs to work together to develop a shared vision on the use of connected vehicle data to inform policy decisions and to ensure that investments in charging infrastructure support equitable adoption of electric vehicles. The article includes links to the data set to provide an opportunity for the ITE community to begin engaging in this technical analysis and provide a framework for further dialogue with policy makers and the automotive OEMs to broaden the vehicles included in this analysis and extend to all 50 states.

5.2.2 Introduction

Sales of electric (EV) and hybrid electric (HV) vehicles increased by approximately 83% and 76% respectively in the past year [134]. The United States government will invest approximately $7.5 billion to expand access to EV chargers with a long term goal of establishing a national charging network [135], [136]. With this investment influx in the EV domain, it is important to incorporate available data sources to ensure strategic and equitable investments in EV chargers and monitor evolving usage patterns for agile adaption of public policy as the charging network is built out.

5.2.3 Data Description

The paper uses an August 2021 data set of connected vehicles (CV) for California, Connecticut, Georgia, Indiana, Minnesota, North Carolina, Ohio, Pennsylvania, Texas, Utah and Wisconsin, to analyze EV and HV usage at the state, city and county level. In this research, a CV refers to a vehicle that shares select on-board data with the original equipment manufacturer (OEM) in real-time. This research focused on identifying fast charging station gaps on long range travel corridors, measuring dwell times near public charging stations, and developing comparative metrics that can be used for inter- and intra-state comparisons. It is believed that the tables, figures and methodologies in this paper will stimulate further dialogue among decision makers and transportation professionals to build upon these CV data driven methodologies to inform public policy and investments.

Table 8 summarizes the coverage of the CV data set utilized as well as details regarding vehicle miles traveled by EV and HV vehicles in those 11 states. Although this is not an exhaustive or unbiased data set, it is a nationally available CV data set that can be obtained in near real-time. Cloud storage and data warehousing services were used to manage and analyze this big data set with modest costs and in a manner that can be easily scaled to all 50 states [2].

Table 8. Summary statistics for 11-state connected vehicle data (August 2021)

State	Counties	CV Records	EV Records	EVMT (mi)	HV Records	HVMT (mi)	Combined EV/HV VMT (mi)
California	58	33.68B	892.67M	18.64M	731.61M	17.06M	35.70M
Connecticut	8	3.31B	17.34M	0.39M	19.24M	0.49M	0.88M
Georgia	159	15.01B	21.49M	0.44M	34.22M	0.80M	1.24M
Indiana	92	11.19B	14.29M	0.34M	34.90M	0.90M	1.23M
Minnesota	87	8.64B	24.74M	0.60M	29.69M	0.84M	1.44M
North Carolina	100	13.12B	26.82M	0.62M	39.70M	1.00M	1.63M
Ohio	88	18.50B	29.84M	0.70M	55.04M	1.43M	2.13M
Pennsylvania	67	14.61B	32.05M	0.68M	47.78M	1.15M	1.82M
Texas	254	54.17B	54.78M	1.13M	82.43M	1.82M	2.95M
Utah	29	2.72B	17.39M	0.38M	18.46M	0.48M	0.86M
Wisconsin	72	9.92B	19.59M	0.51M	30.91M	0.90M	1.41M
Total	**1014**	**184.87B**	**1151.08M**	**24.44M**	**1226.80M**	**26.85M**	**51.29M**

A single connected vehicle trajectory is obtained as a series of waypoints at 1 to 3-second fidelity with a 3-meter geolocation accuracy. Each waypoint provides a timestamp, speed and heading value for the vehicle in addition to a vehicle classification code that helps identify the make and model by using the National Highway Traffic Safety Administration's (NHTSA) Product Information Catalog Vehicle Listing (vPIC) dataset [130] enabling further classification of every record as belonging to an Internal Combustion Engine (ICEV), EV or HV. Each trajectory has a unique anonymized journey identifier attribute, which aids in serializing and connecting the individual waypoints of a single trip. Pairwise haversine distances between consecutive trajectory records of the same vehicle are computed and aggregated to arrive at the electric and hybrid vehicle miles traveled (VMT) numbers shown in Table 8.

Previous studies have indicated this data represents approximately 3-5% of the total vehicles operating in these 11 states [55]. Approximately 218 billion records of third-party crowdsourced CV data, corresponding to over 515 million trips, were distilled down to an aggregated county-level dataset representing nearly 7 million trips and 51 million miles traveled by EVs and HVs in August 2021. California had the highest volume of EVs and HVs in this CV dataset, with more than 892 million and 731 million records respectively, while Texas on the other hand showed the highest overall volume of connected vehicle data with 54.17 billion records.

Data on EV charging stations and number of plugs was obtained using the National Renewable Energy Laboratory's (NREL) alternative fuel stations API [132]. SAE J1772 and Combined Charging System (CCS) are the charging standards for the electric vehicles analyzed by this study.

5.2.4 Aggregation of EV and HV Data by County

Vehicle miles travelled for 1,014 counties in the 11 states were tabulated. To illustrate the spatial variation in EVMT by county, a three-state view spanning Indiana, Ohio and Pennsylvania with counties colored by EVMT is shown in Figure 41a. Franklin county in Ohio (callout i, Columbus area) had the highest miles traveled by EVs for this three-state region for the month of August 2021. Additional high EVMT travel was also observed in the following Ohio counties, Cuyahoga (callout ii, Cleveland area) and Hamilton (callout iii, Cincinnati area). In Pennsylvania, counties with high EVMT were Allegheny (callout iv, Pittsburgh,) and Montgomery (callout v) and Philadelphia (callout vi) in the Philadelphia area. In Indiana, Marion County (callout vii, Indianapolis area) had the sixth highest EVMT in the three-state region.

5.2.5 Interstate Charging Deserts

Fast charging deserts, defined in previous literature [106] as segments of interstate roadway longer than 50 miles with no fast charging station available within a mile of the interstate, are an effective screening tool for charge station siting towards aiding long range EV travel and alleviating range anxiety among current and potential EV adopters. Figure 41b shows the Interstate-70 (I-70) corridor passing through Indiana, Ohio, West Virginia and Pennsylvania, with solid red circles representing DC Fast (Level 3) charging stations in the four states, solid black lines indicating fast charging deserts, and translucent green segments indicating segments of I-70 with adequate access to fast charging. Five distinct deserts are observed on this interstate corridor, passing through counties that show little to no EV activity. Thus, this figure presents a strong case for expanding charging capacity to curb range anxiety, encourage inter-city travel, and to connect rural communities by EV. Of note is the location of charging deserts at the borders of states, emphasizing the importance of collaboration with adjacent states in addressing range anxiety as these types of analysis are performed on a national level for Interstates and perhaps the entire national highway system.

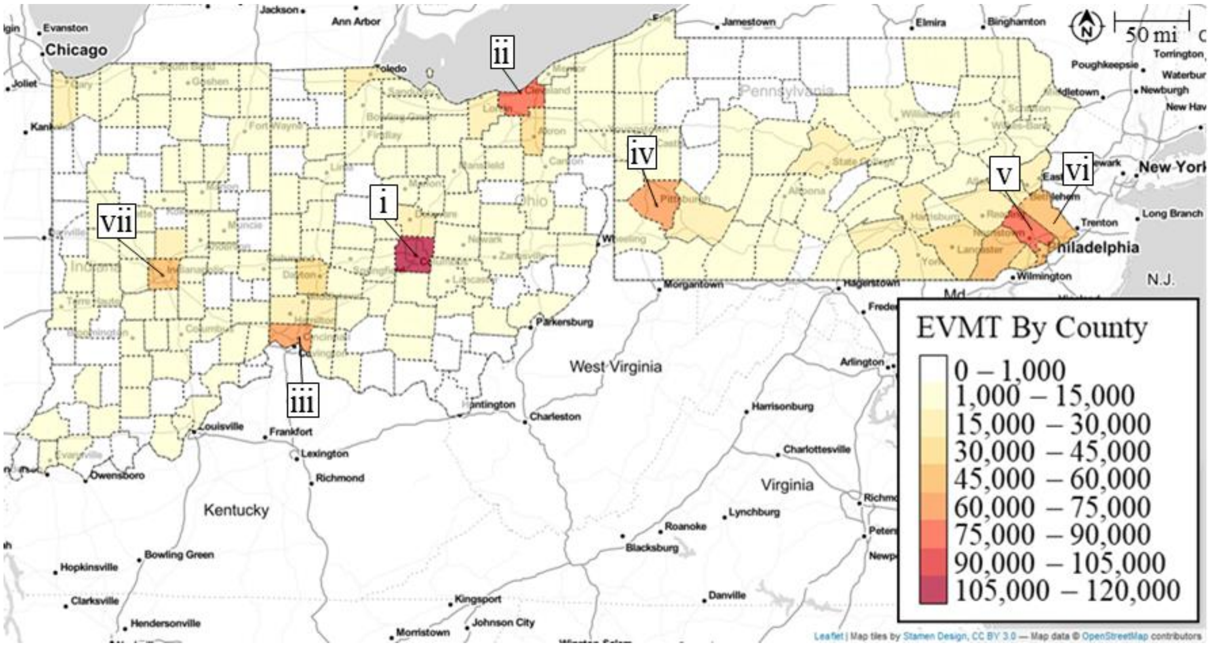

(a) EVMT by county for Indiana, Ohio and Pennsylvania (August 2021)

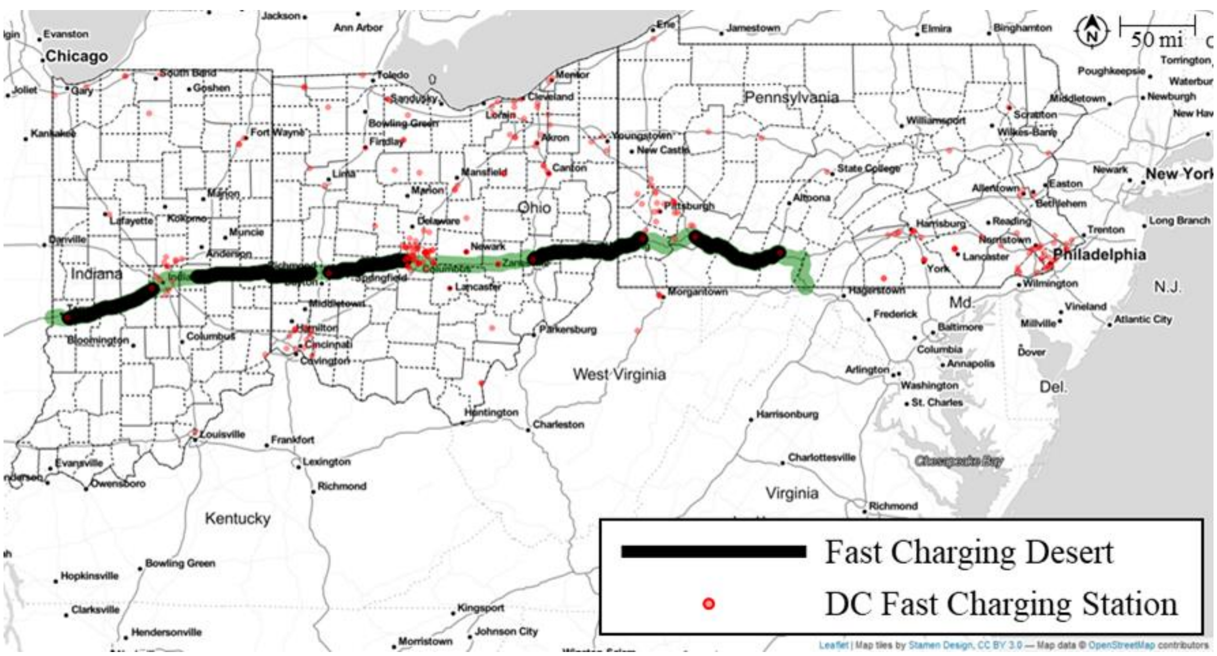

(b) Fast charging deserts on I-70 corridor through Indiana, Ohio, West Virginia and Pennsylvania

Figure 41. Visualization of EVMT and fast charging deserts

5.2.6 EV Dwell Time near Public Charging Stations

Some of the past research has focused on modeling, simulating and subsequently forecasting the demand of EV charging [137]–[139] to identify potential locations for siting new stations primarily at the local level. However, the availability of real-world CV data now provides researchers and policy makers with the ability to evaluate in significant detail real-time charging station usage across the nation to further augment existing models and allow for more informed decision making. In this study, EV trajectories within 100 feet of level 2 and level 3 charging stations were extracted for a parking lot-level analysis of dwell times. The analysis focuses on dwell times instead of charging times due to limitations on the availability of charging status / plugged-in attributes in the CV data set. Pairs of discontinuous electric vehicle journeys which represent the same manufacturer year, make, model, motor and vehicle descriptor, and end and resume within a spatial threshold of 3 meters of each other (nominally a parking spot level resolution), were paired and subsequently classified as dwell sessions. A temporal filter of dwell sessions between 5 minutes and 72 hours was also applied to remove outliers. Locations with both level 2 and level 3 charging points next to each other were also discarded.

Dwell session times in the vicinity of Level 2 and Level 3 charging stations across 1,101 cities spanning the 11 states were aggregated for the month of August and are represented in Figure 42. Due to the comparatively high EV usage in the state of California, two versions of the plot are shown, one that ranks the top ten among all 1,101 cities (Figure 42a), and another that ranks a subset of 612 cities that exclude California (Figure 42c), to provide a more holistic look at the remaining states without their statistics being dwarfed in comparison. Figure 42b and Figure 42d provide similar graphics delving into dwell session times in the vicinity of only Level 3 charging stations, with Sacramento, Los Angeles, Atlanta and Austin showing significantly high total dwell times, with per session dwell time averages of 0.96, 1.00, 1.87 and 0.82 hours respectively. Statewide and multi-state analysis of dwell sessions shown in Figure 42 can help identify cities most in need of additional charging infrastructure. Further analysis at specific sites on an hour by hour level could also be used to identify hour by hour utilization patterns to identify periods where peak demand warrants investment in additional charging points.

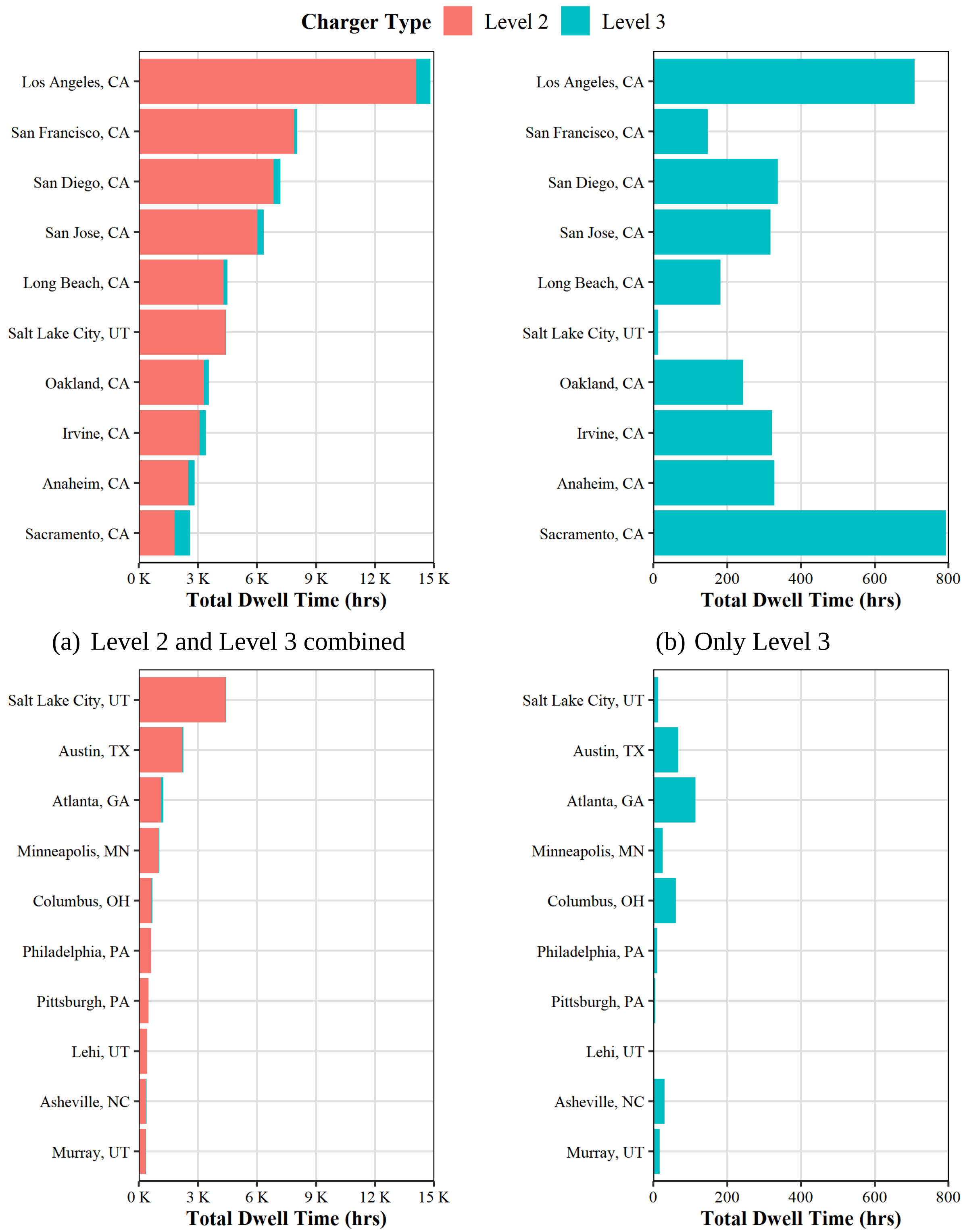

(a) Level 2 and Level 3 combined

(b) Only Level 3

(c) Level 2 and Level 3, excluding CA

(d) Only Level 3, excluding CA

Figure 42. Top 10 cities with highest EV dwell time in the vicinity of Level 2 and Level 3 charging stations (August 2021)

5.2.7 Methodology to compare investment opportunities

A previous study conducted using CV data for a week in the state of Indiana in July 2021, proposed a methodology to compare the relationship between electric vehicle miles traveled (EVMT) aggregated at the county level with the number of EV charging points or plugs (Level 1, 2 and 3) available in a county. This methodology was extended to analyze the 11 states in this study. A representative predicted linear relationship plot for counties in the state of Pennsylvania, along with individual data points for each of the 67 Pennsylvania counties is shown in Figure 43. Counties near the horizontal axis represent areas underserved by charging infrastructure, while those near the vertical axis represent a high availability of charging infrastructure not matched by corresponding EVMT and might be considered overserved.

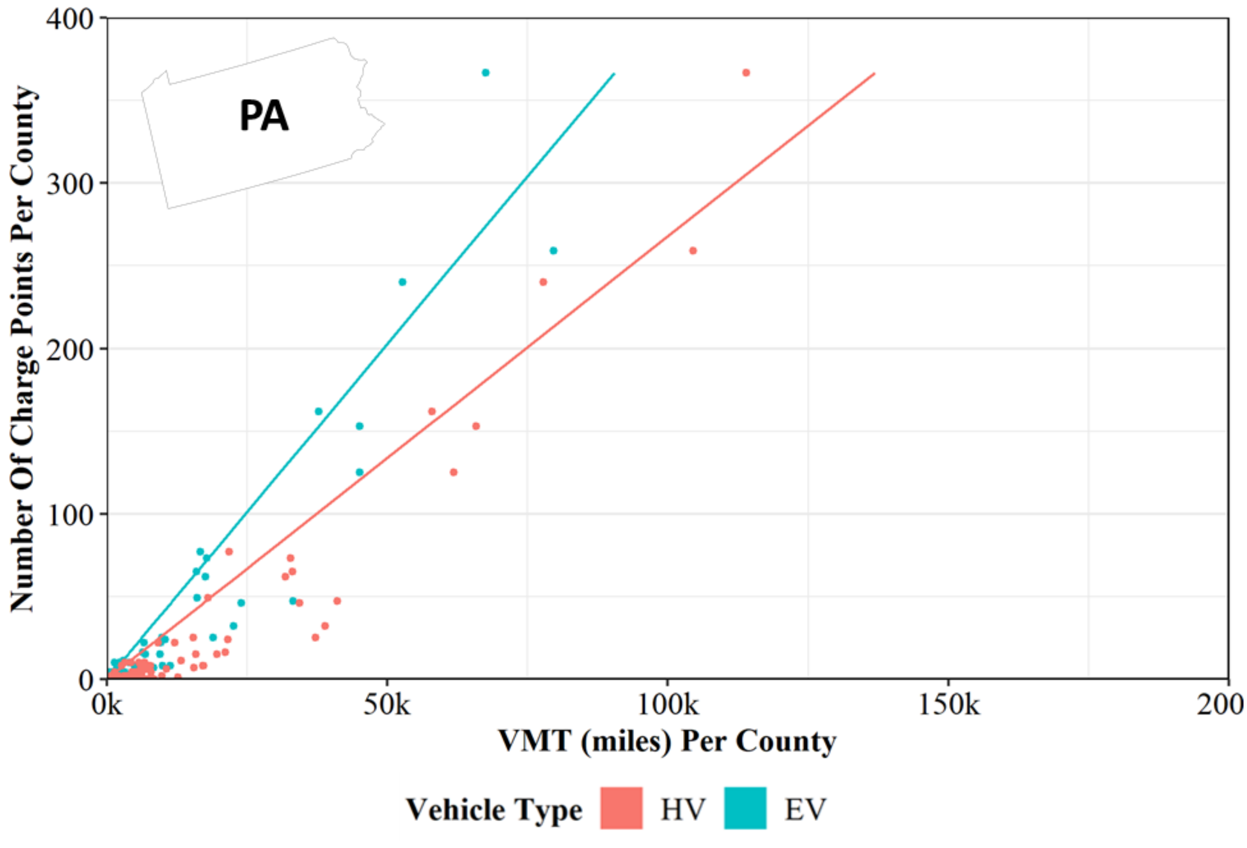

Figure 43. Relationship between number of charge points in a county (Level 1, 2 and 3) and VMT for EVs and HVs in Pennsylvania (August 2021)

5.2.8 Comparative Analysis of Charging Infrastructure Across 11 States

Using the methodology covered in the previous section, a single visualization to compare the current state of charging infrastructure across the 1,014 counties in 11 states is shown in Figure 44 with callouts pointing to the respective predicted linear regression lines for each state. Lines closer to the vertical axis indicate states that may be classified as comparatively overserved by charging infrastructure, while those leaning towards the horizontal axis indicate states underserved by charging infrastructure, showing high number of miles traveled by electric vehicles, however with a low number of charge points per county. Comparative analyses such as these can serve as an effective initial filter in deciding allocation splits for charging infrastructure investments at the statewide and county level.

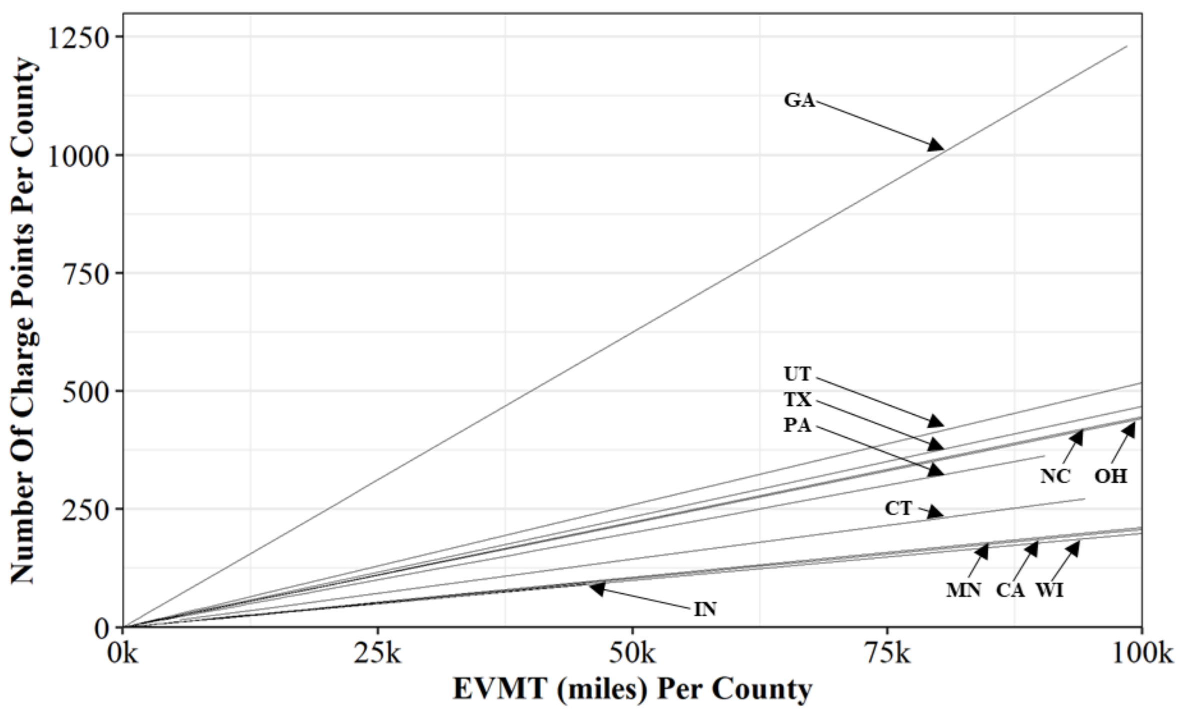

Figure 44. Linear regression lines for number of charge points in a county (Level 1, 2 and 3) versus EVMT for 11 states (August 2021)

5.2.9 Metrics for evaluating equitable charging infrastructure investment opportunities

Using the aggregated dataset of vehicle miles traveled by EVs and HVs spatially grouped by county, an ordinal ranked visualization was developed depicting an average estimate of EVMTs per available charge point in a county. Figure 45 shows this ordinal ranked plot, with the top ten counties in the study location showing the highest EVMT per charge point tabulated along with the number of charge points (Level 1, 2 and 3) and percentage of rural land area in each, led by Columbia County, Wisconsin. The statewide county rankings may be used as a high-level performance measure to easily compare charging infrastructure capacity between multiple states. This visualization provides a quick insight into locations in a state that might be evaluated for further investment in charging capacity to satisfy current consumer demands. Of particular note, the top 10 counties as shown by the inset table in Figure 45 are overwhelmingly rural, with only 1 or 2 charge points per county. Although a large proportion of rural EV owners do in fact charge at home, this graphic suggests that it is important not to overlook rural counties during the early investments in EV charging infrastructure and pay close attention to hourly usage patterns at the relatively small number of charge points.

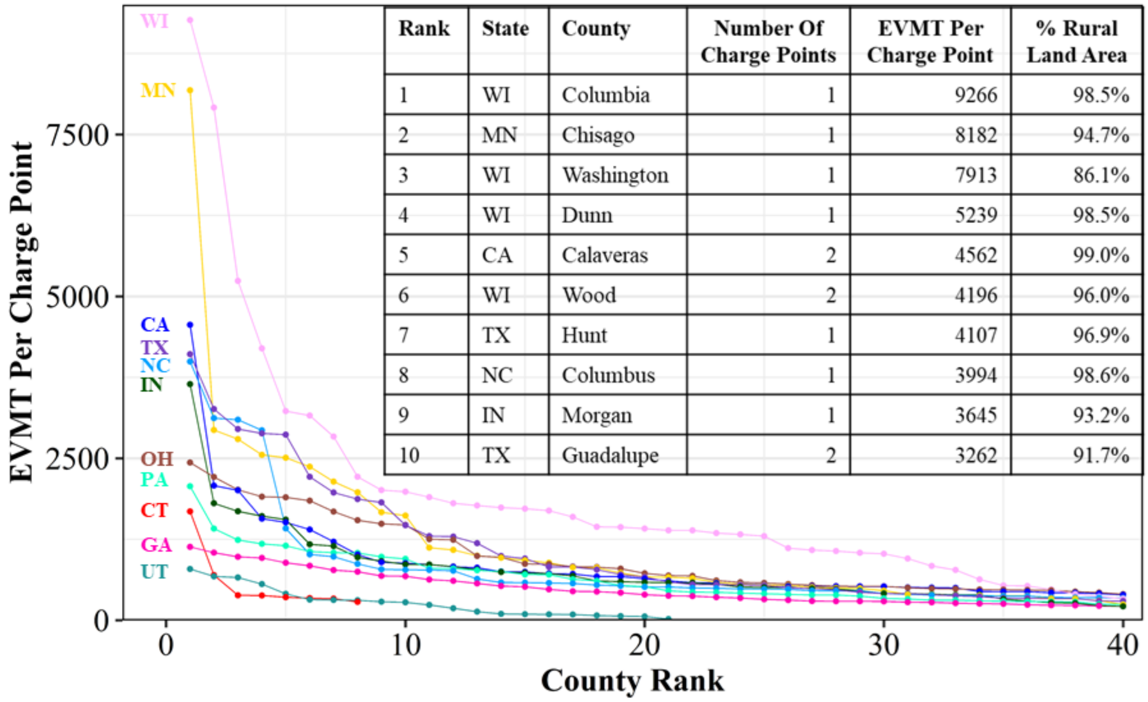

Rank	State	County	Number Of Charge Points	EVMT Per Charge Point	% Rural Land Area
1	WI	Columbia	1	9266	98.5%
2	MN	Chisago	1	8182	94.7%
3	WI	Washington	1	7913	86.1%
4	WI	Dunn	1	5239	98.5%
5	CA	Calaveras	2	4562	99.0%
6	WI	Wood	2	4196	96.0%
7	TX	Hunt	1	4107	96.9%
8	NC	Columbus	1	3994	98.6%
9	IN	Morgan	1	3645	93.2%
10	TX	Guadalupe	2	3262	91.7%

Figure 45. EVMT per charge point by county (Level 1, 2 and 3) and grouped by state (August 2021)

5.2.10 Summary

Significant recent investments from the public and private sector alike merit a growing need for transportation researchers to use CV data to inform policy and resource allocation decisions to ensure a well-planned and equitable investment in EV charging infrastructure. Over 218 billion connected vehicle records across 11 states (Table 8) were utilized in this study to propose easily scalable methodologies and visualizations that can inform this decision-making process. Visualizations that rank charging infrastructure usage at the statewide (Figure 44), county (Figure 45) and city (Figure 42) level were proposed and may help prioritize resource allocation informed by real-world EV usage trends thus providing quantitative evidence to support policy and investment decisions.

While a sample dataset covering 1,014 counties of a total of 3,007 counties in the United States was utilized for this study, the techniques described can easily be scaled to the nationwide level to include data from a broader range of automotive OEMs as well as at further granularity at the

73,057 census tracts and 41,692 zip codes level. To demonstrate the national scalability of this aggregated dataset and to encourage dialogue among the transportation community on additional technical analysis, this aggregated data has been published as a public dataset available at a repository [140].

Connected vehicle data hold immense promise in future research to understand the usage of electric and hybrid vehicles and thus inform policy, without any additional requirement for investing in intelligent transportation systems (ITS) infrastructure. A more granular spatial analysis in close conjunction with sociodemographic census data may help researchers and policy makers analyze factors affecting EV adoption and demand and help forecast market saturation timelines. A nationwide analysis spanning all 50 states and multiple automotive OEM datasets would provide a unique high-level look at strategic opportunities for directing equitable charging infrastructure investment.

Although the current commercially available CV data does not represent the entire EV fleet, nor does it represent all EV OEMs, actively integrating CV data into public policy decisions provides an opportunity to begin developing data driven investments and at the same time open conversations with automotive OEMs on how to most effectively partner with them to inform public policy and not compromise their business interests.

6. ANALYSIS OF ROUTE CHOICE DURING PLANNED AND UNPLANNED ROAD CLOSURES

The information presented in this chapter has been submitted for review to the IEEE Open Journal on Intelligent Transportation Systems.

This chapter discusses visualizations, methodologies and performance measures leveraging CV data towards analyzing route choice behavior among motorists traversing through or around an active freeway incident resulting in roadway capacity reduction by means of a planned or unplanned road closure.

6.1 Overview

The Federal Highway Administration (FHWA) Alternate Route Handbook proposes guidance to identify alternate routes during planned and unplanned road closures. A challenge with this process is the lack of traffic data available to decision-makers. High volume corridors experiencing unplanned closures can provide a rich case history by systematically collecting connected vehicle (CV) data during such incidents. CV data provide the ability to directly measure actual diversion routes and travel times during an ongoing or historical incident. This paper presents methodologies to systematically analyze diversion data to identify the most common alternate route choices and impacted interstate exits, valuable information for public safety and transportation agencies to evaluate the surrounding road network's resiliency in accommodating diverting traffic. Agencies can use this information to proactively deploy resources (officers, signs, barricades) at critical locations during future closures. The scalability of this methodology is demonstrated by evaluating 12 additional cases to assess diversion rates found to be in the range of 58% to 93% for total closures exceeding five hours. The paper concludes by recommending agencies apply these methodologies to develop data-driven diversion strategies on critical routes coupled with real-time CV monitoring in dispatch centers to provide agile adjustment of resources along diversion routes.

6.2 Introduction

The Federal Highway Administration (FHWA) Alternate Route Handbook [141] identifies construction, crashes, inclement weather and natural disasters as events that may result in significant traffic diverting on to alternate routes. The first phase of the three-phase process proposed by the FHWA suggests using historical volumes, travel demand models and anecdotal evidence from public safety to identify alternate routes. In many cases high volume corridors experience sufficient unplanned closures, such that systematically collecting CV data during these incidents provides a rich case history to identify alternate routes used by motorists. Such empirical techniques effectively use crowdsourced data to identify usage patterns during the early phases of an incident as well as later phases of the incident when the network is close to reaching perceived user equilibrium. This real-life empirical data can then be used in conjunction with the FHWA Alternate Route Handbook to develop well-planned diversion management strategies that are consistent with motorists' actual choices.

6.3 Literature Review

Past research has utilized Bluetooth matching, wi-fi scanning, license plate matching among other field observation techniques to capture diversion rates and route choice behavior among motorists in spatially and temporally controlled studies. An unplanned bridge closure in northwest Indiana utilized 11 Bluetooth Monitoring Stations to evaluate the mobility impact of trip distributions along four prescribed alternate routes [51]. Bluetooth probe tracking techniques have been implemented on interstate work zones in the past to assess travel time reliability and evaluate work zone mobility performance [48]. A global positioning system-based vehicle activity data study of 467 instrumented vehicles in Atlanta, Georgia, analyzed driver-level behavior for route choices on morning commutes [142]. Researchers have proposed the use of widespread cellular signal towers and signaling events generated by devices moving from the influence area of one tower to another to track vehicular movement and estimate route choices [143]. One such floating phone data study using 1.4 million records in Germany was able to analyze route choice behavior and its dependence on radio broadcasts, traffic management center notifications and variable message sign recommendations [144]. Probe-vehicle studies have utilized a limited set of vehicles to study dynamic route choice behavior to augment existing static route choice models [145], [146]. Stated preference survey approaches and discrete choice models have captured user-level preference on route choice and the factors affecting it, including variable message signs, radio traffic information among others [147]–[150]. However, results from these existing techniques run the risk of presenting inherent spatial and temporal inaccuracies and may only provide approximate estimates of travel time, limitations that can be addressed by CV data. Concurrently, while researchers have long modeled route choices [151]–[153] at the link, path and system level, CV data has the ability to augment those models with real-world data lending further confidence to modeling estimates.

Segment-based probe-vehicle data have been used by agencies in Indiana to monitor queuing and congestion on a detour route lacking traditional intelligent transportation system (ITS) infrastructure during an unexpected interstate closure on Interstate 65 (I-65) [52]. However, recent studies on short-term and long-term interstate construction work zones in Indiana have already shown promise in the applicability of CV data to evaluate impacts of diverting traffic from interstates on traffic signal performance of the surrounding road network, as well as in computing detour rates and travel time estimates during construction periods [154], [155]. CV data aggregated by a 19-day floating car fleet study on the German freeway network were able to demonstrate the travel time benefits obtained by navigating around freeway congestion, and the progression of these benefits from the occurrence of an incident to eventual road clearance [156]. These encouraging approaches have paved the path for applying large scale real-world CV data towards route choice analysis.

6.4 Objectives

The objective of this study is to use CV data to develop scalable techniques that systematically analyze diversion patterns associated with significant road/lane closures on major highways. The proposed techniques classify trips along the corridor as on-route, diversion, or a trip chaining activity. Associated metrics of travel time and route length are computed. These techniques provide the empirical data-driven foundation for agency after-action reviews, pre-planned diversion strategies, and tactical monitoring during an incident with significant diversion.

6.5 Data Description

A commercially available CV dataset which represents about 4-5% of all passenger vehicles in Indiana was utilized for this study [55]. Trajectory waypoints were obtained at 3-second reporting frequency with a geolocation accuracy of 3-meters. Each waypoint has the following information provided with it: latitude, longitude, timestamp, speed, heading, and an anonymized unique trajectory identifier. A vehicle's journey can be determined using the trajectory identifier as it navigates through or around an active freeway incident.

6.6 CV Visualization of Closure Impact

A bus crash in the northbound (NB) direction on I-65 in White County, Indiana on June 11, 2021 resulted in a complete closure of northbound lanes for approximately 6 hours and slowed traffic in the opposing direction while recovery efforts were underway [157]. Public safety and emergency management resources from neighboring cities and counties were deployed to manage diverting traffic.

Figure 46 presents a trajectory heatmap for this incident occurring at approximately 12:38 PM at mile marker 189. Each of the 535 trajectories shown is linearly referenced to interstate mile markers. The color of the vehicle trajectories at a particular location corresponds to the vehicle speeds shown in the legend. The horizontal axis on the heatmap represents the time of day, while the vertical axis represents the location along the analysis corridor. Mile marker 164 to 200 is shown in order to capture the upstream and downstream impacts of this incident. Each interstate exit within this region is marked by a solid black horizontal line. As vehicles leave the interstate, a drop in CV volumes is visualized. A hollow ellipse at Exit 188 highlights one such group of trajectories that appear to end at mile marker 188, where the interstate was closed to provide a diversion opportunity. A similar hollow ellipse at Exit 193 highlights a location where vehicles rejoined the interstate.

Hard-braking events, representing a deceleration of 8.76 ft/s^2 or greater on a CV trajectory (defined by the data supplier), are depicted by solid red diamonds and clearly indicate vehicles braking at the back of a queue on encountering slow moving or stopped traffic. Queues resulting from this incident at mile marker 189 were found to stretch as far back as mile marker 171 shown by the slow-moving purple trajectories (speeds of 0 to 14 miles per hour) in Figure 46. Blank areas on the heatmap spanning approximately from 1 PM to 7 PM between exits 178 and 193 correspond to total road closure with minimal to no CV trajectories passing through that segment.

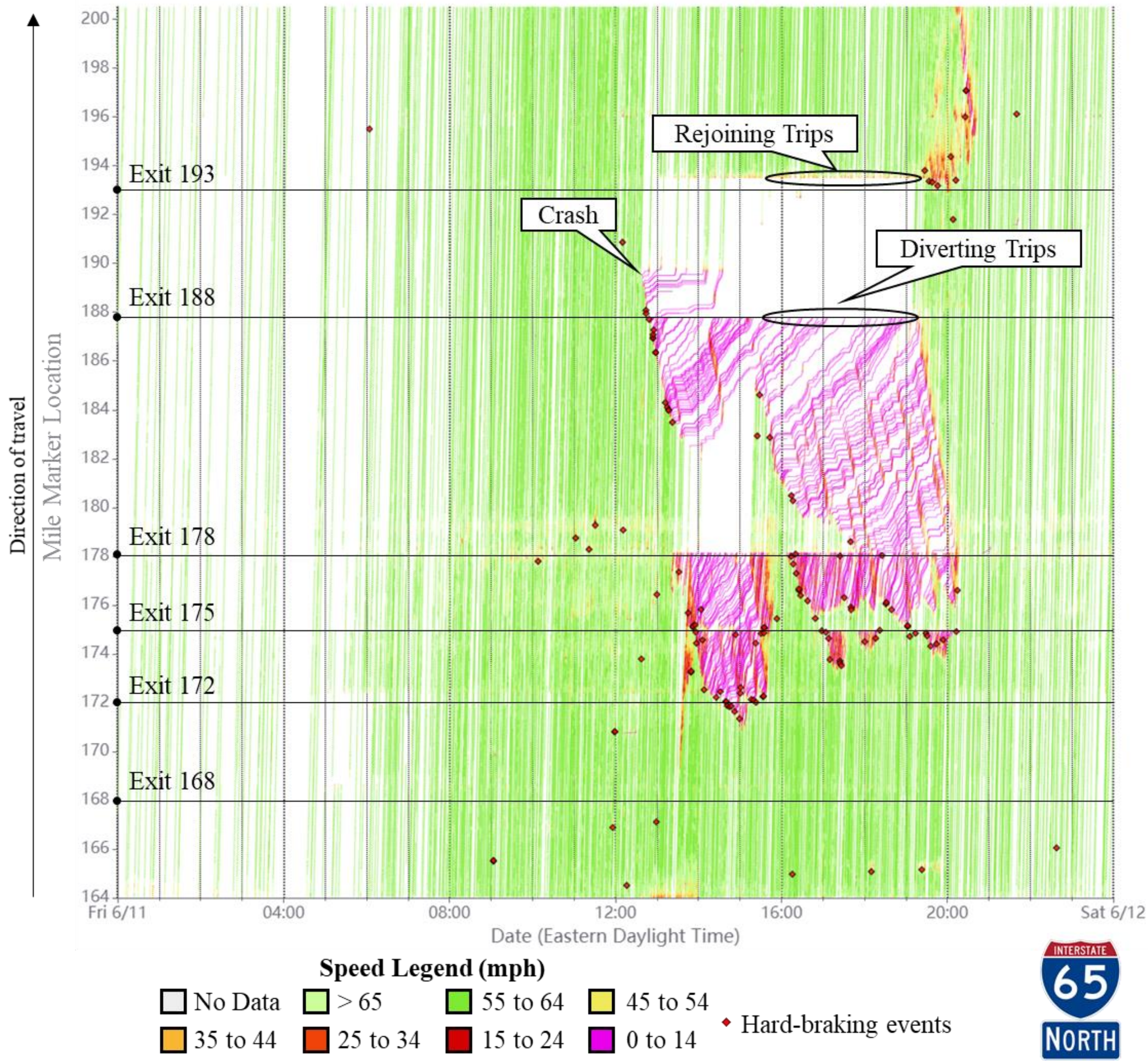

Figure 46. Trajectory heatmap showing CV trajectories and hard-braking events for an unplanned closure caused due to a crash incident on I-65 NB (June 11, 2021)

6.7 Trip Travel Time

Figure 47 shows a scatter plot representation of travel times experienced by trips traversing the 36-mile analysis region of I-65 NB between mile marker 164 and 200. The location of a datapoint on the horizontal axis is determined by the timestamp at which the trip entered the analysis corridor at mile marker 164. The free-flow travel time on this segment is typically 31 minutes.

The crash incident that resulted in the unplanned closure was reported to have occurred at 12:38 PM as indicated by the solid black vertical line on the plot. Callout i points to an example of a free-flowing trip that did not leave the interstate. Callouts ii and iii correspond to examples of trip chaining, confirmed upon further examination showing the trip leaving and rejoining the interstate at the same interchange thus resulting in a higher than expected travel time. Trips entering the study area at mile marker 164 just after 12:00 PM were impacted as they approached the impending crash 25 miles away. Callouts iv, v and vi represent examples of vehicles that chose an alternate route to navigate around the road closure. A significant increase in travel times from a base value of 30 minutes to as high as 4 hours was seen in the period following the incident. The wide range of travel times seen after 12:38 PM highlights the diversity in routes chosen by the CVs, one of the prime analysis objectives for this study.

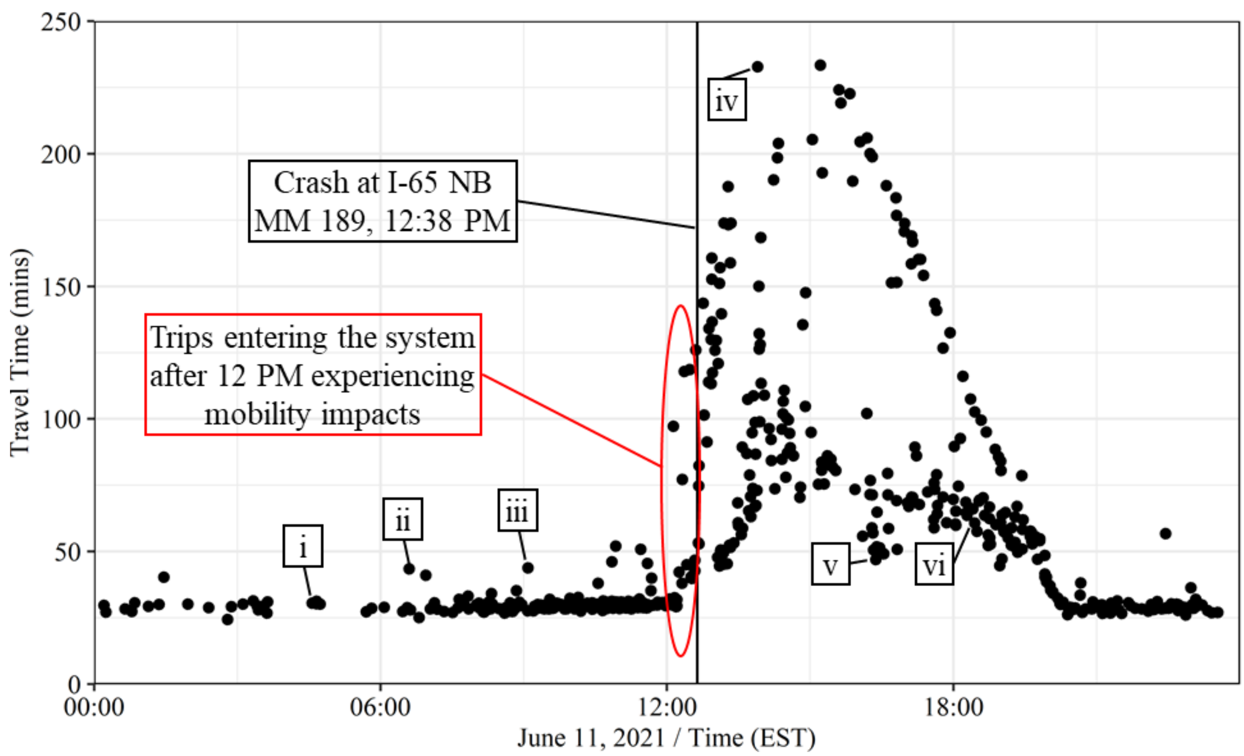

Figure 47. Diversity of travel times experienced by CVs passing through region of unplanned closure on I-65 NB (June 11, 2021)

6.8 Route Choices

It is quite easy to measure which exit observes the most vehicles departing the interstate and then rejoining downstream. Map matching analysis in the vicinity of interstate exits using CV trajectory data allows us to easily identify trips traveling through on the interstate from those utilizing the exit ramps to leave the interstate. Table 9 tabulates the percentage of trips leaving the interstate at each of the six exits shown in Figure 46. Exit 178 observed the highest portion of traffic leaving the interstate (18.5%), while exit 175 saw the highest mean ramp delay (12.7 minutes) experienced by vehicles exiting the interstate. This high delay is likely due to a combination of relatively high diverting volume and an intersecting state road that was relatively close to capacity. The mean ramp delay for each vehicle exiting the interstate was computed as the amount of time taken to pass through a half-mile radius geofence built around the center of the interchange. Metrics such as the percent of trips exiting and ramp delay at exits shown here provide a high-level overview and quantitative indications of queue propagation and mobility impacts caused upstream of a freeway incident.

Table 9. Percentage of trips leaving the interstate and ramp delays experienced at six exits in analysis corridor (June 11, 2021)

Exit	**County**	**% leaving interstate**	**Mean ramp delay experienced (mins)**	**Median ramp delay experienced (mins)**
Exit 168	Tippecanoe	0.8%	3.0	2.6
Exit 172	Tippecanoe	4.3%	9.3	7.3
Exit 175	Tippecanoe	12.1%	12.7	3.2
Exit 178	Tippecanoe	18.5%	6.9	4.8
Exit 188	White	12.3%	9.3	9.0
Exit 193	White	-	-	-

Figure 48 shows a map view of routes taken by vehicles called out in the travel time plot in Figure 47. Figure 48a shows a vehicle that stayed on the interstate throughout before the incident occurred, indicating a free-flowing trajectory. Figure 48b shows a route that involved trip chaining at exit 172 (pointed to by callout ‘Trip chaining’ in the Lafayette area) and rejoined the interstate, resulting, as one would expect, in a longer travel time. Figure 48c and Figure 48d show examples of trips making an alternate route choice. One such alternate route shown in Figure 48e observed a trip leaving the interstate at exit 175 and rejoining at exit 193, while crossing over the Wabash River using a single-lane bridge on state route (SR) 225 (Figure 48f) with a posted weight restriction of 12 tons. This alternate route choice, adopted by many passenger vehicles, unfortunately was also chosen by at least 40 heavy trucks. Subsequently, the SR 225 bridge, which had a weight limit of 12 tons, required emergency closure for inspection and repair [158].

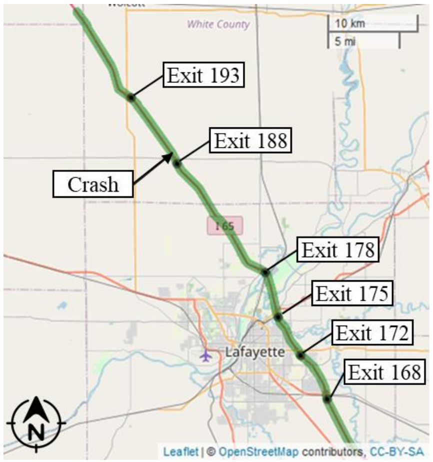

(a) Route corresponding to travel time i

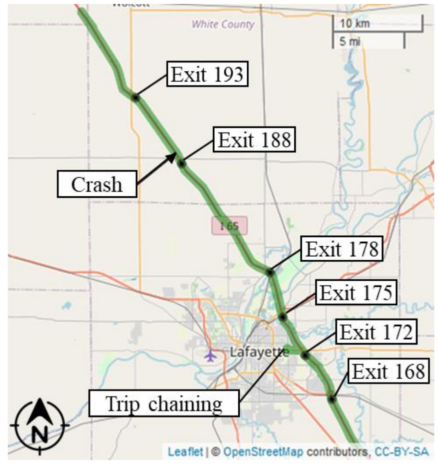

(b) Route corresponding to travel time ii

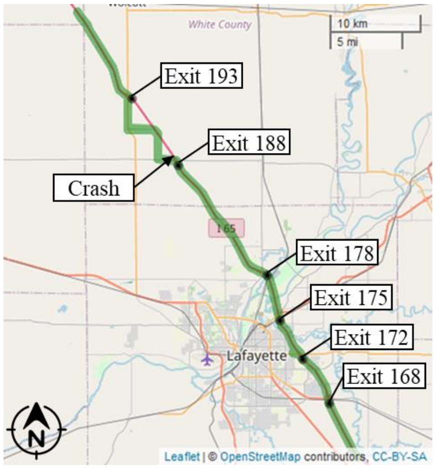

(c) Route corresponding to travel time iv

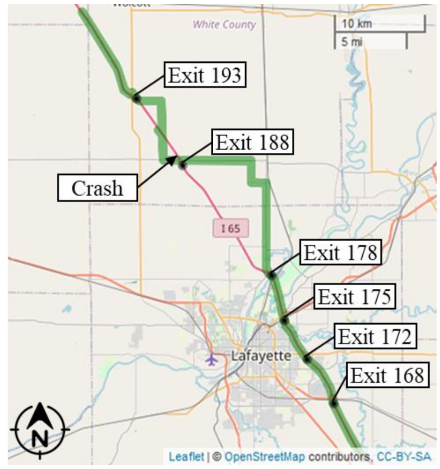

(d) Route corresponding to travel time v

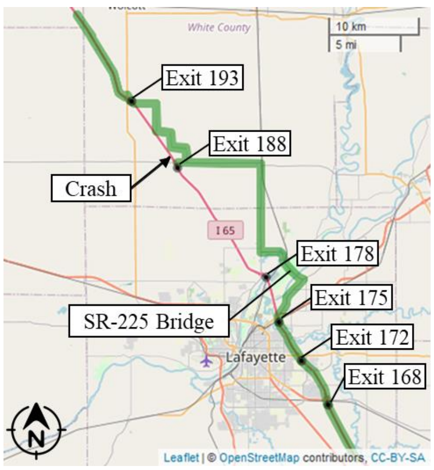

(e) Route corresponding to travel time vi

(f) Single lane bridge on SR-225 [159]

Figure 48. Diversity of route choices adopted by CVs (June 11, 2021)

6.9 Methodology

6.9.1 To Identify Instances of Trip Chaining

While trip chaining as a concept is recognized among transportation practitioners and researchers, multiple different definitions have been utilized to identify a chained trip in past studies. Two of the most commonly accepted ways to define a trip chain involve a start and end at the same anchor location (such as 'home'), or a sequence of trip segments with multiple stops between two anchor locations [160]. For this study, a slightly modified interpretation of trip chaining is broadly defined as a sequence of trip segments between a pair of anchor points, namely the start and end points of the chosen interstate analysis corridor (mile markers 164 and 200 respectively for the I-65 case study presented in Figure 46), involving a significant departure from the base route and subsequent rejoining at the same interchange.

Figure 49 shows an example of such a trip chaining instance, wherein a journey departs the interstate to a rest area (Wolcott Rest Area on I-65 NB in the analysis corridor) and rejoins the interstate after a short break, resulting in a higher than normally expected travel time. However, such trips, if misclassified as an alternate route and not identified to be trip chaining, may lead to mischaracterization of travel time statistics and reliability metrics on a corridor.

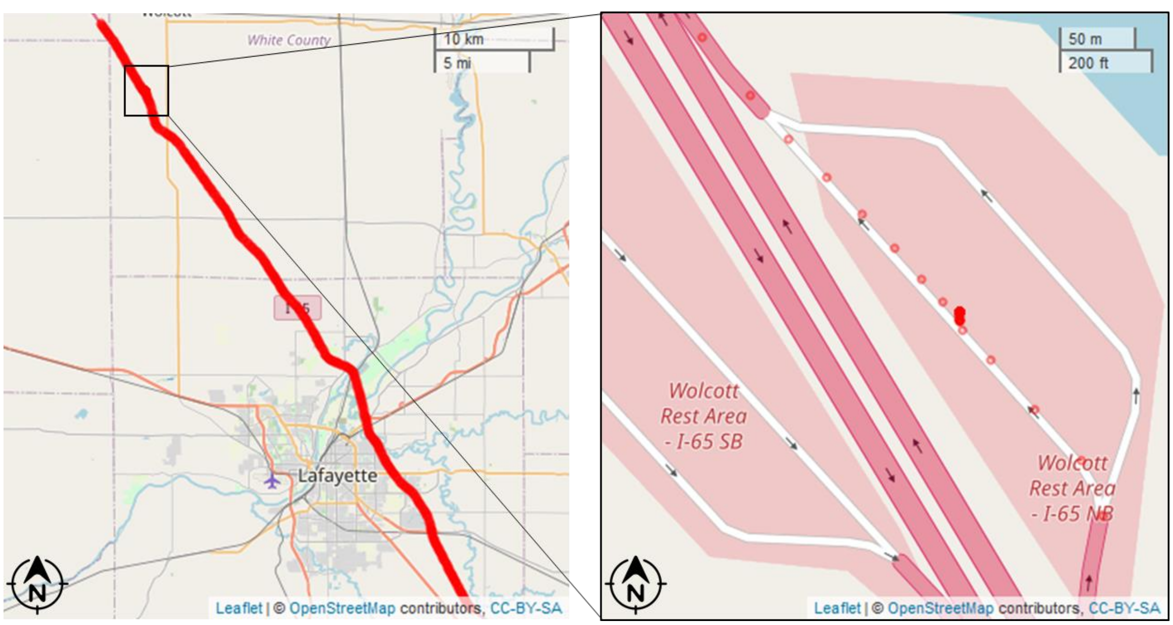

Figure 49. Instances of trip chaining (example corresponding to travel time iii of 43.8 mins from Figure 47)

A methodology proposed in this paper can be used to identify such instances of trip chaining so as to prevent biasing travel time estimates or incident clearance performance measures. Figure 50 shows this methodology in finer detail as a six-step process. The first step (Figure 50a) involves identifying the base route (translucent blue polygon, 120 feet wide to cover all lanes of traffic) defined by the virtual origin and destination gates on the interstate roadway. The second step (Figure 50b) shows an overlay of a CV trajectory's individual waypoints as red circles on the translucent blue polygon showing the base interstate route. This step is then followed by identifying the portion of the CV trajectory that overlaps with the base route (Figure 50c) and identifying parts of the journey not overlapping the interstate (Figure 50d). To determine a trip chaining event, the first (callout F) and last (callout L) waypoints of the non-overlapping portion of a journey are extracted (Figure 50e) and matched to the nearest linear referenced mile marker on the interstate (Figure 50f). If the gap in matched mile marker locations for these waypoints is under a mile, it alludes to a journey having exited and rejoined the interstate at the same interchange/rest area following a brief stoppage, thus confirming a trip chaining event. This methodology is leveraged throughout this study to separate instances of trip chaining from diversions.

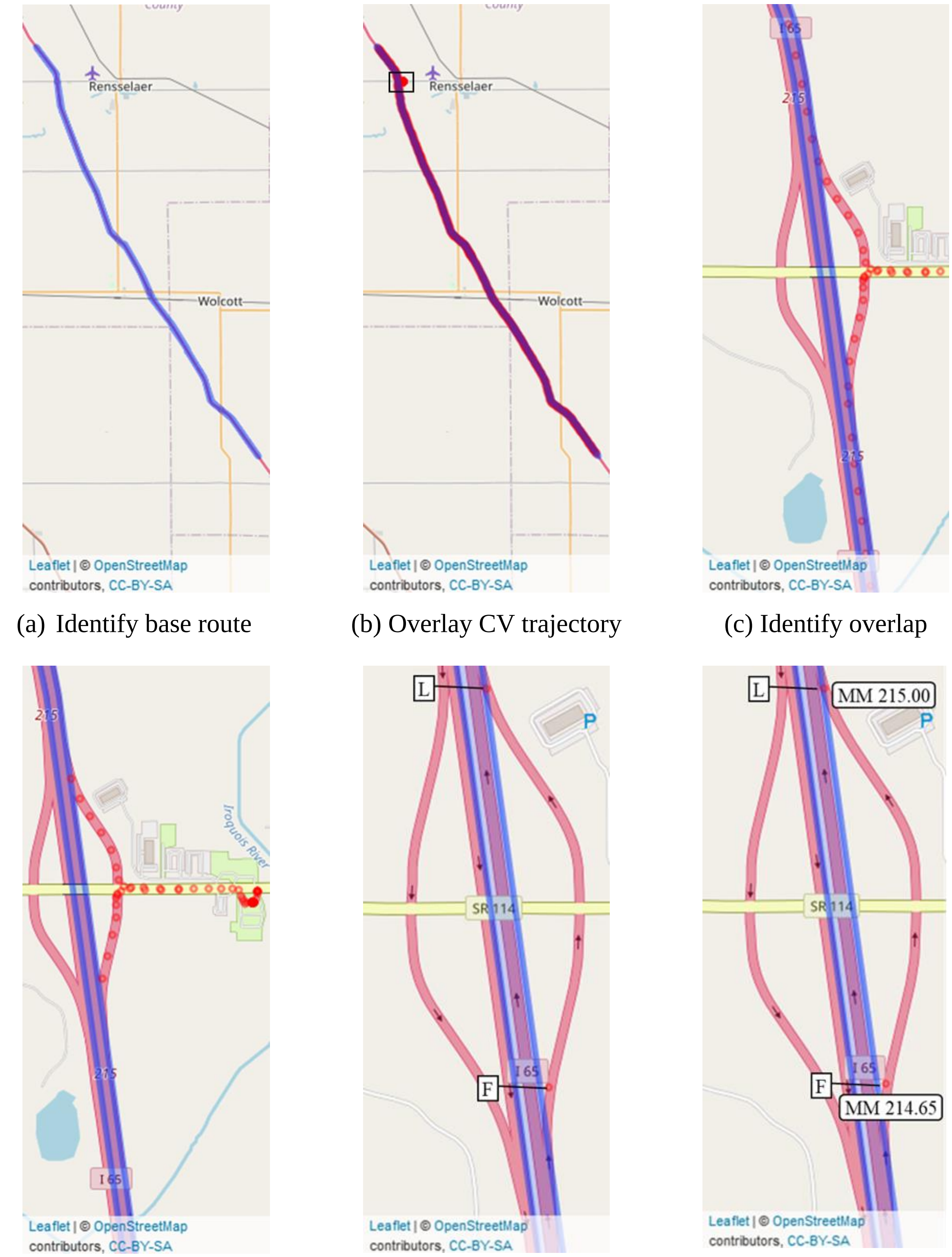

(a) Identify base route

(b) Overlay CV trajectory

(c) Identify overlap

(d) Isolate non-overlapping waypoints

(e) Identify departure and rejoining onto base route

(f) Validate if trip chain occurred at same exit

Figure 50. Methodology to identify instances of trip chaining at interstate exits

6.9.2 To Identify and Group Alternate Route Choices

Origin and destination detectors positioned at the ends of a chosen analysis region, are used to extract journeys having passed through both detectors. For the text that follows, the terms ‘alternate route’ and ‘detour’ are used interchangeably for simplicity in referring to significant diversions from an interstate route. A flowchart representation of the methodology used to categorize and group route choices has been presented in Figure 51. Every trip under analysis is initialized with a match percent of zero, and a matched detour identifier of 0. The algorithm then tries to match each trip with all of the currently classified detours, and detects if a match percentage surpassing the pre-defined threshold (95% in this case) has been detected. A match percentage between a trip and a detour is defined as the percentage of a trip’s waypoints lying completely within the spatial polygon of a detour. If so, the current trip is classified as having matched that detour. If no match is found, a new detour is created and assigned a new detour identifier. The new detour’s spatial polygon is created by extending the line joining the current trip’s waypoints 60 feet in either direction, perpendicular to the direction of travel. A similar process is followed for each trip under analysis until all trips have been classified as belonging to a detour route with an acceptable match percentage. This ensures sufficient matching accuracy among the various trips and allows for the algorithm to be adjusted by modifying the match percentage threshold. For instance, the match percent may need to be modified and the spatial tolerance may need to be increased in dense urban areas where multiple high-volume roadways run fairly close to each other thus increasing the potential for mismatching. Using this methodology, the set of trips under analysis will be condensed down to a much smaller set of identified detours providing an insight into the trip distribution along each alternate route choice, one of which, by virtue of the grouping methodology, will be the base interstate route.

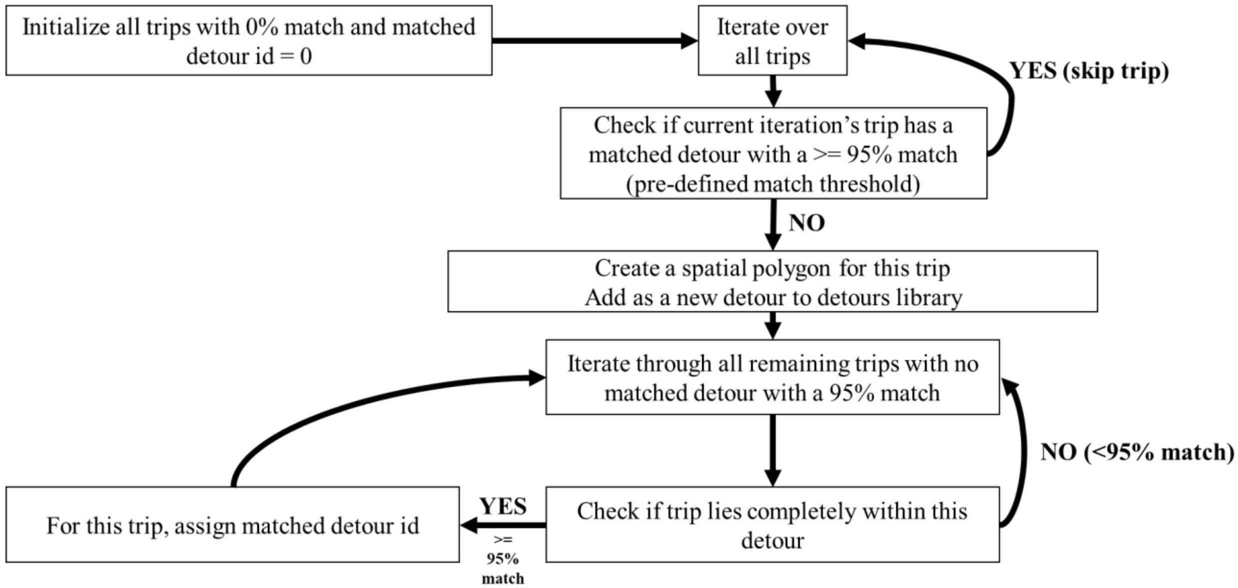

Figure 51. Methodology to identify and group alternate route choices

6.9.3 Sensitivity of Map Matching Percentage Threshold

Figure 52 depicts the sensitivity of the pre-defined trip-to-detour matching percentage threshold utilized by the route choice analysis. Two instances of alternate route choices in Figure 52a and Figure 52b show a 90.4% and 93.4% match respectively with the base interstate route. Concurrently, Figure 52c depicts a case wherein a journey shows a complete match with the base route indicating it did not choose an alternate route. A matching threshold of 95% was chosen for the route choice analyses in this study as this threshold would allow accounting for minor inaccuracies in geolocation reporting, while not grouping together substantially different route choices. For example, if a slightly lenient matching threshold of 90% was used, alternate routes shown in Figure 52a and Figure 52b would be misclassified in the same category as trips taking the base route (100% match, Figure 52c).

(a) 90.4% match (b) 93.4% match (c) 100% match

Figure 52. Sensitivity check on determining map matching percentage threshold

6.10 Results

6.10.1 Identification of Most Frequent Alternate Route Choices

Table 10 shows the most common route choices (with at least two trips observed on each route choice) adopted by motorists during the unplanned closure from Figure 46. The analysis period was chosen by visual inspection of the start of congestion at 12:30 PM, ending with traffic returning to free flow conditions for the analysis corridor by 9 PM on June 11, 2021. Trips that utilized the base route of I-65 NB and chose not to detour represent 55 of a total of 258 trips (21.3%) during the analysis period, with average and median travel times of 88.4 minutes and 62 minutes respectively. Six journeys that were categorized as having trip chained were excluded from the route choice analysis to avoid biasing the resulting travel time statistics. A total of 103 unique detours were identified during this analysis of which the top 22 alternate route choices (47% of all sampled trips in the analysis period) have been summarized in Table 10. The exit on I-65 NB corresponding to each identified detour has also been indicated in Table 10. Ten of the top 22 route choices impacted Exit 178. The top two alternate route choices (detour IDs 10 and 11) show relatively high travel times due to the increased traffic, while a majority of the other detours show modest travel times, suggesting the alternate routes may not have reached equilibrium.

Table 10. Top identified route choices with at least two trips observed on I-65 NB MM 164-200 (12:30 PM – 9 PM, June 11, 2021)

Route Choice	Exit Number on I-65 NB	Number of Trips	% of Total Trips	Avg. Travel Time (mins)	Median Travel Time (mins)
Base Route (I-65 NB)	-	55	21.3%	88.4	62.0
Detour ID 10	188	19	7.4%	117.2	130.1
Detour ID 11	188	12	4.7%	134.0	121.7
Detour ID 45	178	10	3.9%	68.7	65.2
Detour ID 34	178	9	3.5%	75.5	50.5
Detour ID 12	188	8	3.1%	177.0	173.6
Detour ID 33	178	8	3.1%	66.6	59.3
Detour ID 22	178	7	2.7%	57.1	55.5
Detour ID 44	178	6	2.3%	58.5	55.8
Detour ID 51	175	6	2.3%	83.4	79.0
Detour ID 57	178	4	1.6%	78.7	72.2
Detour ID 80	175	4	1.6%	57.3	57.3
Detour ID 19	178	3	1.2%	53.5	51.9
Detour ID 36	178	3	1.2%	67.1	60.9
Detour ID 55	175	3	1.2%	57.9	57.5
Detour ID 64	175	3	1.2%	53.4	53.5
Detour ID 87	175	3	1.2%	89.2	94.7
Detour ID 92	175	3	1.2%	69.3	70.4
Detour ID 41	178	2	0.8%	45.2	45.2
Detour ID 49	178	2	0.8%	84.9	84.9
Detour ID 63	175	2	0.8%	46.0	46.0
Detour ID 79	175	2	0.8%	76.2	76.2
Detour ID 90	175	2	0.8%	77.1	77.1

While Table 9 depicted a high-level data summary of diversion percentage at each exit in the analysis corridor, Figure 53 shows a detailed spatial representation of the base interstate route (Figure 53a) and the top five alternate route choices (Figure 53b-f) adopted by vehicles for this case study during the analysis period of 12:30 PM to 9 PM on June 11, 2021 for traversing a 36-mile stretch of I-65 NB. The crash location along with each of the six interstate exits (exit 168 through exit 193) have been called out on each map for geographical context. The top alternate route choice among motorists (detour ID 10) involved a nearly 2-mile detour by leaving the interstate at exit 188 and rejoining at exit 193, thus navigating around the incident at mile marker 189. Exit 188 was observed to be the top choice as point of departure from I-65 NB for three of the top five alternate routes (detour IDs 10, 11 and 12), with each of them rejoining the interstate at exit 193. CV trajectories that may have witnessed queues building up near exit 178 chose to detour much earlier and are represented by detour IDs 45 (Figure 53d) and 34 (Figure 53e).

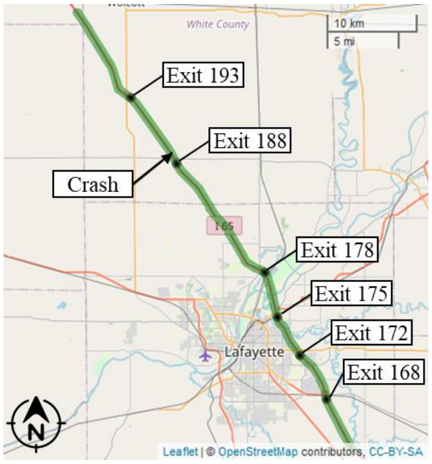

(a) Base route (I-65 NB)

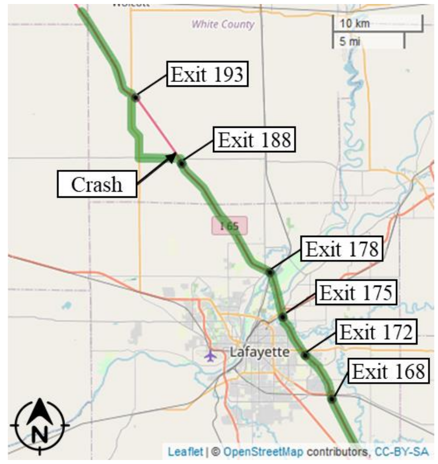

(b) Detour ID 10

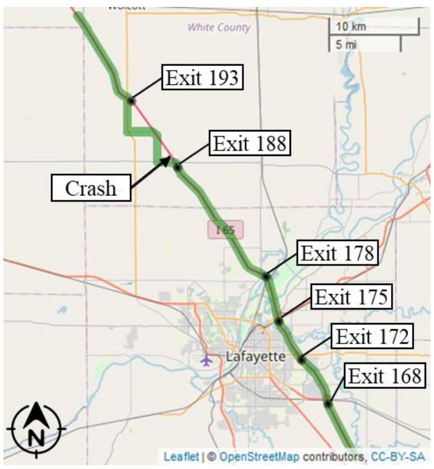

(c) Detour ID 11

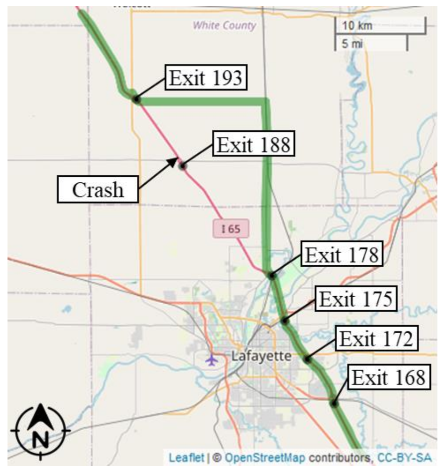

(d) Detour ID 45

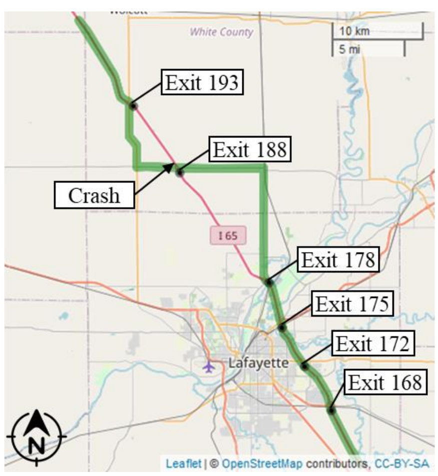

(e) Detour ID 34

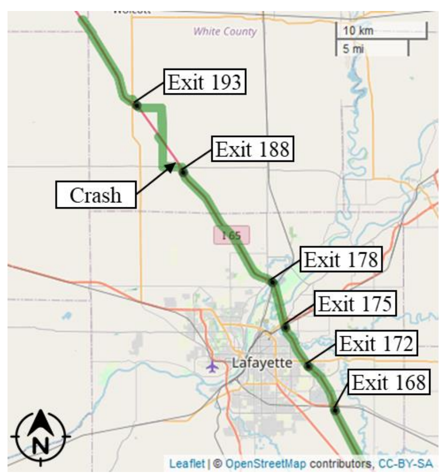

(f) Detour ID 12

Figure 53. Base route and top five identified alternate route choices I-65 NB MM 164-200 (12:30 PM – 9 PM, June 11, 2021)

6.10.2 Travel Time and Frequency of Alternate Route Choices during Incident

Utilizing the methodologies described earlier, 535 unique trips traversing the analysis region on I-65 were classified as either detouring, trip chaining or following the base route throughout. A colorized travel time plot for the analysis corridor for June 11, 2021 is shown in Figure 54a. Solid red circles indicate trips remaining on the interstate, solid blue circles indicate journeys identified as having trip chained, and solid green circles indicate those journeys that exited the interstate and chose an alternate route to navigate around the closure. Additionally, an hourly 100% stacked percentage plot showing trip distribution by route choice in this region is shown in Figure 54b. Alternate routes accounting for more than 3% of total trips are indicated by their individual colors. Journeys that were identified as having trip chained (23 in total) are excluded to visualize a slightly modified and realistic detour percentage by hour plot as shown in Figure 54c. The detour percentage sharply rises in the hour of 12 PM – 1 PM, which also coincides with the hour of the freeway crash incident, and reaches 100% for the next two hours (0% of trips taking the base interstate route) thus providing independent validation to the complete roadway closure. The detour percentage returns to zero by the hour of 10 PM – 11 PM pointing to eventual incident clearance and freeway traffic returning to normal thus not necessitating any detour behavior among drivers.

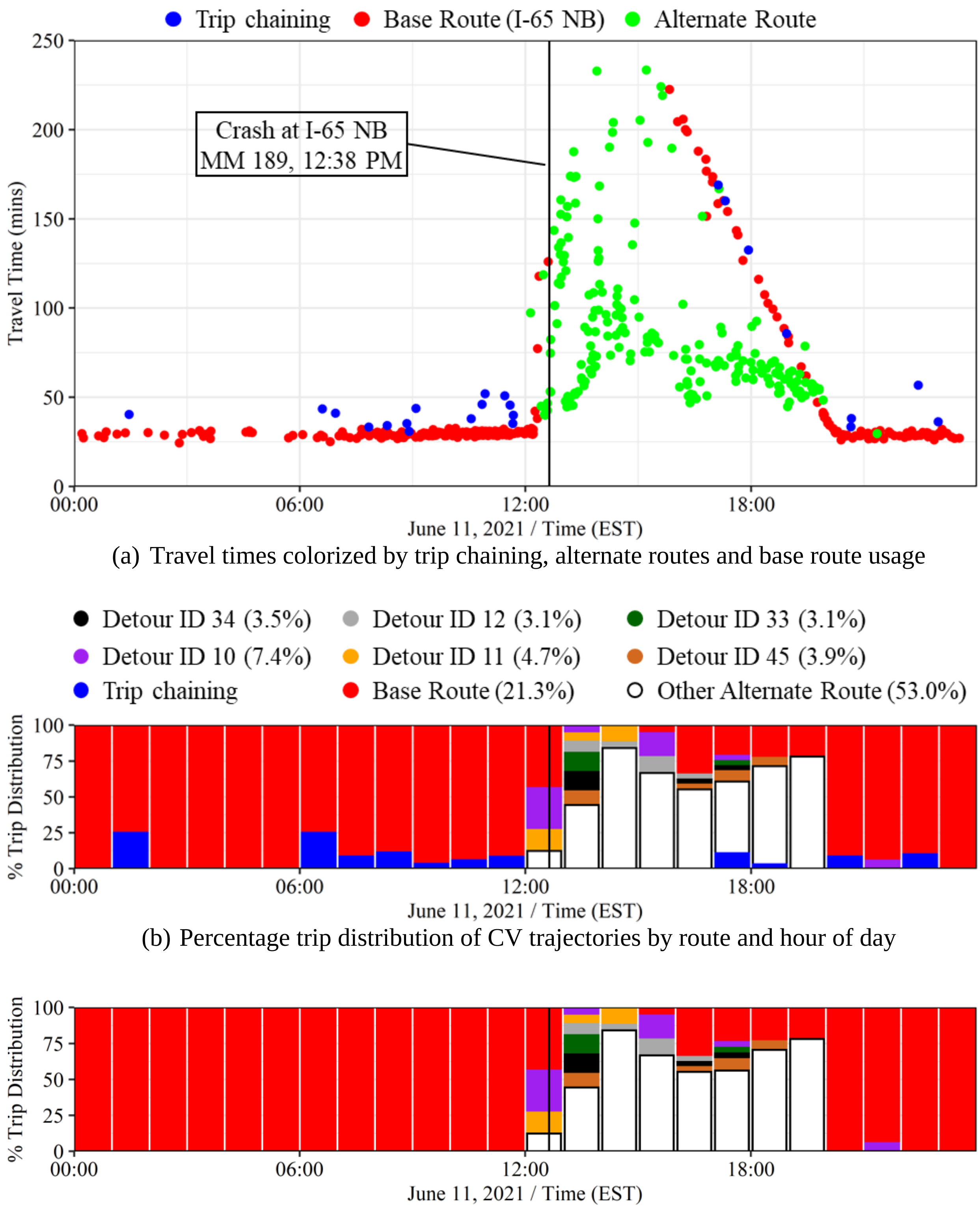

(a) Travel times colorized by trip chaining, alternate routes and base route usage

(b) Percentage trip distribution of CV trajectories by route and hour of day

(c) Percentage trip distribution of CV trajectories by route and hour of day after instances of trip chaining have been excluded

Figure 54. Categorizing CV trajectories as non-detouring, detouring and trip chaining (June 11, 2021)

Figure 55 depicts a scatter plot representation of the number of additional miles vehicles traveled over the base route. Alternate routes accounting for more than 3% of total trips are indicated by individually colored solid circles. 21.3% of trips adhered to the base interstate route, shown by solid red circles on the horizontal axis with no additional distance traveled. A majority of the trip chaining instances (solid blue circles) are observed to have traveled additional distances of five miles or less, with a mean additional distance traveled of 0.74 miles, representing short breaks at interstate exits. Detouring trips saw additional miles of travel ranging from 1.9 miles to 25.4 miles in some cases, with mean additional travel of 6.4 miles across all alternate route choices. Detour ID 10 (solid purple circles) accounted for 7.4% of total trips in the analysis period, with an average travel time approaching two hours while only adding about 2 miles of additional travel. A sharp increase is observed in the number of additional miles traveled by motorists right after the crash incident at 12:38 PM.

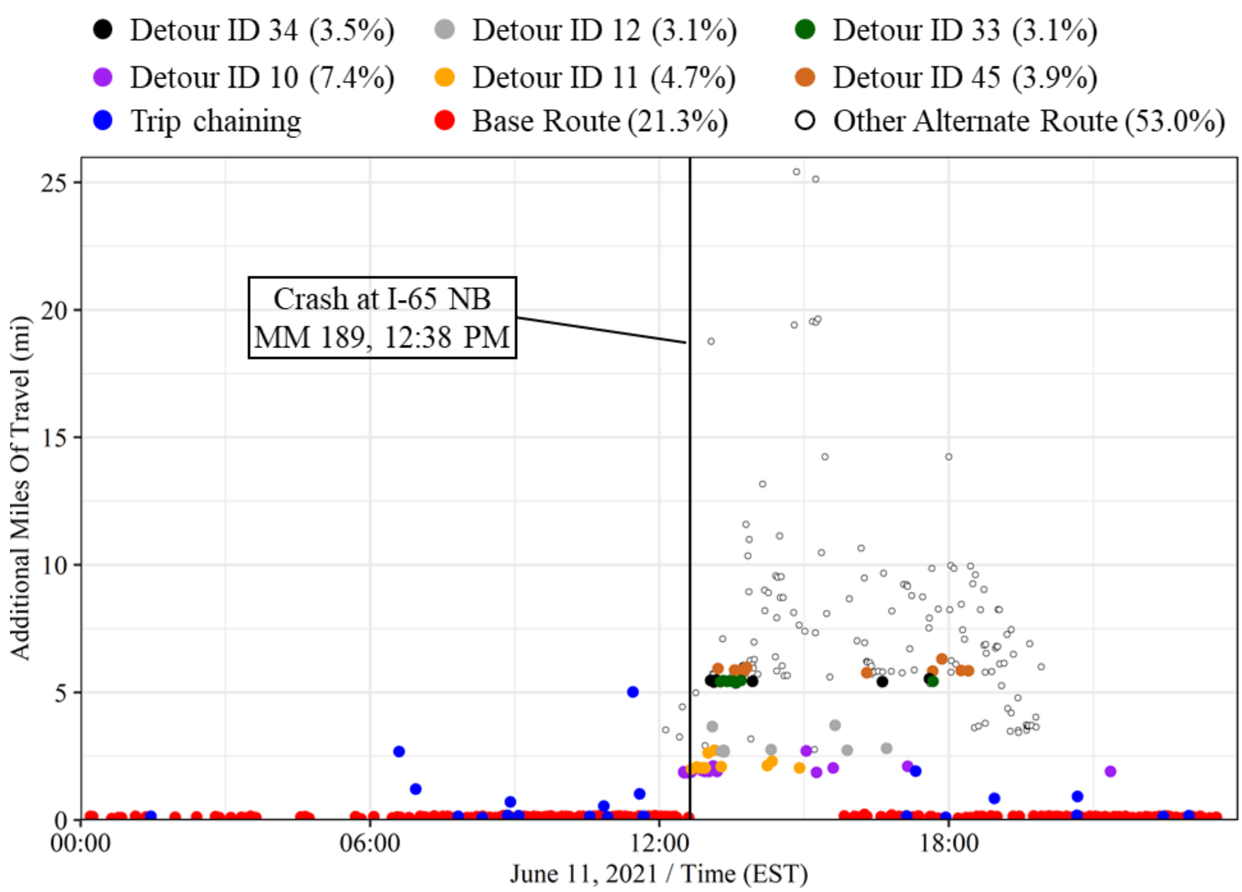

Figure 55. Additional miles of travel compared to interstate travel, routes accounting for more than 3% of all trips individually highlighted (June 11, 2021)

6.10.3 Scalable Application to Interstate Routes

The methodologies proposed and demonstrated for the June 11, 2021 I-65 example earlier in this study are easily scalable and transferable to any interstate or non-interstate route, provided the availability of CV data. A further 11 cases were analyzed around the state of Indiana to present the spatially and temporally independent repeatability of these methods. Figure 56 shows the approximate location of each of these 11 case locations highlighted on a statewide map for geographical context, covering four of the major interstate thoroughfares in Indiana, I-65, I-70, I-74 and I-94. Two of the cases (IN-IL_12 and IN-KY_11) were chosen to demonstrate the usability of this method to evaluate congestion at state borders and alternate state crossing route choices at border towns. Case I-70_08 was chosen to demonstrate the method being used to evaluate trips choosing to detour through rest areas to avoid / bypass a portion of traffic queued upstream of a construction zone. This diversion case is particularly concerning because anecdotal evidence suggests navigation software recommended this “alternate route” and highlights the need for transportation agencies to understand some of the unintended consequences of motorists using navigation software.

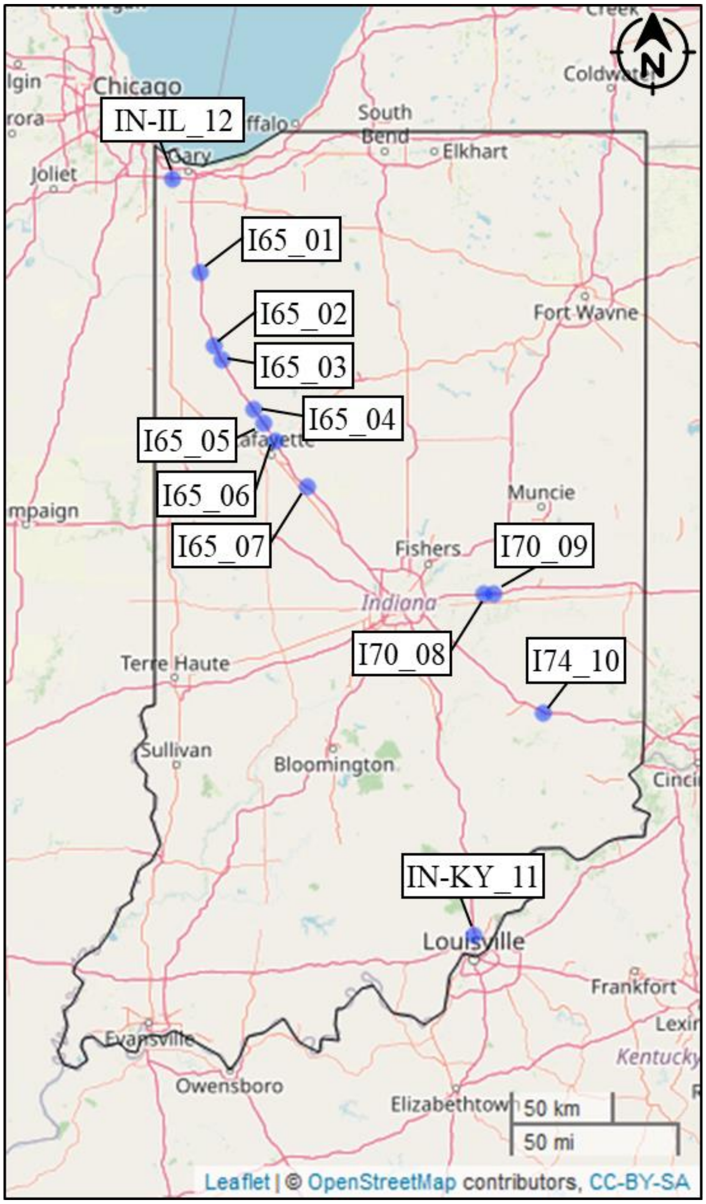

Figure 56. Statewide map of analyzed incidents

The base route distance, detour percentage (number of sampled trips that chose an alternate route as opposed to staying on the base interstate route) during these incidents, average travel times, average travel time differential among detour and base route, and the number of unique exits utilized by motorists for diverting are tabulated in Table 11. These statistics are based upon analysis periods chosen for each incident similar to the period chosen for the unplanned closure case study in this paper from Figure 46. One of the analyzed incidents (I65_03) involved a partial closure while eight cases involved a full closure. While the cases analyzed are examples completely independent of each other, detour percentages are observed to significantly depend on the duration of the full closure irrespective of the route. All analyzed cases with five or more hours of complete road closure had more than 50% of the sampled journeys choose an alternate route.

Table 11. Summary of detour percentage and travel time for analyzed incidents

Incident ID	**Date**	**Type of closure**	**Duration of full closure (hours)**	**Base route distance**	**Detour %**	**Avg. detour travel time (mins)**	**Avg. base route travel time (mins)**	**Avg. detour travel time difference from base route (mins)**	**Unique exits used during incident**
I65_01	09/14/2021	Full	2.25	34.9	39.7%	50.9	43.2	7.7	2
I65_02	09/24/2021	Full	12	29.1	72.5%	72.7	52.5	20.2	3
I65_03	01/24/2022	Partial	-	26.9	4.2%	37.9	25.3	12.7	2
I65_04	06/11/2021	Full	6.5	36	78.7%	86.6	88.4	-1.8	5
I65_05	01/11/2022	Full	10.5	20.1	93.4%	46.6	64.2	-17.6	3
I65_06	07/05/2021	Full	1.5	48.1	39.7%	80.2	62.4	17.8	7
I65_07	07/09/2021	Full	2.25	29	71.6%	53.7	65.4	-11.7	3
I70_08 (Rest Area)	10/10/2021	-	-	1.3	4.2%	7.1	6.5	0.6	-
I70_09	07/15/2021	Full	5	40.9	58.7%	75.5	85.3	-9.8	3
I74_10	01/25/2022	Full	1.75	20	82.6%	57.7	24.3	33.4	2
IN-KY_11	01/25/2022	-	-	15.7	15.4%	17.5	13.6	3.9	3
IN-IL_12	10/09/2021	-	-	10.9	23.4%	45.2	64.6	-19.4	6

6.11 Summary

This study proposed easily scalable methodologies leveraging CV data to identify trip chaining at interstate exits (Figure 50), analyzing route choice distributions (Figure 51, Table 10), and travel times along alternate routes (Figure 54). Knowledge of ramp delays (Table 9) and queues at interstate exits will provide stakeholders with real-time and accurate ground-level information when responding to a freeway incident. The analysis and results presented may be useful for public safety agencies as well as state departments of transportation in providing a data-driven framework for historical as well as real-time alternate route planning. Agencies can apply these methodologies to develop data-driven diversion strategies for critical routes as well as implementation of real-time monitoring to provide agile adjustment of resources along diversion routes during an active incident. Proposed methodologies to detect instances of trip chaining (Figure 50) will allow practitioners and researchers alike to better curate outliers from travel time datasets and enable realistic travel time reliability estimates on corridors not affected by noisy observations.

These methodologies are highly transferable to a host of other transportation research problems such as evaluation of border crossing route usage between neighboring states, monitoring usage/impact of official detour options, and ingress/egress route planning for special events. The sole reliance of the proposed methodologies on CV trajectory waypoint data makes them easily scalable worldwide provided the availability of CV data, without being dependent on cost intensive ITS infrastructure.

7. CONCLUSIONS

The infrastructure bill will provide nearly $643 billion for surface transportation infrastructure over the next five years. Although traditional infrastructure-based sensors, such as loop detectors will still be used, CV data is an important new source of information for agencies to make effective investment choices.

It is estimated that a connected vehicle creates over 25 gigabytes of data every hour [161], and that volume will continue to grow with a larger portion of production vehicles being instrumented for connectivity with every passing year. Stakeholders using CV data require techniques that can draw easily consumable observations from this large-scale data. This dissertation proposed visualizations, methodologies and analysis techniques that allow reducing such big CV data sets down to actionable insights that can inform decision making on mobility, safety and day-to-day operational performance of surface transportation systems. Each chapter of this thesis defined a use case and contribution. A brief summary of these contributions and emerging impact follows.

7.1 Interstate Mobility Impacts of Secondary Crashes

Crash incidents on interstate roadways often result in queuing while the incident is cleared, many a times resulting in secondary crash incidents at the back of a queue. CV data now allows researchers to quantify the mobility impacts of these secondary crashes making the case for increased investment in public safety resources to accelerate scene clearance. A systematic review of 195 incidents was performed for 2019 that involved one or more secondary crashes. Interstate route-level analysis of secondary crash mobility impacts showed an average road closure time of 2 hours and 33 minutes, with an average event duration time of 3 hours and 50 minutes. As a consequence of this study, a project in collaboration with the Indiana Criminal Justice Institute (ICJI) has seen approximately 40 public safety agencies being trained so far on using Unmanned Aircraft Systems (UAS) to quickly map crash scenes and accelerate the clearance of backed up traffic. In fact, both the justification and the UAS program have been highlighted by the USDOT Every Day Counts 5 Program [62].

7.2 Monitoring Mobility through Interstate Construction Work Zones

Agencies have traditionally relied on fixed ITS sensor infrastructure placed in and around construction sites to monitor the progression of traffic through areas under construction. However, this imposes spatial and temporal limits on the ability of practitioners to monitor queuing and congestion. CV data, on the other hand, removes these constraints and allows near real-time monitoring of traffic in any location provided the availability of CV data. A pilot case study on 11 locations in Indiana showed how CV data could be used to inform the Indiana interstate highway closure policy (IHCP) exceptions based on reduced traffic volumes, which may traditionally have not been granted if decision-makers relied upon historical queue forecasting models. Encouraging results from this study enabled further implementations at 25 additional locations around the state, and allowed the Indiana Department of Transportation (INDOT) to take advantage of reduced volumes in the wake of the COVID-19 pandemic to accelerate construction activity while minimizing freeway mobility impacts. An even further granular analysis on a construction work zone on interstate 70 in central Indiana showed the scalable use of CV trajectory data in quantifying diversion rates, travel times and impact on arterial traffic signal performance. Such analyses provide agencies with much needed feedback from real-world CV usage and allows for agile strategy adjustments if and when needed to address critical mobility issues in a work zone.

7.3 Correlating Hard-braking Events and Crash Incident Occurrences in and around Interstate Construction Work Zones

Due to the inherent spatial and temporal inaccuracies and the associated time delay involved in reporting crash incidents, the scope of dynamic safety corrections to construction work zones in response to crash incidents is heavily limited. Hard-braking events on the other hand can be monitored in near real-time and have the potential to provide an initial filter on hot spots in a road network with critical safety performance issues. This chapter demonstrated the correlation between hard-braking events and crash incident occurrences for a system of 23 interstate construction work zones covering six interstate routes in Indiana in 2019. The study found approximately 1 crash per mile occurred for every 147 sampled hard-braking events in and around a construction site in the summer of 2019. While this result corresponds to a 2019 snapshot of construction activity and sampled CV data, the ratio is bound to change as penetration of CVs increases. In spite of the spatially and temporally limited nature of this study, it provides strong quantitative evidence for the immediate implementation of hard-braking events as a surrogate safety performance measure to provide agencies with a first filter on critical safety hot spots that require their further attention. In fact, Indiana now monitors weekly changes in hard-braking events on their interstates to identify emerging safety concerns in work zones. In addition to hard-braking events, this study encourages further research in the use of other in-vehicle events such as hard-acceleration, emergency braking and traction control for near real-time safety performance monitoring of work zones and roadways in general.

7.4 Evaluating Electric and Hybrid Vehicle Charging Infrastructure Usage and Investment Opportunities

The new infrastructure bill provides $100 million for Indiana EV infrastructure and $7.5 billion nationally. With this influx of public and private sector investment into building a nationwide EV charging network by the end of this decade, determining an equitable formula for state-wise funding allocations is of utmost importance to stakeholders. This dissertation presented a case study using CV data from 11 states (California, Connecticut, Georgia, Indiana, Minnesota, North Carolina, Pennsylvania, Ohio, Utah, Texas and Wisconsin) to analyze the current usage trends of EVs, HVs and existing charging infrastructure. Methodologies were presented to identify critical gaps in fast charging availability on freeways, and for ranking charging infrastructure usage at the statewide, county and city level to help real-world EV usage trends provide quantitative supporting evidence for policy decisions and investment allocations. A publicly available aggregated dataset of EV and HV usage at the county level was put forth [140] by this study to stimulate and invite further dialogue among the transportation community on additional technical analysis.

7.5 Analysis of Route Choice during Planned and Unplanned Road Closures

While researchers and practitioners have long modeled, simulated, surveyed and forecasted route choice behavior, very limited research has been conducted on documenting and analyzing real-world route choices. CV data provides easily scalable opportunities to monitor route choice behavior and provide historical evidence to agencies that may help in allocating public safety and traffic management resources for future roadway capacity reduction incidents. This chapter proposed a recursive methodology to group and summarize alternate route choices adopted by motorists navigating through or around a freeway road closure using a bus crash case study from

June 11, 2021 on Interstate 65 (I-65) in Indiana. Colorized visualizations of travel time, distance traveled and diversion rates were proposed to track the progression of an incident. The temporal and spatial scalability of these methodologies was demonstrated by analyzing a further 11 incidents across the state. The study recommended agencies use these methodologies for documenting historical incidents as well as for real-time incident monitoring in dispatch centers. This chapter also proposed a scalable methodology to detect instances of trip chaining, a much-needed solution for discarding outliers to ensure realistic travel time values for any corridor under analysis.

7.6 Summary

Over the course of my research, I have been lead author on 8 CV papers and contributing author on 7 papers. This dissertation provides a holistic overview of that work that provided the following contributions in the CV data analytics space:

- The development of CV data-driven systematic review techniques to quantifying the mobility impacts of secondary crashes on interstate roadways.
- The demonstration of the applicability of CV data for monitoring impact of construction activity on mobility.
- The use of hard-braking events as a surrogate measure identifying emerging safety concerns in construction work zones.
- The development of performance measures for evaluating charging infrastructure usage using CV data for informing present and future investment allocations.
- The development of methodologies that identify trip chaining and analyze route choice during a planned or unplanned road closure to help agencies make informed diversion strategy decisions.

As transportation researchers and practitioners in the public and private sector alike transition from sole reliance on fixed ITS sensor-based monitoring to complementing the same with large-scale CV data-based monitoring of transportation systems, the methodologies and techniques proposed in this dissertation will provide them with a data-driven framework for use in day-to-day monitoring as well as provide quantitative real-world evidence to support future resource allocation and investment decisions.

REFERENCES

[1] L. E. Y. Mimbela and L. a Klein, “Summary Of Vehicle Detection And Surveillance Technologies Used In Intelligent Transportation Systems,” *UC Berkeley Transp. Libr.*, p. 211, 2000.

[2] J. K. Mathew, J. C. Desai, R. S. Sakhare, W. Kim, H. Li, and D. M. Bullock, “Big data applications for managing roadways,” *ITE J. (Institute Transp. Eng.*, vol. 91, no. 2, pp. 28–35, 2021.

[3] J. Chang *et al.*, “Estimated Benefits of Connected Vehicle Applications: Dynamic Mobility Applications , AERIS , V2I Safety , and Road Weather Management Applications,” *U.S. Dep. Transp.*, no. August, 2015.

[4] C. M. Experience, “The Promise of Connected Vehicle Data.”

[5] “The Global Vehicle Data Market - Global study - PTOLEMUS Consulting Group.” [Online]. Available: https://www.ptolemus.com/research/the-vehicle-data-market-global-study/. [Accessed: 26-Feb-2022].

[6] M. Bertoncello, C. Martens, T. Möller, and T. Schneiderbauer, “Unlocking full value from data from connected cars,” *McKinsey & Company*, 2021. [Online]. Available: https://www.mckinsey.com/industries/automotive-and-assembly/our-insights/unlocking-the-full-life-cycle-value-from-connected-car-data. [Accessed: 26-Feb-2022].

[7] “Work Zone Data Exchange (WZDx) | US Department of Transportation,” *Last updated: Monday, March 1, 2021*. [Online]. Available: https://www.transportation.gov/av/data/wzdx. [Accessed: 26-Feb-2022].

[8] M. Pack, N. Ivanov, J. Bauer, and E. Birriel, “Considerations of Current and Emerging Transportation Management Center Data,” 2019.

[9] “President Biden, USDOT and USDOE Announce $5 Billion over Five Years for National EV Charging Network, Made Possible by Bipartisan Infrastructure Law | FHWA.” [Online]. Available: https://highways.dot.gov/newsroom/president-biden-usdot-and-usdoe-announce-5-billion-over-five-years-national-ev-charging. [Accessed: 26-Feb-2022].

[10] The USDOT’s Volpe Center, “Advancing Data-Driven Decision Making in Transportation.”

[11] "GM Tries to Make Sense of All That Connected-Car Data | WardsAuto." [Online]. Available: https://www.wardsauto.com/vehicles/gm-tries-make-sense-all-connected-car-data. [Accessed: 26-Feb-2022].

[12] "Ford Pro – Commercial Vehicles and Connected Fleet Services." [Online]. Available: https://pro.ford.com/en-us/telematics/?searchid=14955766448%7C128984718912%7C1436966495201%7C&ef_id=CjwKCAiAvOeQBhBkEiwAxutUVBvjDCtnvViXXh2aZCQIkZsSZNDWEYh6CUfViDxlDSOWG0KNNklVXRoCk3IQAvD_BwE:G:s&s_kwcid=AL!2519!3!553511868371!p!!g!!ford vehicle data!1495. [Accessed: 26-Feb-2022].

[13] "Honda to Start Selling Smart Car Data." [Online]. Available: https://www.trendmicro.com/en_us/research/21/j/honda-to-start-selling-smart-car-data.html. [Accessed: 26-Feb-2022].

[14] "How Volkswagen Automotive Cloud will help shape the connected car of tomorrow," 2021. [Online]. Available: https://www.volkswagenag.com/en/news/stories/2021/01/how-volkswagen-automotive-cloud-will-help-shape-the-connected.html. [Accessed: 26-Feb-2022].

[15] The White House, "Fact Sheet: The Bipartisan Infrastructure Deal | The White House," *The White House*, 2021. [Online]. Available: https://www.whitehouse.gov/briefing-room/statements-releases/2021/11/06/fact-sheet-the-bipartisan-infrastructure-deal/. [Accessed: 26-Feb-2022].

[16] G. M. Shepherd, "The National Electric Vehicle Infrastructure (NEVI) Formula Program Guidance," pp. 1–31, 2022.

[17] Wejo, "The growth of the Connected Vehicle Data market | Wejo." [Online]. Available: https://www.wejo.com/press/the-growth-of-the-connected-vehicle-data-market. [Accessed: 26-Feb-2022].

[18] J. Desai *et al.*, "Agile Work Zone Management Based on Connected Vehicle Data," *2021 IEEE Int. Intell. Transp. Syst. Conf.*, pp. 4051–4056, Sep. 2021, doi: 10.1109/ITSC48978.2021.9565039.

[19] J. Desai, E. Saldivar-Carranza, J. K. Mathew, H. Li, T. Platte, and D. Bullock, "Methodology for Applying Connected Vehicle Data to Evaluate Impact of Interstate Construction Work Zone Diversions," in *IEEE Conference on Intelligent Transportation Systems, Proceedings, ITSC*, 2021, vol. 2021-Septe, pp. 4035–4042, doi: 10.1109/ITSC48978.2021.9564873.

[20] T. H. Maze and J. Wiegand, "Lane Closure Policy Development, Enforcement, and Exceptions: A Survey of Seven State Transportation Agencies," p. 62p, 2007.

[21] Indiana Department of Transportation, "Interstate Highways Congestion Policy," 2017. [Online]. Available: https://www.in.gov/indot/files/2017 Interstate Highways Congestion Policy.pdf. [Accessed: 24-Jul-2020].

[22] "INRIX U.S. National Traffic Volume Synopsis Issue #15 (June 20 – June 26, 2020) - INRIX." [Online]. Available: https://inrix.com/blog/2020/06/covid19-us-traffic-volume-synopsis-15/. [Accessed: 24-Jul-2020].

[23] R. Owen, L. Koskela, G. Henrich, and R. Codinhoto, "Is agile project management applicable to construction?," in *Understanding and Managing the Construction Process: Theory and Practice - 14th Annual Conference of the International Group for Lean Construction, IGLC-14*, 2006, pp. 51–66.

[24] J. Adut, "Applying agile approaches in public construction and civil engineering projects," 2016.

[25] K. Ozbay and B. Bartin, "Development of Uniform Standards for Allowable Lane Closure (NJDOT Bureau of Research)," New Jersey. Dept. of Transportation, Sep. 2008.

[26] M. M. Mekker, S. M. Remias, M. L. McNamara, and D. M. Bullock, "Characterizing Interstate Crash Rates Based on Traffic Congestion Using Probe Vehicle Data," West Lafayette, IN, Jan. 2020.

[27] M. Mekker, "CONNECTED VEHICLE DATA-BASED TOOLS FOR WORK ZONE ACTIVE TRAFFIC MANAGEMENT," Purdue University, 2018.

[28] O. Ozturk, K. Ozbay, and H. Yang, "Estimating the Impact of Work Zones on Highway Safety," *Transp. Res. Board 93rd Annu. Meet.*, pp. 1–16, 2014.

[29] J. Desai, H. Li, J. K. Mathew, Y.-T. Cheng, A. Habib, and D. M. Bullock, “Correlating Hard-Braking Activity with Crash Occurrences on Interstate Construction Projects in Indiana,” *J. Big Data Anal. Transp.*, vol. 3, no. 1, pp. 27–41, Apr. 2020, doi: 10.1007/s42421-020-00024-x.

[30] FHWA, “FHWA Work Zone Facts and Statistics - FHWA Office of Operations,” 2018. [Online]. Available: https://ops.fhwa.dot.gov/wz/resources/facts_stats.htm. [Accessed: 17-Jun-2020].

[31] “FHWA Office of Operations - Making Work Zones Work Better.” .

[32] O. Jahn, R. H. Möhring, A. S. Schulz, and N. E. Stier-Moses, “System-optimal routing of traffic flows with user constraints in networks with congestion,” *Oper. Res.*, vol. 53, no. 4, pp. 600–616, 2005, doi: 10.1287/opre.1040.0197.

[33] S. A. Bagloee, M. Sarvi, M. Patriksson, and A. Rajabifard, “A Mixed User-Equilibrium and System-Optimal Traffic Flow for Connected Vehicles Stated as a Complementarity Problem,” *Comput. Civ. Infrastruct. Eng.*, vol. 32, no. 7, pp. 562–580, 2017, doi: 10.1111/mice.12261.

[34] L. Zhenlong and Z. Xiaohua, *Integrated-Equilibrium Routing of Traffic Flows with Congestion*, vol. 41, no. 2. IFAC, 2008.

[35] G. E. Cantarella and E. Cascetta, “Dynamic processes and equilibrium in transportation networks: towards a unifying theory,” *Transp. Sci.*, vol. 29, no. 4, pp. 305–329, Nov. 1995, doi: 10.1287/trsc.29.4.305.

[36] J. L. Adler and V. J. Blue, “A cooperative multi-agent transportation management and route guidance system,” *Transp. Res. Part C Emerg. Technol.*, vol. 10, no. 5–6, pp. 433–454, Oct. 2002, doi: 10.1016/S0968-090X(02)00030-X.

[37] S. Peeta and J. L. Ramos, “Driver response to variable message signs-based traffic information,” *IEE Proc. Intell. Transp. Syst.*, vol. 153, no. 1, pp. 2–10, 2006, doi: 10.1049/ip-its:20055012.

[38] L. Kattan, A. G. De Barros, and H. Saleemi, “Travel behavior changes and responses to advanced traveler information in prolonged and large-scale network disruptions: A case study of west LRT line construction in the city of Calgary,” *Transp. Res. Part F Traffic Psychol. Behav.*, vol. 21, pp. 90–102, 2013, doi: 10.1016/j.trf.2013.08.005.

[39] E. Ben-Elia and D. Ettema, "Changing commuters' behavior using rewards: A study of rush-hour avoidance," *Transp. Res. Part F Traffic Psychol. Behav.*, vol. 14, no. 5, pp. 354–368, Sep. 2011, doi: 10.1016/j.trf.2011.04.003.

[40] C. G. Chorus, E. J. E. Molin, and B. Van Wee, "Use and effects of Advanced Traveller Information Services (ATIS): A review of the literature," *Transport Reviews*, vol. 26, no. 2. Routledge, pp. 127–149, Mar-2006, doi: 10.1080/01441640500333677.

[41] A. Memarian, J. M. Rosenberger, S. P. Mattingly, J. C. Williams, and H. Hashemi, "An optimization-based traffic diversion model during construction closures," *Comput. Civ. Infrastruct. Eng.*, vol. 34, no. 12, pp. 1087–1099, 2019, doi: 10.1111/mice.12491.

[42] X. Li, Y. Cao, X. Zhao, and D. Xie, "Drivers' diversion from expressway under real traffic condition information shown on variable message signs," *KSCE J. Civ. Eng.*, vol. 19, no. 7, pp. 2262–2270, 2014, doi: 10.1007/s12205-014-0692-y.

[43] Z. Liang and Y. Wakahara, "Real-time urban traffic amount prediction models for dynamic route guidance systems," *Eurasip J. Wirel. Commun. Netw.*, vol. 2014, no. 1, p. 85, Dec. 2014, doi: 10.1186/1687-1499-2014-85.

[44] Y. Yim, A. J. Khattak, and J. Raw, "Traveler response to new dynamic information sources: Analyzing corridor and areawide behavioral surveys," *Transportation Research Record*, vol. 1803, no. 1803. National Research Council, pp. 66–75, Jan-2002, doi: 10.3141/1803-10.

[45] M. Petrella and J. Lappin, "Comparative analysis of customer response to online traffic information in two cities Los Angeles, California, and Seattle, Washington," in *Transportation Research Record*, 2004, vol. 1886, no. 1886, pp. 10–17, doi: 10.3141/1886-02.

[46] S. Tanvir, I. Ahmed, N. Karmakar, and B. J. Schroeder, "Determination of Diversion Sensitivity at Urban Freeway Work Zones Using Bluetooth Devices," *Present. 96th Annu. Meet. Transp. Res. Board, Pap. No.*, vol. 17–06766, 2017.

[47] J. Effinger, A. J. Horowitz, Y. Liu, and J. Shaw, "Bluetooth Vehicle Reidentification for Analysis of Work Zone Diversion," *Present. 92nd Annu. Meet. Transp. Res. Board, Pap. No.*, vol. 13–2159, 2013.

[48] R. J. Haseman, J. S. Wasson, and D. M. Bullock, "Real-time measurement of travel time delay in work zones and evaluation metrics using bluetooth probe tracking," *Transp. Res. Rec.*, vol. 2169, no. 2169, pp. 40–53, Jan. 2010, doi: 10.3141/2169-05.

[49] Federal Highway Administration, "Comparative Analysis Report: The Benefits of Using Intelligent Transportation Systems in Work Zones," FHWA-HOP-09-002, 2008.

[50] C. Villiers, L. D. Nguyen, and J. Zalewski, "Evaluation of traffic management strategies for special events using probe data," *Transp. Res. Interdiscip. Perspect.*, vol. 2, p. 100052, Sep. 2019, doi: 10.1016/j.trip.2019.100052.

[51] A. M. Hainen, J. S. Wasson, S. M. L. Hubbard, S. M. Remias, G. D. Farnsworth, and D. M. Bullock, "Estimating route choice and travel time reliability with field observations of bluetooth probe vehicles," *Transp. Res. Rec.*, no. 2256, pp. 43–50, Jan. 2011, doi: 10.3141/2256-06.

[52] M. McNamara *et al.*, "Using Real-Time Probe Vehicle Data to Manage Unplanned Detour Routes," *ITE J.*, vol. 85, no. 12, 2015.

[53] S. Umeda, Y. Kawasaki, and M. Kuwahara, "Analysis of traffic state during a heavy rain disaster using probe data," *J. Disaster Res.*, vol. 14, no. 3, pp. 466–477, 2019, doi: 10.20965/jdr.2019.p0466.

[54] J. K. Mathew, J. C. Desai, R. S. Sakhare, W. Kim, H. Li, and D. M. Bullock, "Big data applications for managing roadways," *ITE J. (Institute Transp. Eng.*, vol. 91, no. 2, pp. 28–35, 2021.

[55] M. Hunter, J. K. Mathew, E. Cox, M. Blackwell, and D. M. Bullock, "Estimation of Connected Vehicle Penetration Rate on Indiana Roadways," West Lafayette, 2021.

[56] T. M. Brennan, S. M. Remias, G. M. Grimmer, D. K. Horton, E. D. Cox, and D. M. Bullock, "Probe vehicle-based statewide mobility performance measures for decision makers," *Transp. Res. Rec.*, no. 2338, pp. 78–90, Jan. 2013, doi: 10.3141/2338-09.

[57] C. Day *et al.*, "2015 Indiana Mobility Report and Performance Measure Dashboards," West Lafayette, IN, Nov. 2016.

[58] E. Saldivar-Carranza, H. Li, J. Mathew, M. Hunter, J. Sturdevant, and D. Bullock, "Deriving Operational Traffic Signal Performance Measures from Vehicle Trajectory Data," *Transp. Res. Rec. J. Transp. Res. Board*, 2021, doi: 10.1177/03611981211006725.

[59] E. D. Saldivar-Carranza, "Scalable Operational Traffic Signal Performance Measures from Vehicle Trajectory Data," Purdue University, 2021.

[60] Transportation Research Board (TRB), *Highway Capacity Manual 2010*. Washington DC: National Research Council (NRC), 2010.

[61] J. Desai, R. Sakhare, S. Rogers, J. K. Mathew, A. Habib, and D. Bullock, “Using Connected Vehicle Data to Evaluate Impact of Secondary Crashes on Indiana Interstates,” *2021 IEEE Int. Intell. Transp. Syst. Conf.*, pp. 4057–4063, Sep. 2021, doi: 10.1109/ITSC48978.2021.9564653.

[62] Federal Highway Administration, “EDC-5: Unmanned Aerial Systems (UAS) | Federal Highway Administration,” 2021. [Online]. Available: https://www.fhwa.dot.gov/innovation/everydaycounts/edc_5/uas.cfm. [Accessed: 23-Mar-2022].

[63] N. H. T. S. A. (NHTSA), “Preview of Motor Vehicle Traffic Fatalities In 2019,” 2020.

[64] Federal Highway Administration, “Traffic Congestion and Reliability: Trends and Advanced Strategies for Congestion Mitigation,” Washington, DC, 2005.

[65] J. A. Lindley, “Urban freeway congestion: quantification of the problem and effectiveness of potential solutions.,” *ITE J.*, vol. 57, no. 1, pp. 27–32, 1987.

[66] Z. Chen, X. C. Liu, and G. Zhang, “Non-recurrent congestion analysis using data-driven spatiotemporal approach for information construction,” *Transp. Res. Part C Emerg. Technol.*, vol. 71, pp. 19–31, 2016, doi: 10.1016/j.trc.2016.07.002.

[67] M. G. Karlaftis, S. P. Latoski, N. J. Richards, and K. C. Sinha, “ITS Impacts on Safety and Traffic Management: An Investigation of Secondary Crash Causes,” *ITS J. - Intell. Transp. Syst. J.*, vol. 5, no. 1, pp. 39–52, Jan. 1999, doi: 10.1080/10248079908903756.

[68] M. M. Mekker, S. M. Remias, M. L. McNamara, and D. M. Bullock, “Characterizing Interstate Crash Rates Based on Traffic Congestion Using Probe Vehicle Data,” West Lafayette, IN, 2020.

[69] H. Yang, B. Bartin, and K. Ozbay, “Use of Sensor Data to Identify Secondary Crashes on Freeways,” *Transp. Res. Rec. J. Transp. Res. Board*, vol. 2396, no. 1, pp. 82–92, Jan. 2013, doi: 10.3141/2396-10.

[70] R. A. Raub, “Occurrence of Secondary Crashes on Urban Arterial Roadways,” *Transp. Res. Rec. J. Transp. Res. Board*, vol. 1581, no. 1, pp. 53–58, Jan. 1997, doi: 10.3141/1581-07.

[71] Y. Chung, “Identifying Primary and Secondary Crashes from Spatiotemporal Crash Impact Analysis,” *Transp. Res. Rec. J. Transp. Res. Board*, vol. 2386, no. 1, pp. 62–71, Jan. 2013, doi: 10.3141/2386-08.

[72] C. C. Sun and V. Chilukuri, “Dynamic incident progression curve for classifying secondary traffic crashes,” *J. Transp. Eng.*, vol. 136, no. 12, pp. 1153–1158, 2010, doi: 10.1061/(ASCE)TE.1943-5436.0000187.

[73] A. Haghani, M. Hamedi, and K. F. Sababadi, “I-95 Corridor Coalition Vehicle Probe Project : Validation of INRIX data July-September 2008 Final Report,” *I-95 Corridor Coalit.*, no. January, pp. 1–110, 2009.

[74] T. M. Brennan, S. M. Remias, G. M. Grimmer, D. K. Horton, E. D. Cox, and D. M. Bullock, “Probe vehicle-based statewide mobility performance measures for decision makers,” *Transp. Res. Rec.*, no. 2338, pp. 78–90, 2013, doi: 10.3141/2338-09.

[75] K. Jijo Mathew, J. C. Desai, R. Suryakant Sakhare, W. Kim, H. Li, and D. M. Bullock, “Big Data Applications for Managing Roadways,” *ITE J.*, vol. 91, no. 2, pp. 28–35, 2021.

[76] R. S. Sakhare, J. C. Desai, J. K. Mathew, J. D. McGregor, and D. M. Bullock, “Evaluation of the Impact of Presence Lighting and Digital Speed Limit Trailers on Interstate Speeds in Indiana Work Zones,” *J. Transp. Technol.*, vol. 11, no. 02, pp. 157–167, 2021, doi: 10.4236/jtts.2021.112010.

[77] J. Desai, H. Li, J. K. Mathew, Y.-T. Cheng, A. Habib, and D. M. Bullock, “Correlating Hard-Braking Activity with Crash Occurrences on Interstate Construction Projects in Indiana,” *J. Big Data Anal. Transp.*, vol. 3, no. 1, pp. 27–41, Apr. 2020, doi: 10.1007/s42421-020-00024-x.

[78] FHWA, “Traffic Incident Management (TIM) Performance Measurement: On the Road to Success,” 2018.

[79] H. Li, S. M. Remias, C. M. Day, M. M. Mekker, J. R. Sturdevant, and D. M. Bullock, “Shock Wave Boundary Identification Using Cloud-Based Probe Data,” *Transp. Res. Rec.*, vol. 2526, no. 1, pp. 51–60, 2015, doi: 10.3141/2526-06.

[80] C. Day *et al.*, “2015 Indiana Mobility Report and Performance Measure Dashboards,” West Lafayette, IN, Nov. 2016.

[81] T. M. Brennan, S. M. Remias, G. M. Grimmer, D. K. Horton, E. D. Cox, and D. M. Bullock, “Probe Vehicle–Based Statewide Mobility Performance Measures for Decision Makers,” *Transp. Res. Rec. J. Transp. Res. Board*, vol. 2338, no. 1, pp. 78–90, Jan. 2013, doi: 10.3141/2338-09.

[82] J. L. Bullock, R. Hainje, A. Habib, D. Horton, and D. M. Bullock, “Public Safety Implementation of Unmanned Aerial Systems for Photogrammetric Mapping of Crash Scenes,” *Transp. Res. Rec. J. Transp. Res. Board*, vol. 2673, no. 7, pp. 567–574, Jul. 2019, doi: 10.1177/0361198119850804.

[83] J. Desai, H. Li, J. K. Mathew, Y.-T. Cheng, A. Habib, and D. M. Bullock, “Correlating Hard-Braking Activity with Crash Occurrences on Interstate Construction Projects in Indiana,” *J. Big Data Anal. Transp.*, vol. 3, no. 1, pp. 27–41, Apr. 2021, doi: 10.1007/s42421-020-00024-x.

[84] Federal Highway Administration, “EDC-6: Crowdsourcing for Advancing Operations,” 2021. [Online]. Available: https://www.fhwa.dot.gov/innovation/everydaycounts/edc_6/crowdsourcing.cfm. [Accessed: 23-Mar-2022].

[85] G. Ullman, T. Lomax, and T. Scriba, “A Primer on Work Zone Safety and Mobility Performance Measurement,” *Report*, no. September 2011, Jan. 2011.

[86] Y. Li and Y. Bai, “Development of crash-severity-index models for the measurement of work zone risk levels,” *Accid. Anal. Prev.*, vol. 40, no. 5, pp. 1724–1731, Sep. 2008, doi: 10.1016/j.aap.2008.06.012.

[87] R. J. Haseman, J. S. Wasson, and D. M. Bullock, “Real-Time Measurement of Travel Time Delay in Work Zones and Evaluation Metrics Using Bluetooth Probe Tracking,” *Transp. Res. Rec. J. Transp. Res. Board*, vol. 2169, no. 1, pp. 40–53, Jan. 2010, doi: 10.3141/2169-05.

[88] M. Mekker, H. Li, J. McGregor, M. Kachler, and D. Bullock, “Implementation of a real-time data driven system to provide queue alerts to stakeholders,” in *IEEE Conference on Intelligent Transportation Systems, Proceedings, ITSC*, 2018, vol. 2018-March, pp. 1–6, doi: 10.1109/ITSC.2017.8317648.

[89] K. H. Janstrup, S. Kaplan, T. Hels, J. Lauritsen, and C. G. Prato, “Understanding traffic crash under-reporting: Linking police and medical records to individual and crash characteristics,” *Traffic Inj. Prev.*, vol. 17, no. 6, pp. 580–584, Aug. 2016, doi: 10.1080/15389588.2015.1128533.

[90] A. Tarko, *Measuring Road Safety with Surrogate Events*. 2019.

[91] T. Yamamoto, J. Hashiji, and V. N. Shankar, “Underreporting in traffic accident data, bias in parameters and the structure of injury severity models,” *Accid. Anal. Prev.*, vol. 40, no. 4, pp. 1320–1329, Jul. 2008, doi: 10.1016/j.aap.2007.10.016.

[92] L. Blincoe *et al.*, “The Economic Impact of Motor Vehicle Crashes, 2000 6. Performing Organization Code NHTSA Technical Report None None,” May 2002.

[93] G. A. Davis, J. Hourdos, H. Xiong, and I. Chatterjee, “Outline for a causal model of traffic conflicts and crashes,” *Accid. Anal. Prev.*, vol. 43, no. 6, pp. 1907–1919, Nov. 2011, doi: 10.1016/j.aap.2011.05.001.

[94] A. P. Tarko, “Use of crash surrogates and exceedance statistics to estimate road safety,” *Accid. Anal. Prev.*, vol. 45, pp. 230–240, Mar. 2012, doi: 10.1016/j.aap.2011.07.008.

[95] M. M. Haque and S. Washington, “The impact of mobile phone distraction on the braking behaviour of young drivers: A hazard-based duration model,” *Transp. Res. Part C Emerg. Technol.*, vol. 50, pp. 13–27, Jan. 2015, doi: 10.1016/j.trc.2014.07.011.

[96] J. Kamla, T. Parry, and A. Dawson, “Analysing truck harsh braking incidents to study roundabout accident risk,” *Accid. Anal. Prev.*, vol. 122, pp. 365–377, Jan. 2019, doi: 10.1016/j.aap.2018.04.031.

[97] G. Jun, J. Ogle, and R. Guensler, “Relationships between crash involvement and temporal-spatial driving behavior activity patterns: Use of data for vehicles with global positioning systems,” *Transp. Res. Rec.*, no. 2019, pp. 246–255, 2007, doi: 10.3141/2019-29.

[98] O. Musicant, H. Bar-Gera, and E. Schechtman, “Electronic records of undesirable driving events,” *Transp. Res. Part F Traffic Psychol. Behav.*, vol. 13, no. 2, pp. 71–79, Mar. 2010, doi: 10.1016/j.trf.2009.11.001.

[99] D. Mollicone *et al.*, “Predicting performance and safety based on driver fatigue,” *Accid. Anal. Prev.*, vol. 126, pp. 142–145, May 2019, doi: 10.1016/j.aap.2018.03.004.

[100] R. J. Kiefer, D. J. Leblanc, and C. A. Flannagan, “Developing an inverse time-to-collision crash alert timing approach based on drivers’ last-second braking and steering judgments,” *Accid. Anal. Prev.*, vol. 37, no. 2, pp. 295–303, Mar. 2005, doi: 10.1016/j.aap.2004.09.003.

[101] “Central Indiana Local Climate Info.” [Online]. Available: https://www.weather.gov/ind/localcli. [Accessed: 23-Oct-2020].

[102] H. Li, S. M. Remias, C. M. Day, M. M. Mekker, J. R. Sturdevant, and D. M. Bullock, “Shock Wave Boundary Identification Using Cloud-Based Probe Data,” *Transp. Res. Rec. J. Transp. Res. Board*, vol. 2526, no. 1, pp. 51–60, Jan. 2015, doi: 10.3141/2526-06.

[103] T. M. Brennan, S. M. Remias, G. M. Grimmer, D. K. Horton, E. D. Cox, and D. M. Bullock, “Probe Vehicle–Based Statewide Mobility Performance Measures for Decision Makers,” *Transp. Res. Rec. J. Transp. Res. Board*, 2013, doi: 10.3141/2338-09.

[104] M. M. Mekker *et al.*, “Application of LiDAR and Connected Vehicle Data to Evaluate the Impact of Work Zone Geometry on Freeway Traffic Operations,” *Transp. Res. Rec. J. Transp. Res. Board*, vol. 2672, no. 16, pp. 1–13, Dec. 2018, doi: 10.1177/0361198118758050.

[105] AASHTO, *A Policy on Geometric Design of Highways and Streets, 7th Edition*. 2018.

[106] J. Desai, J. K. Mathew, H. Li, and D. M. Bullock, “Analysis of Electric and Hybrid Vehicle Usage in Proximity to Charging Infrastructure in Indiana,” *J. Transp. Technol.*, vol. 11, no. 04, pp. 577–596, Aug. 2021, doi: 10.4236/jtts.2021.114036.

[107] J. Desai, J. K. Mathew, H. Li, and D. M. Bullock, “Using Connected Vehicle Data for Assessing Electric Vehicle Charging Infrastructure Usage and Investment Opportunities,” *ITE Journal (Institute of Transportation Engineers)*, vol. 95, no. 3. 2022, doi: 10.36548/jaicn.2022.1.

[108] “Global EV Outlook 2021 – Analysis - IEA.” [Online]. Available: https://www.iea.org/reports/global-ev-outlook-2021?mode=overview. [Accessed: 29-Jul-2021].

[109] “EVO Report 2021 | BloombergNEF | Bloomberg Finance LP.” [Online]. Available: https://about.bnef.com/electric-vehicle-outlook/. [Accessed: 29-Jul-2021].

[110] M. McCormick and C. Bushey, “Biden sets electric vehicle target in drive to cut emissions | Financial Times,” *Financial Times*. [Online]. Available: https://www.ft.com/content/7fbc2d70-5365-4d3b-97ec-cea2756de28d?accessToken=zwAAAXsbyTPAkc9_vC1wU2VNO9OX7M6idW3ijQ.MEUCIQCCFN3pibkmvpKfALJsyr65UsVacw57IkJiuAYsxLyZWgIgcYiGfGbevq6AKLEWpWLlBaLsBkYCQAH4dgBEafpVHA8&sharetype=gift?token=c507fd08-660d-4871-a983. [Accessed: 06-Aug-2021].

[111] "Global electric vehicle sales: why 2020 proved a tipping point | World Economic Forum." [Online]. Available: https://www.weforum.org/agenda/2021/01/electric-vehicles-breakthrough-tesla-china/. [Accessed: 29-Jul-2021].

[112] "Electric Vehicle Market Status-Update."

[113] G. Inc, "Addressing the barriers to EV adoption | Geotab." [Online]. Available: www.geotab.com/energy. [Accessed: 30-Jul-2021].

[114] T. Franke, I. Neumann, F. Bühler, P. Cocron, and J. F. Krems, "Experiencing Range in an Electric Vehicle: Understanding Psychological Barriers," *Appl. Psychol.*, vol. 61, no. 3, pp. 368–391, Jul. 2012, doi: 10.1111/j.1464-0597.2011.00474.x.

[115] S. Hardman and G. Tal, "Understanding discontinuance among California's electric vehicle owners," *Nat. Energy 2021 65*, vol. 6, no. 5, pp. 538–545, Apr. 2021, doi: 10.1038/s41560-021-00814-9.

[116] J. H. Lee, D. Chakraborty, S. J. Hardman, and G. Tal, "Exploring electric vehicle charging patterns: Mixed usage of charging infrastructure," *Transp. Res. Part D Transp. Environ.*, vol. 79, p. 102249, Feb. 2020, doi: 10.1016/j.trd.2020.102249.

[117] C. Bingham, C. Walsh, and S. Carroll, "Impact of driving characteristics on electric vehicle energy consumption and range," *IET Intell. Transp. Syst.*, vol. 6, no. 1, pp. 29–35, Mar. 2012, doi: 10.1049/iet-its.2010.0137.

[118] K. Kambly and T. H. Bradley, "Geographical and temporal differences in electric vehicle range due to cabin conditioning energy consumption," *J. Power Sources*, vol. 275, pp. 468–475, Feb. 2015, doi: 10.1016/j.jpowsour.2014.10.142.

[119] E. Yao, Z. Yang, Y. Song, and T. Zuo, "Comparison of electric vehicle's energy consumption factors for different road types," *Discret. Dyn. Nat. Soc.*, vol. 2013, 2013, doi: 10.1155/2013/328757.

[120] G. Wager, J. Whale, and T. Braunl, "Driving electric vehicles at highway speeds: The effect of higher driving speeds on energy consumption and driving range for electric vehicles in Australia," *Renewable and Sustainable Energy Reviews*, vol. 63. Pergamon, pp. 158–165, 01-Sep-2016, doi: 10.1016/j.rser.2016.05.060.

[121] X. Yuan, L. Li, H. Gou, and T. Dong, "Energy and environmental impact of battery electric vehicle range in China," *Appl. Energy*, vol. 157, pp. 75–84, Nov. 2015, doi: 10.1016/j.apenergy.2015.08.001.

[122] H. Yang, Y. Gao, K. B. Farley, M. Jerue, J. Perry, and Z. Tse, “EV usage and city planning of charging station installations,” in *2015 IEEE Wireless Power Transfer Conference, WPTC 2015*, 2015, doi: 10.1109/WPT.2015.7139139.

[123] C. Li, Z. Dong, G. Chen, B. Zhou, J. Zhang, and X. Yu, “Data-driven Planning of Electric Vehicle Charging Infrastructure: A Case Study of Sydney, Australia,” *IEEE Trans. Smart Grid*, 2021, doi: 10.1109/TSG.2021.3054763.

[124] T. Bräunl, D. Harries, M. McHenry, and G. Wager, “Determining the optimal electric vehicle DC-charging infrastructure for Western Australia,” *Transp. Res. Part D Transp. Environ.*, vol. 84, p. 102250, Jul. 2020, doi: 10.1016/j.trd.2020.102250.

[125] M. Kavianipour *et al.*, “Electric vehicle fast charging infrastructure planning in urban networks considering daily travel and charging behavior,” *Transp. Res. Part D Transp. Environ.*, vol. 93, p. 102769, Apr. 2021, doi: 10.1016/j.trd.2021.102769.

[126] R. Maia, M. Silva, R. Araujo, and U. Nunes, “Electric vehicle simulator for energy consumption studies in electric mobility systems,” in *2011 IEEE Forum on Integrated and Sustainable Transportation Systems, FISTS 2011*, 2011, pp. 227–232, doi: 10.1109/FISTS.2011.5973655.

[127] Y. Dashora, J. W. Barnes, R. S. Pillai, T. E. Combs, M. Hilliard, and M. S. Chinthavali, “The PHEV charging infrastructure planning (PCIP) problem,” *Int. J. Emerg. Electr. Power Syst.*, vol. 11, no. 2, Jun. 2010, doi: 10.2202/1553-779X.2482.

[128] P. Morrissey, P. Weldon, and M. O’Mahony, “Future standard and fast charging infrastructure planning: An analysis of electric vehicle charging behaviour,” *Energy Policy*, vol. 89, pp. 257–270, Feb. 2016, doi: 10.1016/j.enpol.2015.12.001.

[129] M. Hunter, J. Mathew, E. Cox, M. Blackwell, and D. Bullock, “Estimation of Connected Vehicle Penetration Rate on Indiana Roadways,” *JTRP Affil. Reports*, Jan. 2021, doi: 10.5703/1288284317343.

[130] W. A. P. I. Specifications, “Vehicle API,” 2012. [Online]. Available: https://vpic.nhtsa.dot.gov/api/. [Accessed: 30-Jul-2021].

[131] INDOT, “INDOT: Wireless Electric Vehicle Charging Solution for Highway Infrastructure.” [Online]. Available: https://www.in.gov/indot/4320.htm. [Accessed: 27-Jul-2021].

[132] National Renewable Energy Laboratory, “All Stations API.” [Online]. Available: https://developer.nrel.gov/docs/transportation/alt-fuel-stations-v1/all/. [Accessed: 28-Jul-2021].

[133] “Tested: InsideEVs Reveals Real World Range Of Today’s Electric Cars.” [Online]. Available: https://insideevs.com/reviews/443791/ev-range-test-results/. [Accessed: 10-Mar-2022].

[134] H. Jin, “U.S. hybrid electric car sales hit record highs | Reuters,” *Reuters*, 2022.

[135] “FACT SHEET: The Biden-Harris Electric Vehicle Charging Action Plan | The White House.” [Online]. Available: https://www.whitehouse.gov/briefing-room/statements-releases/2021/12/13/fact-sheet-the-biden-harris-electric-vehicle-charging-action-plan/. [Accessed: 21-Jan-2022].

[136]“Officials highlight Biden’s electric vehicle goals, importance of charger rollout - UPI.com,” *UPI*, 2022.

[137] M. B. Arias and S. Bae, “Electric vehicle charging demand forecasting model based on big data technologies,” *Appl. Energy*, vol. 183, pp. 327–339, Dec. 2016, doi: 10.1016/J.APENERGY.2016.08.080.

[138] E. Xydas, C. Marmaras, L. M. Cipcigan, N. Jenkins, S. Carroll, and M. Barker, “A data-driven approach for characterising the charging demand of electric vehicles: A UK case study,” *Appl. Energy*, vol. 162, pp. 763–771, Jan. 2016, doi: 10.1016/J.APENERGY.2015.10.151.

[139] R. Pagany, A. Marquardt, and R. Zink, “Electric Charging Demand Location Model—A User- and Destination-Based Locating Approach for Electric Vehicle Charging Stations,” *Sustain. 2019, Vol. 11, Page 2301*, vol. 11, no. 8, p. 2301, Apr. 2019, doi: 10.3390/SU11082301.

[140] J. Desai, J. K. Mathew, H. Li, and D. M. Bullock, “Electric and Hybrid Vehicle Miles Travelled Dataset.” Purdue University Research Repository, 31-Jan-2022, doi: 10.4231/MTDC-3C27.

[141] “FHWA Office of Operations - Alternate Route Handbook - Alternate Route Plan Development.” [Online]. Available: https://ops.fhwa.dot.gov/publications/ar_handbook/arh1.htm. [Accessed: 04-Feb-2022].

[142] H. Li, R. Guensler, and J. Ogle, “Analysis of Morning Commute Route Choice Patterns Using Global Positioning System–Based Vehicle Activity Data,” *Transp. Res. Rec. J. Transp. Res. Board*, vol. 1926, no. 1, pp. 162–170, Jan. 2005, doi: 10.1177/0361198105192600119.

[143] T. Tettamanti, H. Demeter, and I. Varga, “Route choice estimation based on cellular signaling data,” *Acta Polytech. Hungarica*, vol. 9, no. 4, pp. 207–220, 2012.

[144] J. Schlaich, “Analyzing route choice behavior with mobile phone trajectories,” *Transp. Res. Rec.*, no. 2157, pp. 78–85, Jan. 2010, doi: 10.3141/2157-10.

[145] T. Morikawa and T. Miwa, “Preliminary analysis on dynamic route choice behavior: Using probe-vehicle data,” in *Journal of Advanced Transportation*, 2006, vol. 40, no. 2, pp. 140–163, doi: 10.1002/atr.5670400204.

[146] J. Gong, Z. Yu, and N. Chen, “An analysis of drivers’ route choice behavior in urban road networks based on GPS data,” in *International Conference on Transportation Engineering 2007, ICTE 2007*, 2007, pp. 515–520, doi: 10.1061/40932(246)85.

[147] P. H. L. Bovy and M. A. Bradley, “ROUTE CHOICE ANALYZED WITH STATED-PREFERENCE APPROACHES.,” *Transp. Res. Rec.*, no. 1037, pp. 1–11, 1985.

[148] R. H. M. Emmerink, P. Nijkamp, P. Rietveld, and J. N. Van Ommeren, “Variable message signs and radio traffic information: An integrated empirical analysis of drivers’ route choice behaviour,” *Transp. Res. Part A Policy Pract.*, vol. 30, no. 2, pp. 135–153, Mar. 1996, doi: 10.1016/0965-8564(95)00016-X.

[149] H. Dia, “An agent-based approach to modelling driver route choice behaviour under the influence of real-time information,” *Transp. Res. Part C Emerg. Technol.*, vol. 10, no. 5–6, pp. 331–349, Oct. 2002, doi: 10.1016/S0968-090X(02)00025-6.

[150] M. A. Abdel-Aty, R. Kitamura, and P. P. Jovanis, “Using stated preference data for studying the effect of advanced traffic information on drivers’ route choice,” *Transp. Res. Part C Emerg. Technol.*, vol. 5, no. 1, pp. 39–50, Feb. 1997, doi: 10.1016/S0968-090X(96)00023-X.

[151] H. Xu, H. Yang, J. Zhou, and Y. Yin, “A Route Choice Model with Context-Dependent Value of Time,” *https://doi.org/10.1287/trsc.2016.0710*, vol. 51, no. 2, pp. 536–548, Feb. 2017, doi: 10.1287/TRSC.2016.0710.

[152] M. Fosgerau, E. Frejinger, and A. Karlstrom, “A link based network route choice model with unrestricted choice set,” *Transp. Res. Part B Methodol.*, vol. 56, pp. 70–80, Oct. 2013, doi: 10.1016/J.TRB.2013.07.012.

[153] V. Henn, “Fuzzy route choice model for traffic assignment,” *Fuzzy Sets Syst.*, vol. 116, no. 1, pp. 77–101, Nov. 2000, doi: 10.1016/S0165-0114(99)00039-1.

[154] E. D. Saldivar-Carranza, M. Hunter, H. Li, J. Mathew, and D. M. Bullock, “Longitudinal Performance Assessment of Traffic Signal System Impacted by Long-Term Interstate Construction Diversion Using Connected Vehicle Data,” *J. Transp. Technol.*, vol. 11, no. 04, pp. 644–659, Aug. 2021, doi: 10.4236/jtts.2021.114040.

[155] J. Desai, E. Saldivar-Carranza, J. K. Mathew, H. Li, T. Platte, and D. Bullock, “Methodology for Applying Connected Vehicle Data to Evaluate Impact of Interstate Construction Work Zone Diversions,” *2021 IEEE Int. Intell. Transp. Syst. Conf.*, pp. 4035–4042, Sep. 2021, doi: 10.1109/ITSC48978.2021.9564873.

[156] M. Auer and K. Bogenberger, “Empirical Analysis of Dynamic Route Choice Behavior on German Freeway A8 Based on Large Scale Vehicle Fleet Data Matching Algorithm for Dynamic Ride Sharing Problem View project Park Spot Routing View project,” *6th Symp. Eur. Assoc. Res. Transp.*, no. September, 2017.

[157] “Greyhound bus crash leaves two people dead in Indiana - CNN.”

[158] “Indiana 225 bridge over Wabash River closed indefinitely over concern.” [Online]. Available: https://www.jconline.com/story/news/2021/06/15/indiana-225-bridge-wabash-river-closed/7707349002/. [Accessed: 31-Jan-2022].

[159] “Google Maps.” [Online]. Available: https://www.google.com/maps/@40.493997,-86.82286,192a,35y,39.43t/data=!3m1!1e3. [Accessed: 01-Feb-2022].

[160] F. Primerano, M. A. P. Taylor, L. Pitaksringkarn, and P. Tisato, “Defining and understanding trip chaining behaviour,” *Transportation*, vol. 35, no. 1. Springer, pp. 55–72, 19-Jan-2008, doi: 10.1007/s11116-007-9134-8.

[161] F. Richter, “Big data on wheels | The Big Data Hub,” 2017. [Online]. Available: https://www.statista.com/chart/8018/connected-car-data-generation/. [Accessed: 23-Mar-2022].